ISTANBUL TECHNICAL UNIVERSITY ★ GRADUATE SCHOOL OF SCIENCE ENGINEERING AND TECHNOLOGY

MORPHOLOGICAL, ELECTRONIC AND OPTICAL PROPERTIES OF NOVEL NANO-SCALE STRUCTURES

M.Sc. THESIS

Merve ALTAY

Department of Physics Engineering

Physics Engineering Programme

JUNE 2012

ISTANBUL TECHNICAL UNIVERSITY ★ GRADUATE SCHOOL OF SCIENCE ENGINEERING AND TECHNOLOGY

MORPHOLOGICAL, ELECTRONIC AND OPTICAL PROPERTIES OF NOVEL NANO-SCALE STRUCTURES

M.Sc. THESIS

Merve ALTAY
(509081108)

Department of Physics Engineering

Physics Engineering Programme

Thesis Advisor: Assoc. Prof. Dr. Oğuzhan GÜRLÜ

JUNE 2012

İSTANBUL TEKNİK ÜNİVERSİTESİ ★ FEN BİLİMLERİ ENSTİTÜSÜ

NANO-BOYUTLU FARKLI YAPILARIN MORFOLOJİK, ELEKTRONİK VE OPTİK ÖZELLİKLERİ

YÜKSEK LİSANS TEZİ

Merve ALTAY
(509081108)

Fizik Mühendisliği Anabilim Dalı

Fizik Mühendisliği Programı

Tez Danışmanı: Doç. Dr. Oğuzhan GÜRLÜ

HAZİRAN 2012

Merve ALTAY, a **M.Sc.** student of ITU **Graduate School of Science, Engineering and Technology** student ID **509081108**, successfully defended the **thesis** entitled "**MORPHOLOGICAL, ELECTRONIC AND OPTICAL PROPERTIES OF NOVEL NANO-SCALE STRUCTURES** ", which she prepared after fulfilling the requirements specified in the associated legislations, before the jury whose signatures are below.

Thesis Advisor :	**Assoc. Prof. Dr. Oğuzhan GÜRLÜ** Istanbul Technical University	.....
Jury Members :	**Assoc. Prof. Dr. H.Özgür ÖZER** Istanbul Technical University	.....
	Assist. Prof. Dr. Alper Tunga AKARSUBAŞI Istanbul Technical University	.....

Date of Submission : 4 May 2012
Date of Defense : 8 June 2012

To my father,

FOREWORD

In this study, morphological, electronic and optical properties of novel nano-scale structures, which are composed of T7 Primer molecules, Tris-EDTA buffer and Tris-HCl buffers, CdSe quantum dots, graphene and graphitic flakes, are investigated.

I am really greatful to my supervisor Assoc. Prof. Dr. Oğuzhan Gürlü for his guidance and encouragement during the whole study. I have learned lots of things from him and I will never forget his great support and advices.

I would like to thank Prof. Dr. Fatma Tepehan from Physics Engineering Department, ITU for giving the opportunity to study with atomic force microscopy. I am thankful to Assist. Prof. Dr. Alper Tunga Akarsubaşı from Molecular Biology and Genetics Department,ITU for supplying the DNA molecules and buffer solutions. I would like to thank Prof. Dr. Atilla Aydınlı from Physics Department, Bilkent University for giving the opportunity to study with Micro Raman Spectroscopy.

I am very thankful to all Gürlü Group's members for their help and friendships.

Special thanks to Mehmet Selman Tamer for his great support, patience and unconditional love.

Finally, I would like to thank to my family for their love and unlimited support.

May 2012

Merve ALTAY
(Physicist)

TABLE OF CONTENTS

Page

ABBREVIATIONS

2D	**:** Two dimensional
AFM	**:** Atomic Force Microscopy
CVD	**:** Chemical Vapour Deposition
DNA	**:** Deoxyribonucleic Acid
EDTA	**:** Ethylenediaminetetraacetic acid
HOPG	**:** Highly Oriented Pyrolytic Graphite
MRS	**:** Micro Raman Spectroscopy
NUS	**:** National University of Singapore
QD	**:** Quantum Dot
STM	**:** Scanning Tunneling Microscopy
SPM	**:** Scanning Probe Microscopy
TE	**:** Tris-EDTA
Tris	**:** Tris(hydroxymethyl)aminomethane

LIST OF FIGURES

Page

MORPHOLOGICAL, ELECTRONIC AND OPTICAL PROPERTIES OF NOVEL NANO-SCALE STRUCTURES

SUMMARY

Investigations of novel nanostructures are of great interest to many research groups since the advent of scanning probe microscopy. Atomic Force Microscopy and Scanning Tunneling Microscopy are widely used for investigation of novel nanostructures. Some examples of nanostructures can be listed as quantum dots, biomolecules and allotropes of carbon such as graphene and carbon nano tubes. These nanostructures are not only of scientific interest but also promising for future applications in various fields such as electronics, optics and molecular biology.

Biomolecules are one of the most noteworthy nanostructures and they have been investigated by scanning probe microscopy techniques. In biological studies, the molecules are generally kept in buffer solutions to stabilize their activity, but the buffer solutions may prevent the observation of biomolecules when studying with scanning probe microscopy. Quantum dots are examples to the nano-sturctures in recent years. They have many different features such as discrete enery levels, larger band gaps compared to their bulk crystal forms and the relation between their size and emission wavelength is quite notable. The main motivation to work on quantum dots is the possible application areas such as transistors, solar cells and LEDs. Resarch primarily focusing on the nanoscale properties of materials has a special interest in graphene. Its unusual electronic, thermal and mechanical properties make it a unique material.

In this study, preparation of novel structures at nanoscale and investigation of their morphological, electronic and optical properties were looked upon by optical microscopy, scanning probe microscopy techniques and micro Raman spectroscopy. First, T7 Primers were investigated on HOPG surface by using scanning probe microscopy techniques. However, the solution of T7 Primer molecules formed different film structures on HOPG surface and prevented the observation of T7 Primer molecules on the surface. Then, the solution of T7 Primer molecules, which is Tris-EDTA buffer solution was investigated and the solution created hexagonal structures on solid substrates due to the Tris-HCl in the buffer. Second, preparation of quantum dot surface systems were studied in this study. CdSe type quantum dot surfaces systems were prepared in different ratio. The CdSe quantum dots were observed by AFM, but in cluster form. Third, an alternative method for graphene production was also attempted in this study. The method involves preparation of a solution using both mechanical exfoliation method and chemical materials. By using micro Raman spectroscopy and current-voltage characterization technique, the alternative method for graphene production results in multi layer graphene and graphitic flakes.

NANO-BOYUTLU FARKLI YAPILARIN MORFOLOJİK, ELEKTRONİK VE OPTİK ÖZELLİKLERİ

ÖZET

Farklı nano yapıların incelenmesi, taramalı uç mikroskoplarının bulunmasından beri pek çok araştıma grubunun ilgi odağı olmuştur. Atomik kuvvet mikroskobu ve taramalı tünelleme mikroskobu çeşitli nano yapıların incelenmesinde sıklıkla kullanılmaktadır. Bu nano yapılardan bazıları, kuantum noktalar, biyomoleküller ile grafin ve karbon nano tüpler gibi karbon allotropları olabilir. Bu nano yapılar sadece bilimsel ilgi odağı değil, gelecekte elektronik, optik ve moleküler biyoloji gibi alanlarda umut vaat eden yapılardır.

Biyomoleküller en çok ilgi çeken nano yapılardan biridir ve taramalı uç mikroskobu teknikleri ile yıllardır incelenmektedirler. Taramalı uç mikroskobu özellikle DNA moleküllerinin görüntülenmesinde çok önemlidir. Çok farklı yapılardaki DNA moekülleri atomik kuvvet mikroskobu ile incelenmektedir. Bu moleküller ayrıca iletken özellikte oldukları için taramalı tünelleme mikroskobu ile de incelenebilirler. Taramalı uç mikroskobu çalışmalarında bazı zorluklar ile karşılaşılmaktadır. Örneğin, DNA moleküllerini gözlemlenmesi ve elde edilen görüntülerin tekrarlananması taramalı uç mikroskobu çalışmalarında karşılaşılan zorluklardandır.

Biyolojik çalışmalarda, biyomoleküllerin özelliklerini koruyabilmek için biyomoleküller genellikle tampon çözeltilerin içerisinde tutulurlar. Bu tampon çözeltiler molekülleri korur, aktifliklerinin devam etmesini sağlar. Ancak, bu tampon çözeltiler taramalı uç mikroskopları ile çalışırken biyomoleküllerin gözlemlenmesini engelleyebilirler. Biyomoleküllerin taramalı uç mikroskopları ile incelenmesi çalışmaları oldukça geniş bir yere sahip olmasına rağmen, taramalı uç mikroskopları ile çalışmaları engellediği bilinen tampon çözeltiler ve bunların etkilerinin incelenmesi yok denecek kadar azdır.

Nano yapılara diğer bir örnek ise son yıllarda oldukça popüler çalışma konusu olan kuantum noktalardır. Kuantum noktalar, kesikli enerji seviyesi, bulk kristalden daha geniş bant aralığı, boyutuna bağlı olarak uyarılması ve ışık yayınlaması gibi bir çok özelliğe sahip nano boyutlu yapılardır. Bu ilginç özelliklerin yanı sıra asıl önemli olan kuantum noktaların transistörler, güneş pilleri ve LEDler gibi pek çok uygulama alanlarında kullanılabilmesidir. Kuantum noktaların pek çok uygulama alanları vardır ve genellikle yapılan çalışmalar bu yöndedir. Fakat kuantum noktaların yüzey üzerinde incelenmesi ve tek başına gözlemlenmesi çalışmaları henüz başlangıç seviyededir.

Malzemelerin nano boyutta özelliklerinin incelenmesinde grafin önemli bir yere sahiptir. Grafinin deneysel olarak gözlemlenmesi çok yeni olmasına rağmen, grafin ile ilgili pek çok çalışma bulunmaktadır. Sıradışı elektronik, mekanik ve termal özellikleri grafini çok ilgi çekici bir malzeme yapmaktadır.Bu tez çalışmasında, nano

boyuttaki farklı yapıların yüzey üzerinde incelenmesi, ve bu yapıların morfolojik, elektronik ve optik özelliklerinin optik mikroskop, taramalı uç mikroskobu teknikleri ve mikro Raman spektroskopisi ile incelenmesi üzeride çalışılmıştır.

İlk olarak, T7 Primer DNA molekülleri grafit yüzeyi üzerinde taramalı uç mikroscopları kullanılarak incelenmeye çalışılmıştır. Ancak T7 Primer molekülleri içeren çözelti grafit yüzeyi üzerinde farklı film gibi yapılar oluşturmuş ve T7 Primer moleküllerinin gözlenmesini engellemiştir. Bu sonuçların ardından, elde edilen verilerin anlaşılabilmesi için T7 Primer moleküllerini içeren çözelti tek başına yüzey üzerinde incelenmiştir. Bu çözelti Tris-EDTA tampon çözeltisidir ve tris(hydroxymethyl)aminomethane ile ethylenediaminetetraacetic acid bileşenlerinden oluşmaktadır. Tris-EDTA tampon çözeltisi T7 Primer moleküllerini içermeksizin grafit yüzeyi üzerinde incelenmiştir. Bu incelemeler sonucu Tris-EDTA tampon çözeltisi grafit yüzeyi üzerinde altıgenimsi yapılar oluşturmuştur. Ancak birkaç deneme sonucunda altıgen gibi yapılardan farklı başka film gibi yapılar gözlemlenmiştir. Bu sonuçları anlayabilmek için ise Tris ve EDTA tampon çözeltileri ayrı ayrı incelenmiştir.

İlk olarak Tris-HCl çözeltisi grafit yüzeyi üzerinde denenmiş ancak atomic kuvvet mikroskopisinde gözlemlenemeyecek kadar yüksek yapılar oluştuğu için bu yapılardan kurtulabilmek adına altın kaplanmış mica kullanılarak damlat-sürükle-çek metodu uygulanmıştır. Bu metod uyguladıktan sonra altın kaplı mika yüzeyi üzerinde altıgenimsi yapılar atomic kuvvet mikroskopisi ile ve optik mikroskop ile incelenmiştir. Ayrıca Tris-HCl çözeltisi farklı derişimlerde hazırlanarak damlat-sürükle-çek metodu uygulanmadan HOPG yüzeyi üzerinde altıgenimsi yapılar gözlemlenebilmiştir. Ayrıca EDTA çözeltisi aynı şekilde denenmiş ancak böyle yapılara rastlanılmamıştır. Yüzey üzerinde gözlemlenen keskin ve çok belirgin altıgen yapıların Tris-EDTA tampon çözeltisinin içerisindeki Tris-HCl bileşiminden kaynaklandığı sonucuna ulaşılmıştır. Bu çalışma özellikle tampon çözeltilerin yüzey üzerindeki etkilerini anlayabilmek için önemlidir.

Bu tez çalışmasında ikinci olarak, kadmiyum-selen (CdSe) kuantum nokta yüzey sistemleri çalışılmıştır. CdSe tipindeki kuantum noktalar farklı derişimlerde hazırlanarak yüzey üzerinde film oluşturacak şekilde yüzeye uygulanmış ve ardından taramalı uç mikroskopisi ile en ideal kuantum nokta görüntüsü elde edilmeye çalışılmıştır. Kuantum noktaları içeren çözeltinin etkilerinden kurtulabilmek için durulama işlemi ve Hidrojen-Argon atmosferinde fırınlama işlemi uygulanarak kuantum nokta adacıkları atomik kuvvet mikroskopisi ile gözlemlenmiştir. Buradaki en önemli ayrıntı fırınlama sıcaklığıdır ve fırınlama ortamının temiz olmasıdır.

Son olarak, Grafin eldesi için şimdiye kadar bilinen yöntemlerden dışında bir metod üzerinde çalışılmıştır. Bu tez çalışmasında kullanılan yöntem hem mekanik olarak grafinin katmanlara ayrılmasını hem de kimyasal çözeltiler yardımı ile bu katmanların daha da inceltilmesini içermektedir. Basit bir yapışkan bant grafit yüzeyine yapıştırılıp çekilir ve ardından bant yüzeyindeki grafit katmanları tekrar tekrar banta yapıştırılıp çekilir. Bu işlem bantın üzerindeki grafit yapı incelene kadar ve homojen hale gelene kadar tekrarlanır. Bunun sonunda elde edilen yapı saf aseton içerisinde bant mukus yapı olana kadar ultra sonic banyo kullanılarak çözülür. Ardından bu mukus yapı ultra temiz cam lamel üzerine sürtülür ve bu lamel propanoliçerisinde yıkanır. Elde edilen çözelti damlatılarak film hazırlama yöntemi ile yüzey üzerine damlatılır. Çözelti altın kaplanmış mika, silicon ve silikon oxide üzerinde değişik renklerde katmanlar bırakır. Elde edilen bu katmanlar taramalı uç

mikroskopları, micro Raman spektroskopisi ve akım-voltaj karakterizasyon yöntemi ile incelenmiştir. Ayrıca elde edilen katmanları ayırt edebilmek için ve karşılaştırabilmek için bir referans grafin örneği kullanılmıştır ve ayrıca bu örnek taramalı tünelleme mikroskobu, atomik kuvvet mikroskobu ve micro Raman spektroskopisi ile incelenmiştir. Hazır olan bu referans grafin örneği taramalı tünelleme mikroskobu ile incelendiğinde, grafinin tespit edilmesi ve grafin katmanından atomik çözünürlük alınabilmesinin oldukça zor olduğunu görülmüştür. Bu çalışmada elde edilmeye çalışılan grafin katmanların taramalı uç mikroskopları ile incelendiğinde çözeltis etkisi gözlemlenmiştir bu etkinin yok edilmesi için fırınlama metodu kullanılmıştır. Ancak micro Raman spektroskopisi incelemelerine göre elde edilen katmanlar çok katmanlı grafin veya grafit yapılarıdır. Ayrıca bu yapıların akım-voltaj karakteristik incelemesinde de grafitik olduğu ortaya çıkmıştır.

Bu tez çalışmasında kısaca, ilk olarak T7 Primer moleküllerinin taramalı uç mikroskopları ile incelenmesi hedeflenmiştir. Yapılan deneyler T7 Primer moleküllerinin Tris-EDTA tampon çözeltisi içinde tutulduğunda ve yüzey üzerine damlatma işlemi ile uygulandığında gözlenmenmesinin imkansız olduğunu göstermiştir. Bu nedenle, Tris-EDTA çözeltisi incelenmiş ve sonradan anlaşıldığı üzere bu çözelti içerisindeki Tris-HCl çözeltisi yüzey üzerinde altıgen yapılar oluşturmaktadır. Ayrıca bu çalışmada CdSe tipi kuantum nokta yüzey sistemleri hazırlanması ve bu kuantum noktaların gözlemlenmesi çalışılmıştır. CdSe tipi kuantum noktalar grafit yüzeyi üzerinde adacıklar halinde gözlemlenmiştir. Son olarak ise farklı bir yöntem geliştirilerek grafin elde edilmesi çalışılmıştır ve sonuç olarak elde edilen yapılar daha çok grafitik çıkmıştır.

Bugüne kadar pek çok farklı nano-boyutta yapılar incelenmiştir ve incelenmeye devam edilmektedir. Bu çalışmadaki incelenen yapıların nano-boyuttaki yüzey çalışmalarına, taramalı uç mikroskopları çalışmalarına katkı sağlayacağı ve bu çalışmaların gelişmesine yardımcı olması hedeflenmiştir.

1. .INTRODUCTION

The invention of Scanning Probe Microscopy (SPM) techniques started a new era for investigations at the nanometer scale [1,2]. Scanning Tunneling Microscopy (STM) and Atomic Force Microscopy (AFM) are the corner stones of SPM. These techniques make it possible to investigate various nanostructures with atomic resolution. These nanostructures can be biomolecules, quantum dots, carbon nanotubes, buckyballs, graphene and nanowires.

Investigations on morphological properties of biomolecules started at the beginning of 1990s using atomic force microscopy and scanning tunneling microscopy [3-5]. One of the most important biomolecule is DNA. Atomic force microscopy is a powerful technique for imaging DNA [6]. Many types of DNA molecules such as long, short, single-, double-, triple-stranded DNA molecules have been studied by AFM [3,4,6]. Atomic resolution of DNA molecules have been achieved by STM. In STM studies, helix structure of DNA, periodicity [7-9] and also purine bases are shown [10]. However, there are some difficulties to study DNA with scanning probe microscopy such as immobilization of DNA molecules on solid substrates, low repeatability with STM and appropriate substrate for the molecules [11]. In the biological studies, DNA or other biomolecules are stored in various buffer solutions to keep them stable and maintain their pH. Despite these useful features of buffer solutions, salt in buffer solution or buffer itself may prevent the observation of biomolecules when studying these molecules casted on surfaces, using scanning probe microscopy techniques[12]. In many SPM studies, remnants from buffer solutions are observed rather than the molecules themselves on the surface with biomolecules [12-14].

The effects of Tris-EDTA (TE) buffer were determined, on hydrophobic and hydrophilic surfaces using atomic force microscopy by H.Wang et. al. They showedthe effects of the chemicals in TE buffer, on HOPG surface. The TE buffer solution was consisted of Tris-HCl, NaCl and EDTA, these chemicals are self-organized parallel nanofilaments [12]. However, studies on the effects of buffer solutions on solid substrates are far from complete. In this study, T7 Primer

molecules and the most commonly used buffers (Tris-EDTA and Tris-HCl) were investigated with scanning probe microscopy.

Another example for the most notable nanostructures are the quantum dots [15]. They were suggested by A.Ekimov et. al. [16] and experimentally realized by L.E.Brus et. al. [17]. Quantum dots are semiconductor nanocrystals with several nanometer sizes [18] and they have interesting features such as discrete energy levels, large band gap, relationship between their sizes and their emission wavelength [15,19,20]. Quantum dots are generally synthesized by chemical process and by changing their size and shape, their optoelectronic properties also change [20]. Quantum dots can be in different structures (core, core/shell) and they can have different types of ligands [20-22].

Quantum dots have a wide application area (like in transistors, solar cells, LEDs, diode lasers and medical imaging) due to their unique optical and electronic properties [22-24]. These properties of quantum dots create great motivation for studies on their local electronic properties. This can be achieved by scanning probe microscopes. Although there have been many studies on imaging quantum dots, these studies had generally observed quantum dots in cluster forms [19,20]. In a study of quantum dots with scanning probe microscopy, types of ligands, shapes and sizes of quantum dots and the substrates are important parameters. Several methods have been employed (evaporation of ligands or solution, rinsing) in order to increase conductivity between the quantum dots and the substrate, to establish the higher resolution in STM and AFM images [15,19,20]. In this study, CdSe quantum dots, which are 6.5 nm size, core type semiconductor nanocrystals with Hexadecylamine / Trioctylphosphine (HDA/TOPO) ligands, were investigated with AFM.

Graphene attracted great interest by nanotechnology researches since its suggestion [28], but especially after its observation in 2004 [25]. Its unusual electronic, thermal and mechanical properties make graphene a unique material [25-27, 29]. With all its amazing properties, graphene can be employed in transistor technology, solar cells and ultracapacitors [30]. Graphene is commonly prepared by four methods; chemical vapour deposition [31,32], mechanical exfoliation of graphite using scotch tape [25], epitaxial growth on insulating or semiconductor surfaces (high temperature treatment of SiC) [33] and the formation of colloidal suspensions (graphene-oxide) [34,35].

In this study, an alternative method for graphene production was attempted and large multi layers of graphene and graphitic flakes were obtained.

In brief, the main purpose of this research was the preparation of novel nanostructures and investigation of their morphological, electronic and optical properties using scanning probe techniques. T7 Primer molecules and the most commonly used buffers, such as Tris-EDTA and Tris-HCl buffers, were investigated on solid substrates. CdSe quantum dots surface systems were investigated on highly oriented pyrolytic graphite surfaces. Additionally, an alternative method for graphene production was studied.

1.1 Novel Nanostructures on Solid Substrates

Nanostructures commonly refer to materials that have dimensions at nanometers. These materials have unique physical properties. The properties of nanometer-sized materials show differences compared to their bulk properties. Some examples of the nanostructures are semiconductor quantum dots, DNA molecules, nanotubes, nanowires, graphene and fullerenes. Their structures, electronic and morphologic features have been intriguing since the advent of SPM techniques [1,2].

Biomolecular nanostructures is a very fruitful research area in nanotechnology and surface science. DNA is the well-known genetic material of the living systems. A new field focusing solely on this material is DNA nanotechnology, which includes the construction of nanoscale objects, devices from DNA and self-assembled DNA complexes. The molecular identification of DNA and other nucleic acids are used to create self-assembled DNA systems [36, 37] (Fig.1.1). These systems have been investigated on solid substrates using scanning probe microscopy techniques [38,39]. Self-assembled DNA nanostructures have great importance for biomedical applications [40] (Fig.1.1).

Other examples for self-assembled nanostructures are quantum dots. Quantum dot clusters were observed on solid substrates [19,20]. Quantum dots nanostructures are important not only in surface studies, but also they have a very important role in nanoscale applications, because of their optoelectronic properties [21-23]. Quantum dots are used in both electronics and optics such as in transistors, LEDs, solar cells

and diode lasers. Moreover, quantum dots are recently used in crucial applications, such as medical imaging and disease detection [41].

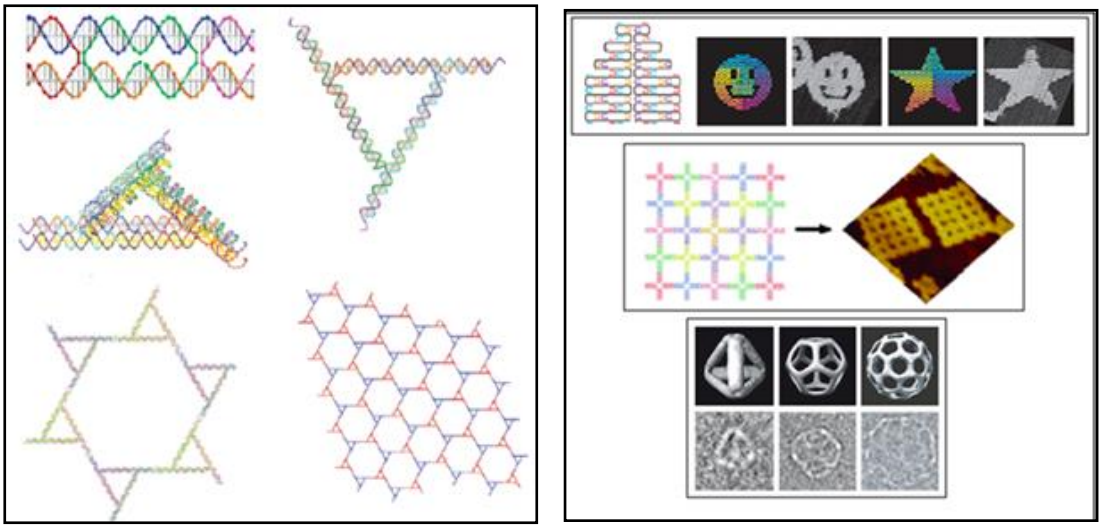

Figure 1.1: Left: DNA motifs [37], Right: Examples of DNA nanostructures [40].

Allotropes of carbon are also important nanostructures from research perspective, like fullerenes, carbon nanotubes and graphene [25]. Many research groups have studied electronic, thermal and mechanical properties of these nano structures in recent years. Especially, carbon nanotubes and graphene have wide application areas. For instance, carbon nanotubes are used as tip material for STM and AFM probes [42], graphene is recently employed in transistor technology [30].

The need for smaller size structures for medical science, electronic devices and optical devices create a great motivation for fundamental research at a smaller size scale. Many novel nanostructures have been observed and there are many of them are waiting to be observed. In this study, we worked on producing, imaging and analyzing nanostructures that may contribute to nanoscale science studies.

2. METHODS

2.1 Sample Preparation Techniques

2.1.1 Drop Casting Method

Drop casting is a very simple method to produce thin films from solutions on solid substrates. Drop casting is the most commonly used method to prepare samples in this study.

The required amount of solution is taken with a micropipette and it is dropped on a substrate (Figure 2.1). According to the characteristics of the surfaces and the solutions, the drop may spread or it may stay intact in a semi-spherical like form on the surface.

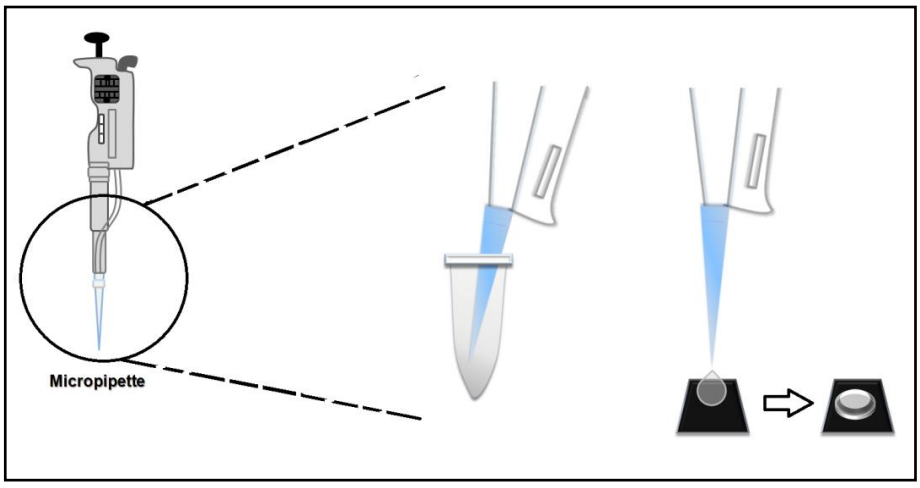

Figure 2.1: Drop casting method by using a micropipette.

2.1.2 Drying in Desiccator

After drop casting method, the samples are placed in a desiccator to dry under a relatively clean and dry environment. Desiccator is generally made of glass and used for keeping the samples dry using a desiccant material such as silica gel (Figure 2.2).

2.1.3 Rinsing

In this study, some of the prepared samples by drop casting method are rinsed by double-distilled water (ddH_2O, Merck Water for chromatography LiChrosolv®) to

eliminate the effects of solutions such as buffer remnants. Before drying or after drying in the desiccator, the prepared samples by drop casting method are rinsed by several drops of double-distilled water (ddH_2O) and then the samples are dried in the desiccator again.

Figure 2.2: Dessicator.

2.1.4 Annealing

Annealing process is important for quantum dot samples and graphene samples. In this study, the quantum dots are covered by ligands and the graphene samples contain residues from the graphitic solution. Annealing method is applied in order to get rid of unwanted residues and ligands on the samples by H-etching. Because the residues and ligands may prevent the investigation of the desired materials (such as a quantum dots or a single layer graphene) using scanning probe techniques. A tube oven is used and the samples were annealed under hydrogen-argon (H_2-Ar) atmosphere (Figure 2.3). Moreover, the temperature should be appropriate for substrates and samples. The temperatures are employed between 200-400^{0}C range for HOPG and graphene samples [43-45]; and between 120-150^{0}C range for quantum dot samples [19], [15], [20].

2.2 Imaging and Analysis

2.2.1 Optical Microscopy

The first step in the characterization of novel nano-structures is optical microscopy investigation. Before using other characterization instruments, investigation of the samples with an optical microscope was very important in this study. For instance, optical microscopy investigation is necessary to distinguish the graphitic flakes, whether they are multi-layer or mono-layer graphene sheets on oxidized silicon

(SiO_2) surface [25]. Moreover, optical microscopy is used for investigation of DNA, Tris-EDTA buffer, Tris-HCl buffer and quantum dot samples. In this study, Olympus BX51 Microscope was used for optical investigation (Figure 2.4).

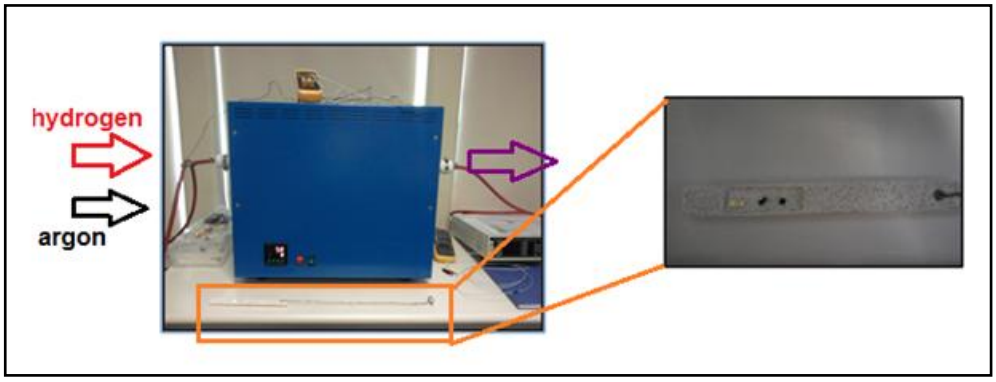

Figure 2.3: Annealing process using tube oven.

Figure 2.4: Optical Microscope, Olympus BX51.

2.2.2 Scanning Tunneling Microscopy

Scanning Tunneling Microscope (STM) was first developed by Gerd Binnig and Heinrich Rohrer in 1982 [2]. STM enables imaging the surfaces of conducting or semiconducting materials at nano scale. STM does not only enable imaging surfaces with atomic precision, but also atoms and molecules on the surface can be manipulated or their electronic and optical properties can be studied using related spectroscopic techniques.

The STM is based on the quantum mechanical tunneling effect of electrons. When two conducting or semi conducting materials are very close to each other, electrons have a fine probability of tunneling from one to the other. In figure 2.5, STM is schematically explained (more detailed information about the STM is available in [46], [47]):

In figure 2.5 (a) tip approaches to conducting or semiconducting sample. The tip is assumed to be atomically sharp. A bias voltage is applied to the tip for a net quantum mechanical tunneling current to pass from the tunnel junction. The tunneling current is kept constant by a feedback mechanism. Feedback mechanism controls the z-piezo, which moves tip and keeps the distance between the tip and the surface constant in the constant current mode. Piezo ceramics are used for tip motion with 1 picometer precision in all the axis. Z piezo is in the vertical axis and used to determine the relative height of each point and x, y piezos move in the horizontal axis and they are used to scan the surface.

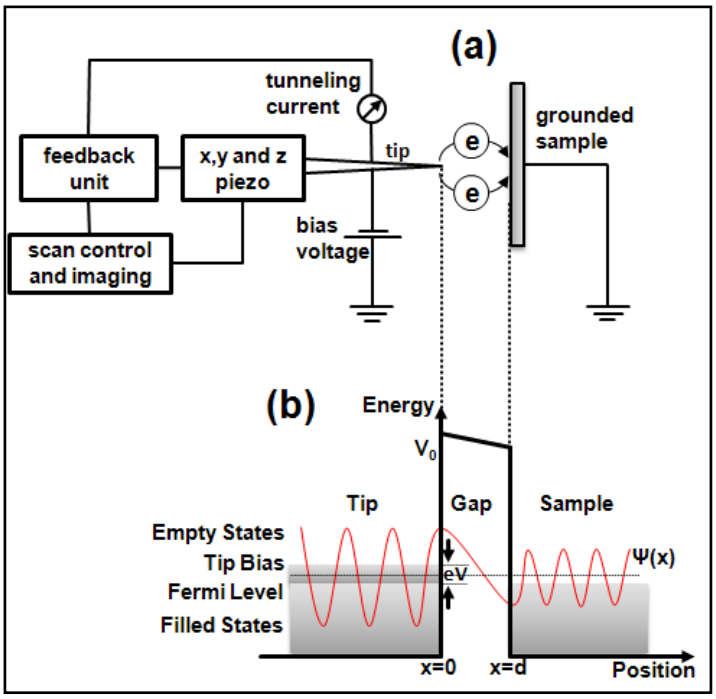

Figure 2.5: The Schematic of Scanning Tunneling Microscope.

In figure 2.5 (b) simple energy level diagram for STM is shown. Electrons can tunnel through the gap from a filled state at the Fermi level in the tip to an empty state at the Fermi level of the sample. The gap is considered as a potential barrier with height V_0, the electrons have energy E. One dimensional Schrödinger equation for the electron can be written as **(2.1)**.

Nanosurf EasyScan2 STM system is a commercial educational purpose STM that works under ambient conditions (Figure 2.6). This system was used during all STM measurements. STM is used to study surface structures of Highly Oriented Pyrolytic Graphite (HOPG), graphene-like structures and Tris-HCl buffer samples.

$$\frac{\hbar^2}{2m}\frac{d^2\psi(x)}{dx^2} + [E - V(x)]\psi(x) = 0 \qquad \textbf{(2.1)}$$

V=0 for x<0 and x>d, V=V_0 for 0<x<d.

Figure 2.6: Nanosurf EasyScan2 STM.

2.2.3 Atomic Force Microscopy

Atomic Force Microscope (AFM) was invented in 1986 by Gerd Binning, Calvin Quate and Christoph Gerber to examine the non-conductive samples at nano-scale [1]. AFM consists of a cantilever with a sharp tip, which is used to probe the surface. Briefly, AFM visualizes topography of the surface at nanoscale by measuring forces between the tip and the sample.

The operational principle of AFM is quite straight forward. When the tip approaches to the surface about 50 nm, surface and tip starts interacting through Van der Waals interaction. This attractive force between the tip and the sample bends the cantilever at a detectable amount. This deflection on the cantilever is measured using an optical system. A laser beam is shined on the reflective cantilever surface at its initial, relaxed position. The reflected laser beam, from the cantilever, is aligned to the center of a position sensitive photodiode (Figure 2.7). When the interaction between

tip and sample bends the cantilever, reflected laser beam changes its position on photodiode. Change in the position of the reflected laser beam on photodiode let us calculate how much the cantilever is deflected. The amount of the force between the tip and the sample depends on the distance between them and the spring constant of the cantilever (the cantilever acts as a spring).

The force defined by Hooke's Law **(2.2)**:

$$F = - k.x \qquad \textbf{(2.2)}$$

F: interaction force between the tip and the sample

k: spring constant (the cantilever acts like a spring)

x: deflection of cantilever

There are also other interaction types between the sample and the tip such as mechanical contact force, electrostatic force and magnetic force. If the distance between the tip and the sample is short, the interactions are Van Der Waals. However, if the distance is long, electrostatic or magnetic forces become important [48,49].

The cantilever is generally made of silicon(Si), silicon oxide(SiO_2) or silicon nitride(Si_3N_4). Cantilever length, material and shape change the spring constant and the resonant frequency. The tips can be coated different materials for other applications such as magnetic force microscopy (MFM) and electrostatic force microscopy (EFM).

There are three types of imaging modes in AFM; contact mode, tapping mode and non-contact mode (Figure 2.8).

Contact mode AFM: When the height of the tip from the surface is more than ~50nm, there is no attractive force on the tip and the tip stays on relaxed position. When the distance between the tip and the surface is less than ~50 nm, Van der Waals interaction bends the tip towards the surface. At a critical point the cantilever bends very much and touches the surface of the sample and cannot relax to its initial position. The tip is in contact with surface and surface structure is imaged by scanning any area on the surface and feedback mechanism keeps the deflection of the cantilever constant. For the contact mode AFM, the spring constant or stiffness constant must be less than the surface. This means when the tip touches the surface

very gently, cantilever should be able to bend upward without damaging the surface even at the atomic level.

The deflection on the cantilever is kept constant by z-piezo, which is perpendicular to the sample surface. Z-piezo is directly controlled by the feedback mechanism. The position sensitive photodiode measures the deflection on the cantilever and informs the feedback electronics about the deflection. Feedback electronics apply a voltage to the z-piezo to keep the laser spot in the center of the detector. The z-piezo voltage is plotted for each x and y coordinates on the surface to obtain the surface topography. When feedback mechanism is closed (active), system always measures the deflection of the cantilever and controls the z piezo.

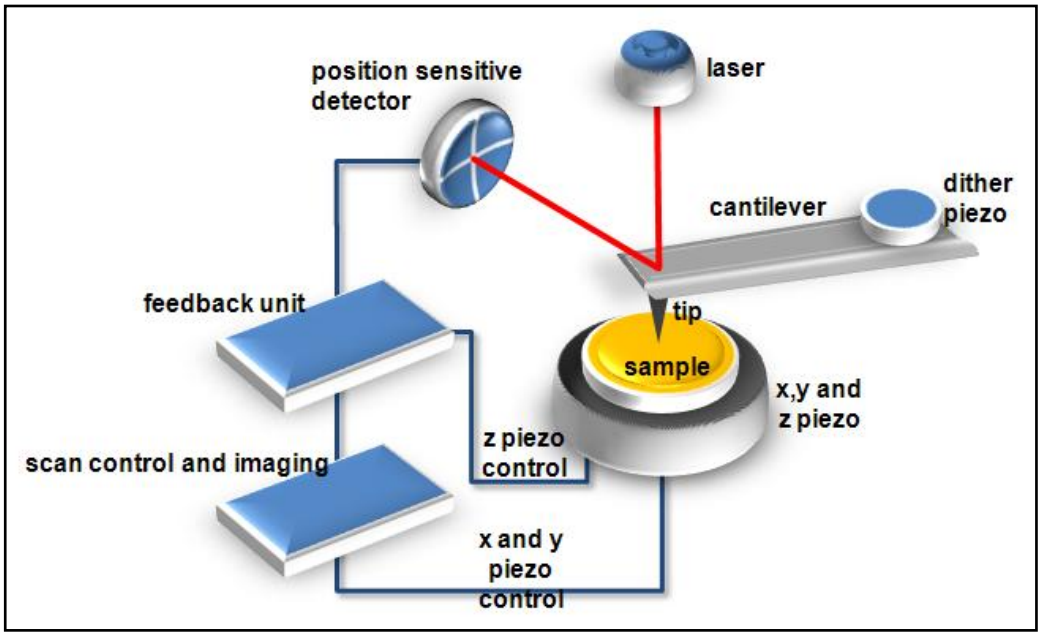

Figure 2.7: The Schematic of Atomic Force Microscope.

Non-contact mode AFM: The tip does not touch to the surface during the scan, but the tip is very close to the surface. The z-piezo voltage is modulated to make the tip vibrate at its resonant frequency f_0. f_0 is mostly between 10 – 100 kHz as the tip approaches to the surface. This oscillation on the cantilever generates an oscillating signal on the photodiode. When the tip is scanning the surface, it can approach or retract from the surface and this shifts the frequency of oscillation by amount of Δf. Δf can be calculated as **(2.3)**.

Tapping mode AFM: In the tapping mode, the tip is periodically in contact with the surface (slightly taps on the surface). The principle is very similar to non-contact

mode but in the tapping mode each time the cantilever goes downwards, tip touches the surface very gently. Tip is oscillated on z-axis upward and downward and tip touches the sample and releases. The oscillation measured on the photodiode as an oscillating signal. During the scan oscillation frequency changes with respect to the surface topography but feedback mechanism keeps the frequency constant by applying a voltage to the z-piezo, the tip-sample interaction is maintained and surface topography is obtained.

$$\Delta f = f_0 \frac{1}{2k} \frac{df}{dz} \qquad \textbf{(2.3)}$$

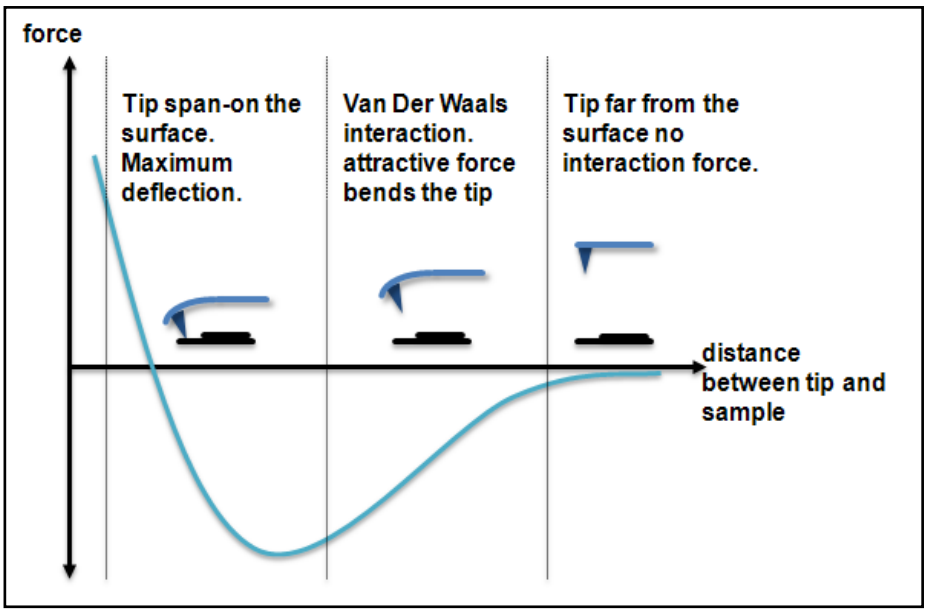

Figure 2.8: Forces vs cantilever bending on AFM.

SPM-9500J3 SHIMADZU and Nanomagnetics Instruments AFM were used in tapping mode during whole AFM measurements. The type of cantilevers were silicon "Tap300 Al-G".

2.2.4 Micro Raman Spectroscopy

In 1928, Sir Chandrasekhra Venkata Raman discovered a new phenomenon using the sunlight as a light source and his eyes as a detector, which turned into one of the most important material characterization method [51]. Raman spectroscopy is used to study vibrational, rotational and other low-frequency modes in a system. In many Raman spectroscopy systems, a laser beam at a certain wavelength is sent to a sample and scattered light and its wavelength are investigated with an optical system.

Laser at a fixed wavelength is used as monochromated light source. Optical system consists of lenses to collect the light scattered from sample, monochromator to measure the wavelength and a detector to observed the power of the scattered light (Figure 2.9).

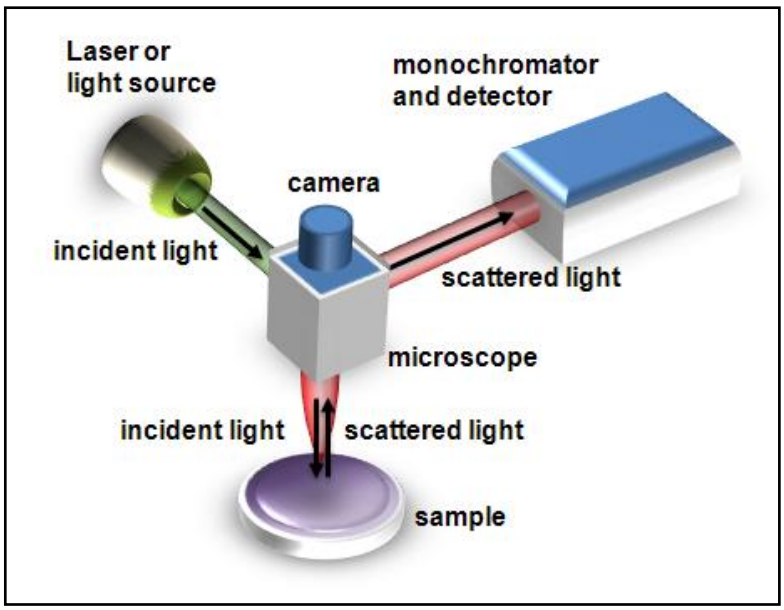

Figure 2.9: The Schematic of Micro Raman Spectroscopy.

Main principle behind the Raman spectroscopy is the inelastic scattering of monochromatic light. When the sample material is hit by photons, it can absorb the photon, gain energy and be exited to an upper vibrational energy state. When the sample material relaxes back to its initial energetic state and it loses energy. This energy loss can emit photon. If this emitted photon has a lower energy and higher wavelength, this is called as stokes Raman scattering. In opposite cases it is called as anti-stokes Raman scattering.

In Raman spectroscopy, the energy difference between incident and emitted light is not expressed with spectral wavelength. Wavelength is converted into wave numbers and Raman shift is calculated by subtracting the excitation wave number from scattered wave number **(2.4)**.

$$\text{Raman Shift: } \Delta\omega = \left(\frac{1}{\lambda_0} - \frac{1}{\lambda_1}\right) \times 10^7 \left(\frac{nm}{cm}\right) \qquad \textbf{(2.4)}$$

If the investigated sample or surface is in micrometer scale, this type of Raman spectroscopy is called as Micro Raman Spectroscopy [50-52]. Micro Raman

Spectroscopy is quite valuable in the characterization of graphene and graphitic structures [53].

2.3 Common Substrates

2.3.1 Highly Oriented Pyrolytic Graphite

Highly Oriented (or Ordered) Pyrolytic Graphite (HOPG) is a very common substrate in surface studies. HOPG consists of stacked two-dimensional (2D) sheets of carbon atoms, which are arranged in a hexagonal lattice. In each layer, an atom is bonded to three nearest neighbor carbon atoms at 0.142 nm. The distance between the layers is 0.335 nm (Figure 2.10).

The layers of graphite are not bonded tightly to one another, however carbon atoms of each layer are bonded very tightly to each other.

HOPG is a hydrophobic, smooth and inert surface that is why it is preferred in experimental studies and especially in surface science under ambient conditions. Moreover, it can be easily cleaned using mechanical exfoliation method (separation of the layers by scotch tape).

The atomic parameters (interatomic and between the layers distance) of HOPG are well known, so it is used as a common calibration sample in STM and AFM studies.

2.3.2 Mica and Gold-Coated Mica

Mica is a very useful substrate for atomic force microscopy studies. It is hydrophilic, dielectric and chemically inert surface.

Mica is known as group of sheet silicate minerals and its chemical formula is $K_2O.Al_2O_3.SiO_2$. Mica is composed of stacked mica sheets and they can be cleaved into layers. Therefore, the most important characteristic of mica is its ability to cleave almost perfectly (Figure 2.11).

Mica sheets can be coated by gold, using thermal vacuum evaporator. Pure gold is thermally evaporated under 10^{-5}-10^{-6} mbar pressure in vacuum system and the mica sheets are coated by pure gold.

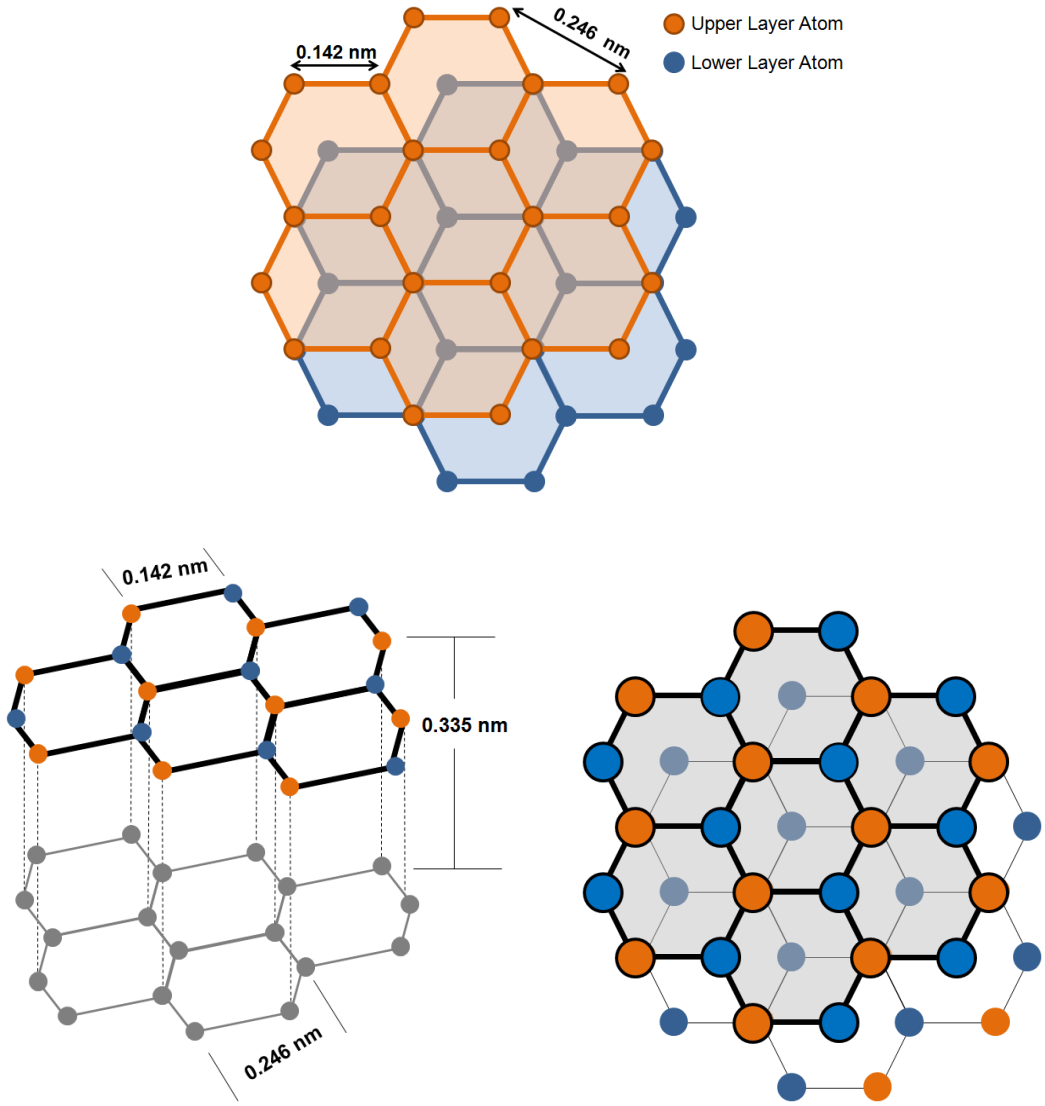

Figure 2.10: Highly Oriented Pyrolytic Graphite (HOPG).

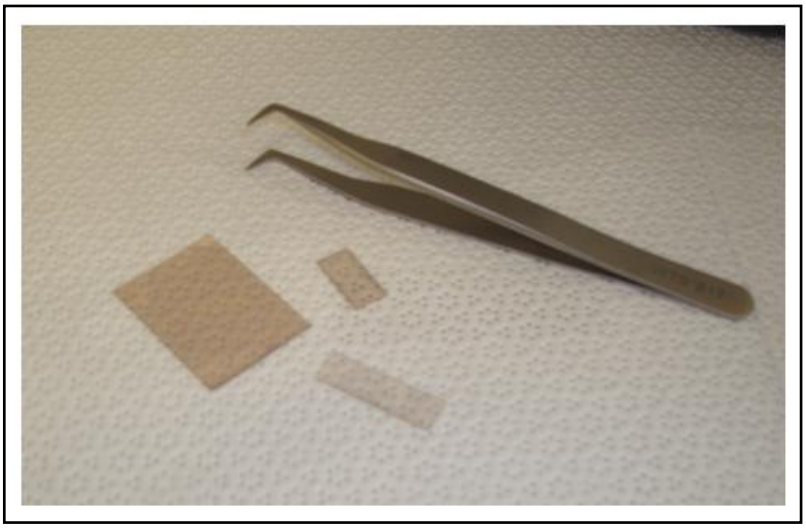

Figure 2.11: Mica sheets.

2.3.3 Silicon (Si) and Silicon Dioxide (SiO_2)

Silicon and silicon dioxide are used as substrates for drop casting of liquid samples on to them or thermal evaporation of gold. These substrates are cleaned with 2-propanol, methanol and ethanol and they can be used repetitively (Figure 2.12).

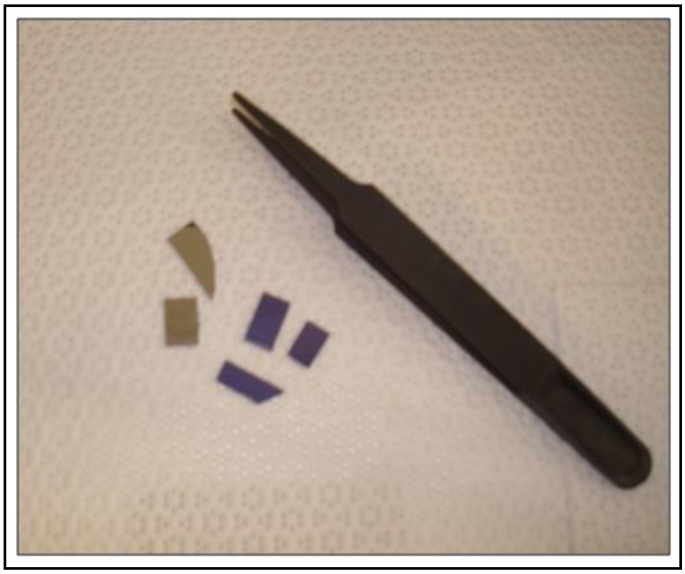

Figure 2.12: Silicon (Si) and Silicon Oxide (SiO_2) wafers.

In most of the studies, thickness of oxide of SiO_2 is important. For instance, in the optical investigation of graphene flakes, the thickness of oxide of SiO_2 should be about 290nm. Because monolayer of graphene is well distinguishable with optical microscope on 290nm oxidized silicon substrate as clearly reported in the literature [25].

3. INVESTIGATION OF T7 PRIMER MOLECULES, TRIS- EDTA BUFFER SOLUTION AND TRIS-HCl SOLUTION

3.1 Literature Review

Investigation of biomolecules with scanning probe techniques started by the end of 1980s. Especially, the atomic force microscopy has become an effective tool for investigating biomolecules since its invention in 1986 [1]. DNA, which plays an important role in molecular biology, is extensively studied using AFM. The investigation includes DNA morphology and DNA interaction with other molecules or materials, which broadens understanding of life processes and mechanisms [54]. The key point is immobilizing DNA when imaging DNA by AFM. Many types of DNA molecules, such as double or single stranded [4], long or short [6] and plasmid, have been studied by atomic force microscopy [12,13,55] and scanning tunneling microscopy [5],[10].

For imaging DNA molecules by scanning probe microscopy, strands and length of DNA are important parameters. Moreover, buffer solution which is used to stabilize the biomolecules is also important [12]. Until now, many types of DNA molecules or nucleotides were investigated, which were suspended in the various buffer solutions and drop casted on substrates [6]. However, the effects of buffer solutions on the surface were almost completely ignored.

In this section, investigation of T7 Primer molecules and the effects of buffer solution of these molecules on solid substrates using scanning probe techniques will be discussed.

T7 Primer, which is known as T7 Phage Promoter Primer, is a type of DNA molecule and it has a particular nucleotide sequence. In this study, T7 Primer has the following nucleotide sequence: 5’d(TAATACGACTCACTATAGGG)3’. T7 Primer was supplied in TE buffer solution. The main components of TE buffer are Tris and EDTA (figure 3.1).

Tris, known as tris(hydroxymethyl)aminomethane with the formula $(HOCH_2)_3CNH_2$ or $C_4H_{11}NO_3$, provides the necessary pH level to maintain biomolecules and micro-organisms. EDTA is a molecule that chelates metal ions and abridgement of a polyamino carboxylic acid known as ethylenediaminetetraacetic acid, with the formula $C_{10}H_{16}N_2O_8$ (Figure 3.1).

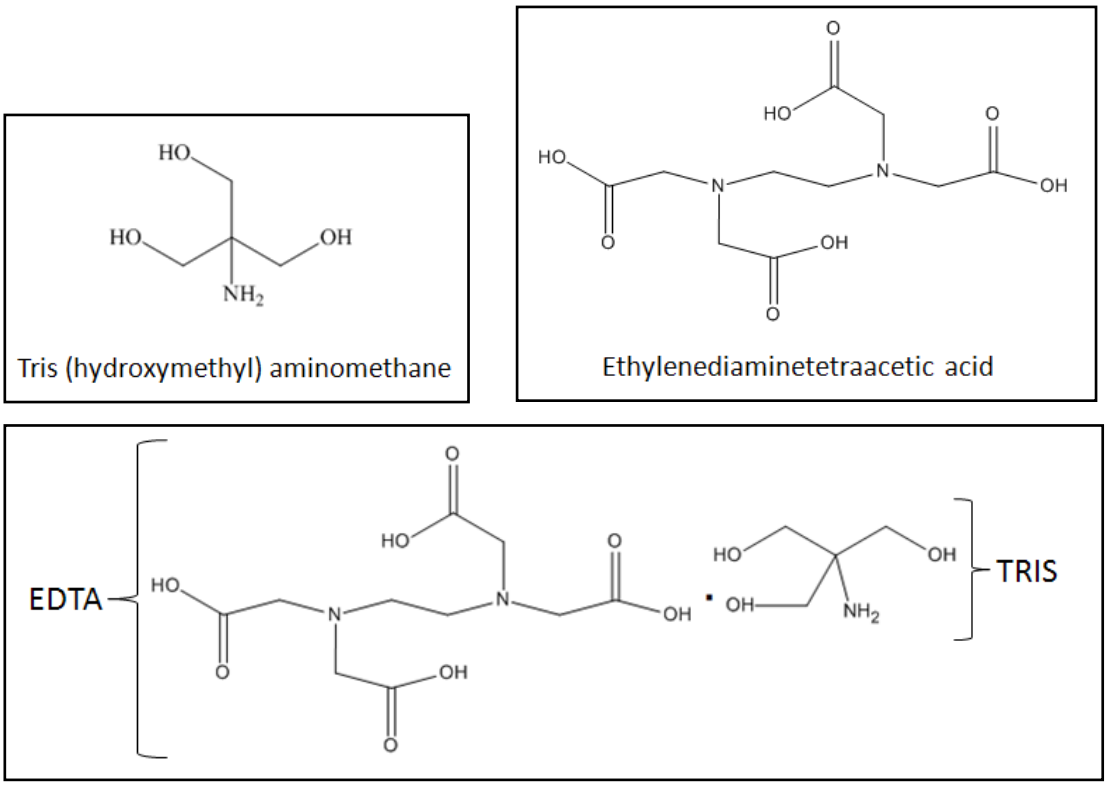

Figure 3.1: Chemical Formula of Tris, EDTA and Tris-EDTA.

Tris and its pH balancing feature was applied by G.Gomori, for the first time, in 1946 [56]. Its crystallization property and molecular structure were determined in 1978 [57]. One of the most important feature of Tris is to be found in two phases; crystalline phase and plastic phase [57, 58]. Under ambient conditions, Tris crystallizes in the orthorhombic lattice, however above 134^0C the structure changes to the orientationally disordered base centered cubic lattice [57]. Tris has been used in medicine and solar cell systems as an organic thermal energy storage material [59,60] . The vibrational spectra, the polarized and high pressure Raman spectra of Tris were observed [61,62] , and Tris was also characterized in the far-infrared [60]. Moreover, EDTA was used for chelating metal ions in many biological and chemical studies. Despite these important applications and characterizations, investigation of

Tris itself and its compounds, such as Tris-HCl (figure 3.2) and Tris-EDTA, on solid substrates by using scanning probe microscopy techniques are very poor. H.Wang et al. showed the effects of Tris-EDTA buffer on hydrophobic and hydrophilic surfaces using AFM. TE buffer solution, which is used in their study, was consisted of Tris-HCl, NaCl and EDTA. This TE buffer solution creates self-organized parallel nanofilaments on HOPG surface [12]. TE buffer may contain different components according to the desired pH, such as ddH_2O, HCl, NaCl, $MgCl_2$ etc. In experiments, which will be discussed in this chapter, TE buffer consists of Tris, EDTA, HCl and ddH_2O.

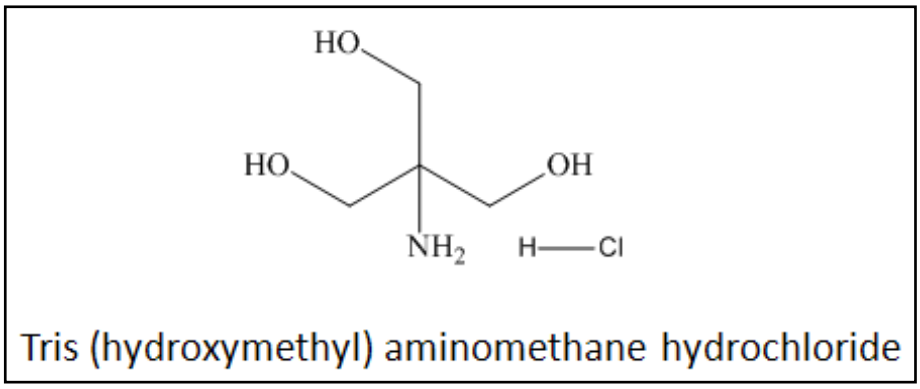

Figure 3.2: Chemical formula of Tris-HCl.

3.2 Experiments

In this study, T7 Primer was used, which has the following nucleotide sequence: 5'd(TAATACGACTCACTATAGGG)3'. T7 Primers were supplied in TE buffer solution. The amount of the solution is 50µl, Tris-EDTA as the buffer, with pH 7.5. Its density is 1picomole/µl. 1µl of the solution contains 1.514 x 10^{12} T7 Primer molecules (see Appendix A.1).

The solution was diluted by 1/100 with ddH_2O. 1µl from this solution was taken with a micropipette and carefully drop casted on HOPG surface at room temperature. Then, the sample was placed in a desiccator to dry. This sample, which was coded as Sample 152, is shown in figure 3.3. In figure 3.3(a) optical microscope image of the sample is shown. Figure 3.3(b) and 3.3(c) are AFM images of the sample. Spherically symmetric structures are observed and HOPG steps can be distinguished in figure 3.3(b). Not only spherically symmetric structures, but also solution effects are plainly observed on the surface, in figure 3.3(c).

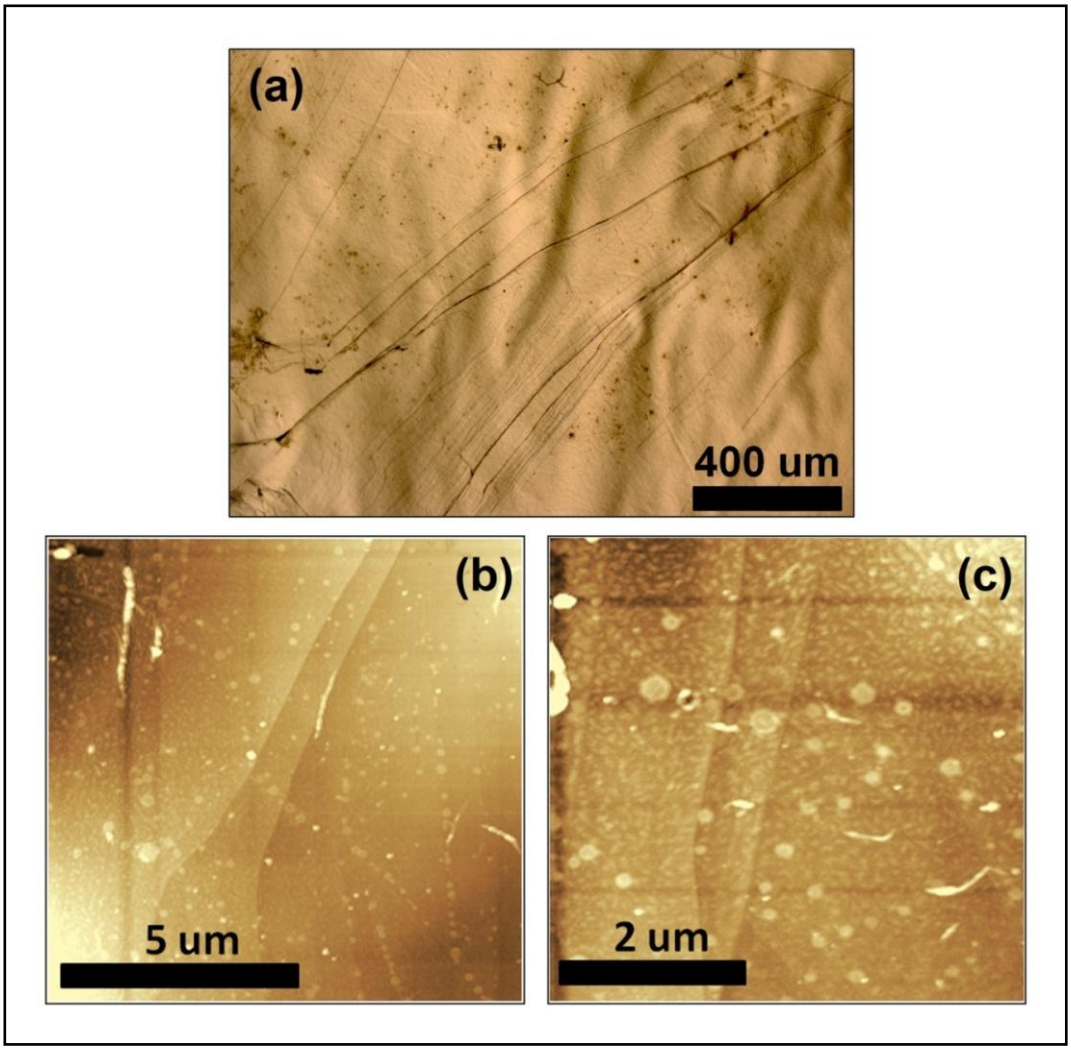

Figure 3.3: Sample 152, the solution with T7 Primer molecules drop casted on HOPG surface. (a) is an optical microscope image of the sample, (b) and (c) are AFM images of the sample. Scan area of (b) is 10µmX10µm, (c) is 5µmX5µm, scan rate is 1Hz for both.

Another sample, which was coded as Sample 153, was prepared with the same method on HOPG surface and it is shown in figure 3.4. However, different results were obtained. The optical microscope image of Sample 153 is shown in figure 3.4(a). AFM images are shown in 3.4(b) and 3.4(c). From the AFM images of this sample, a film formation is observed on the surface and this film seems to be cracked in some areas. The height of a crack structure, which is marked in 3.4(c) and shown in 3.4(d), is ~5 nm.

Sample 162, its AFM images are shown in figure 3.5. This sample was prepared with the same method on HOPG surface. In figure 3.5, HOPG steps are distinguishable and the surface seems to be coated with a different film formation.

Sample 166 was prepared with the same method on HOPG surface. In figure 3.6, AFM images of the sample are shown. Here, the film structure formed differently.

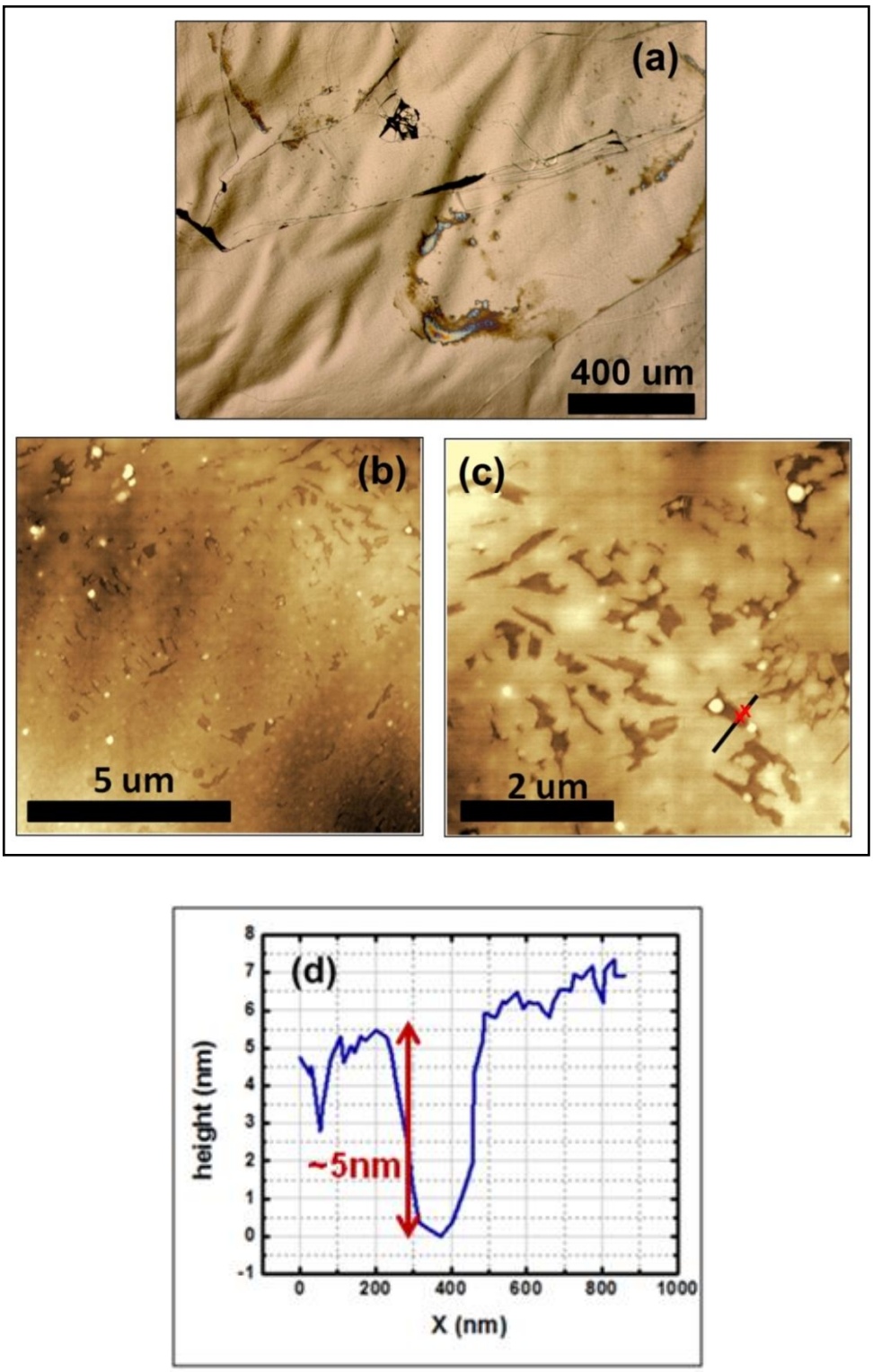

Figure 3.4: Sample 153, the solution with T7 Primer molecules drop casted on HOPG surface. (a) is optical microscope image, (b) and (c) are AFM images. Scan area of image (b) is 10µmX10µm, image (c) is 5µmX5µm, scan rate is 1Hz for both. (d) is height of a crack as marked in (c), ~5nm.

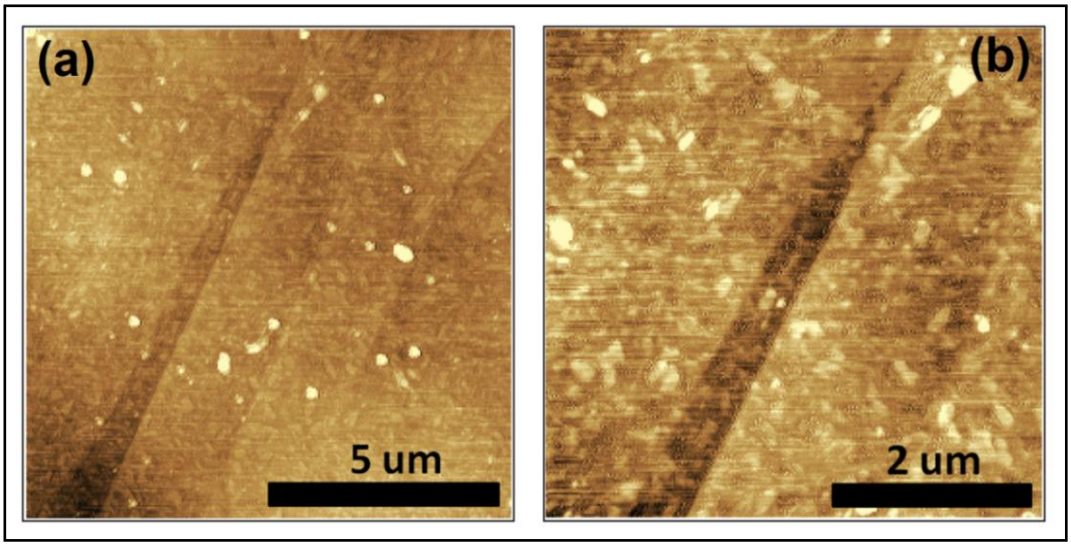

Figure 3.5: Sample 162, the solution with T7 Primer molecules drop casted on HOPG surface. Scan area of image (a) is 10µmX10µm, image (b) is 5µmX5µm. Scan rate is 1Hz for both.

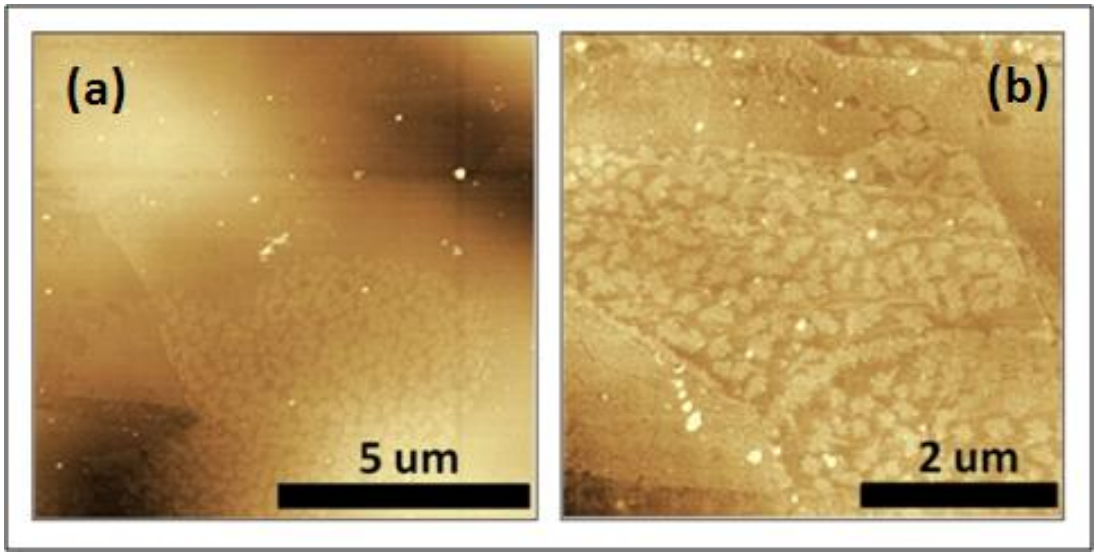

Figure 3.6: Sample 166, the solution with T7 Primer molecules drop casted on HOPG. Scan area of image (a) is 10µmX10µm, image (b) 5µmX5µm, scan rate is 1Hz for both.

The results have shown many types of film formations (figure 3.7) on the HOPG surface using the same solution and same preparation method. According to these results, it can clearly be stated that: "The identification of T7 Primer molecules is not possible when T7 Primer molecules are kept in TE buffer and drop casted directly on HOPG surface without further treatment". Since the solution does not contain any material other than T7 Primer molecules and TE buffer, we can also state that we mainly observe the effect of the buffer solution on the surface.

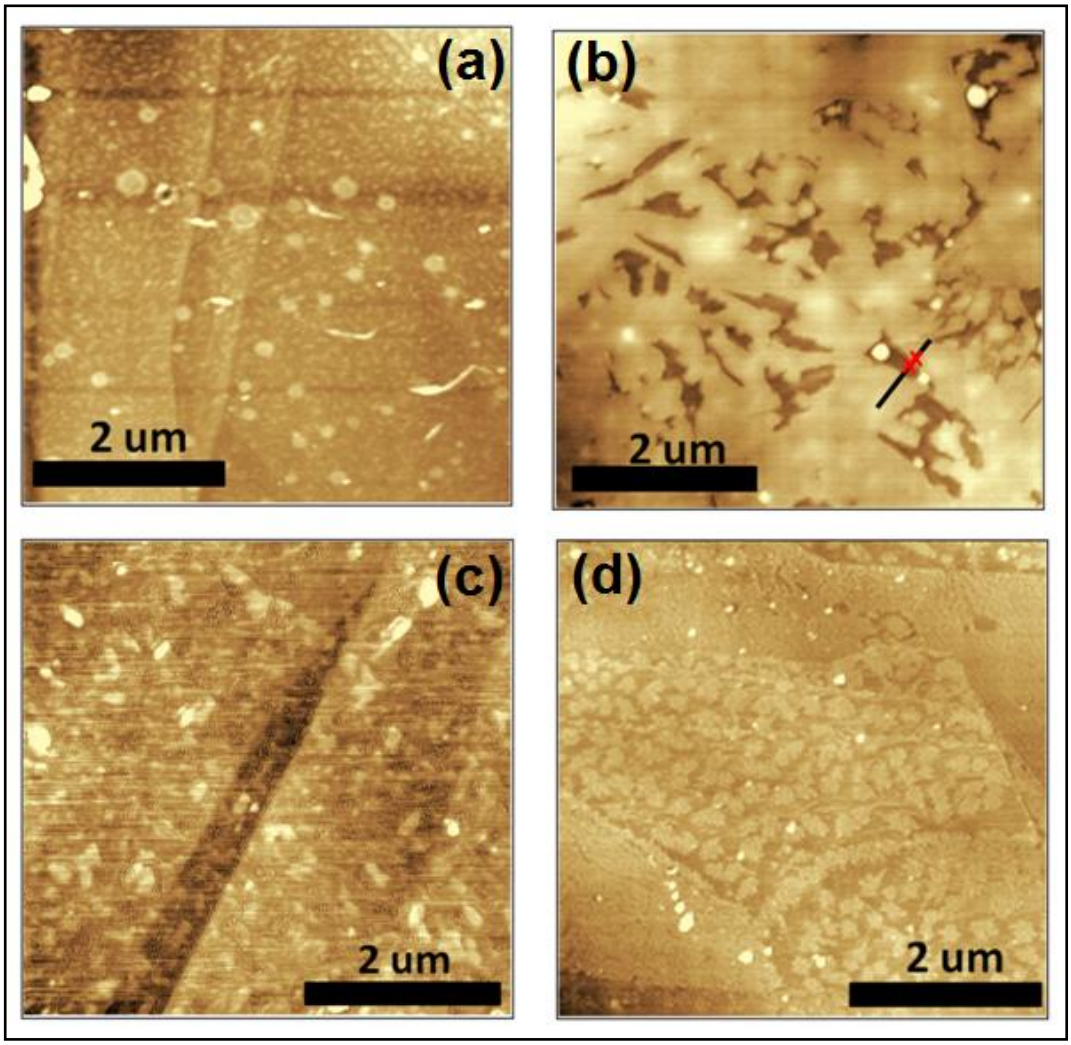

Figure 3.7: Different types of film formations on HOPG surface, using the same sample preparation method. (a) Sample 152, (b) Sample 153, (c) Sample 162, (d) Sample 166.

Since the identification of T7 Primer molecules was not possible, we started investigating TE buffer solution itself. Here, the aim was to examine the effects of Tris-EDTA buffer on solid substrates with no T7 Primer molecules in the buffer.

As in the investigation of T7 Primer molecules described above, 1µl from 1M Tris-EDTA buffer solution was taken with the micropipette and it was carefully drop casted on HOPG surface at room temperature. Then, the sample was placed in the desiccator to dry. This sample was coded as Sample 176 and investigated by optical microscope and atomic force microscope as it is seen in figure 3.8 and figure 3.9. In figure 3.8, AFM image 3.8(b) show that quite large hexagonal nanostructures. The height of them as in image figure 3.8(c) is ~380nm. The hexagonal structures are even observable in optical microscope as in figure 3.8(a).

AFM images of different part of Sample 176 are shown in figure 3.9. Different size hexagonal structures are observed and the height of them is ~300nm.

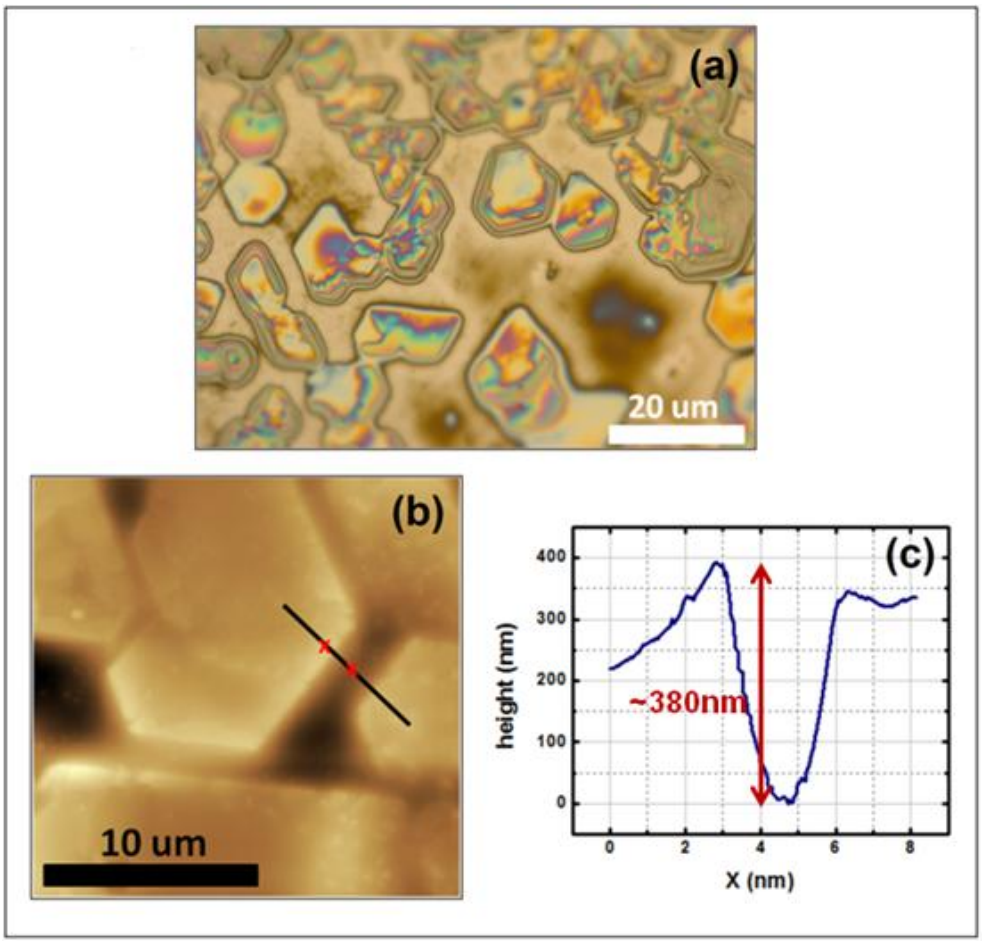

Figure 3.8: Sample 176, Tris-EDTA buffer solution on HOPG surface. (a) is an optical microscope image of the sample, (b) is an AFM image of the sample. Scan area of (b) 20µmX20µm, image. The scan rate is 1Hz. The height of a hexagonal structure is ~380nm as shown in (c).

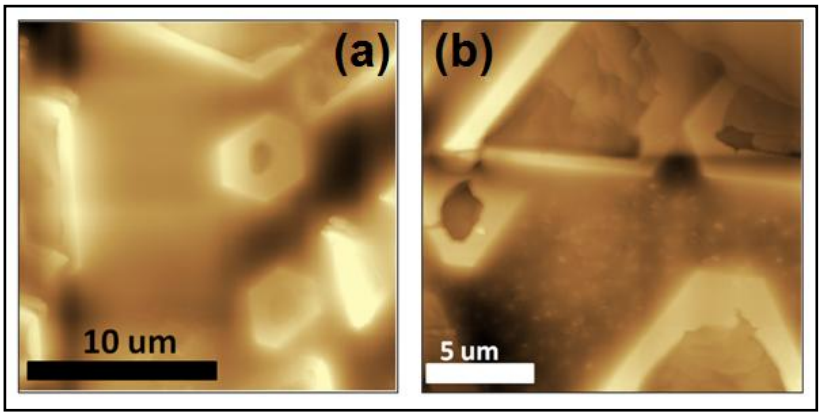

Figure 3.9: AFM images of different part of Sample 176. Scan size of (a) is 20µmX20µm, (b) is 18.38µmX18.38µm. Scan rate is 1Hz for both.

Moreover, Sample 184 was prepared with the same method on Si(001) and the hexagonal structures are also observed as shown in figure 3.10 but, the structures are more adjacent to each other and the hexagons appeared vaguely.

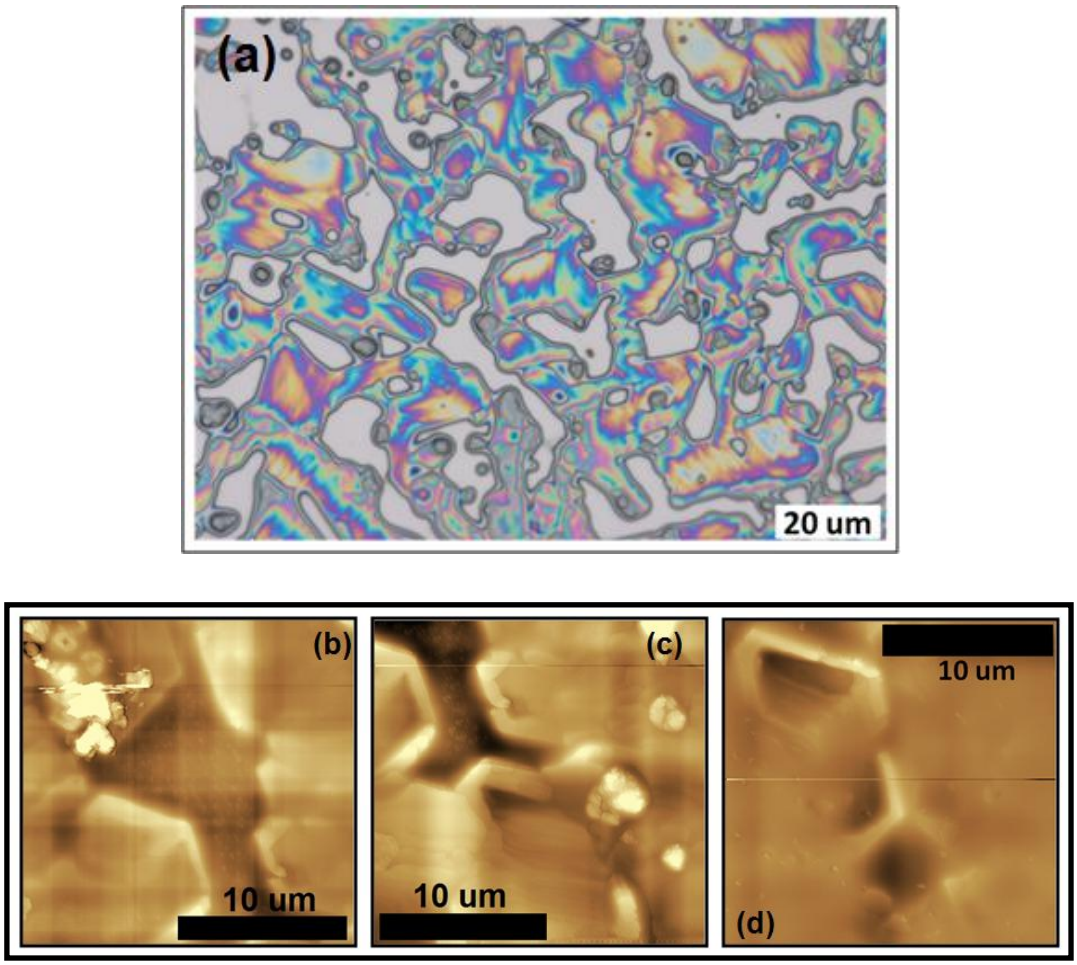

Figure 3.10: Sample 184, TE buffer solution on Si(001) surface. Optical microscopy images and AFM images showed the hexagonal structures. Height of them ~370 nm. Scan size of (b), (c) and (d) are 20µmX20µm. Scan rate is 1Hz for both.

Using the same method, different samples were prepared on HOPG surface and Si(001) surface. However, each sample showed different results and the hexagonal structures could not be observed when using drop casting method of Tris-EDTA buffer solution. AFM images of some of the samples, which were prepared with the same method, are shown in figure 3.11.

Therefore, to understand these results the components of Tris-EDTA were investigated on solid substrates. Tris-EDTA buffer composed of Tris, EDTA, HCl (to adjust the pH of solution) and ddH_2O water (Merck Water for chromatography LiChrosolv®). First, Tris-HCl solution was investigated on HOPG surface using

drop casting method (for preparing Tris-HCl solution see Appendix A.2). 1µl from 1M, pH 7.2 Tris-HCl solution was taken with the micropipette and it was carefully drop casted on HOPG surface at room temperature. Then, the sample was placed in the desiccator to dry. This sample was coded as Sample 235.

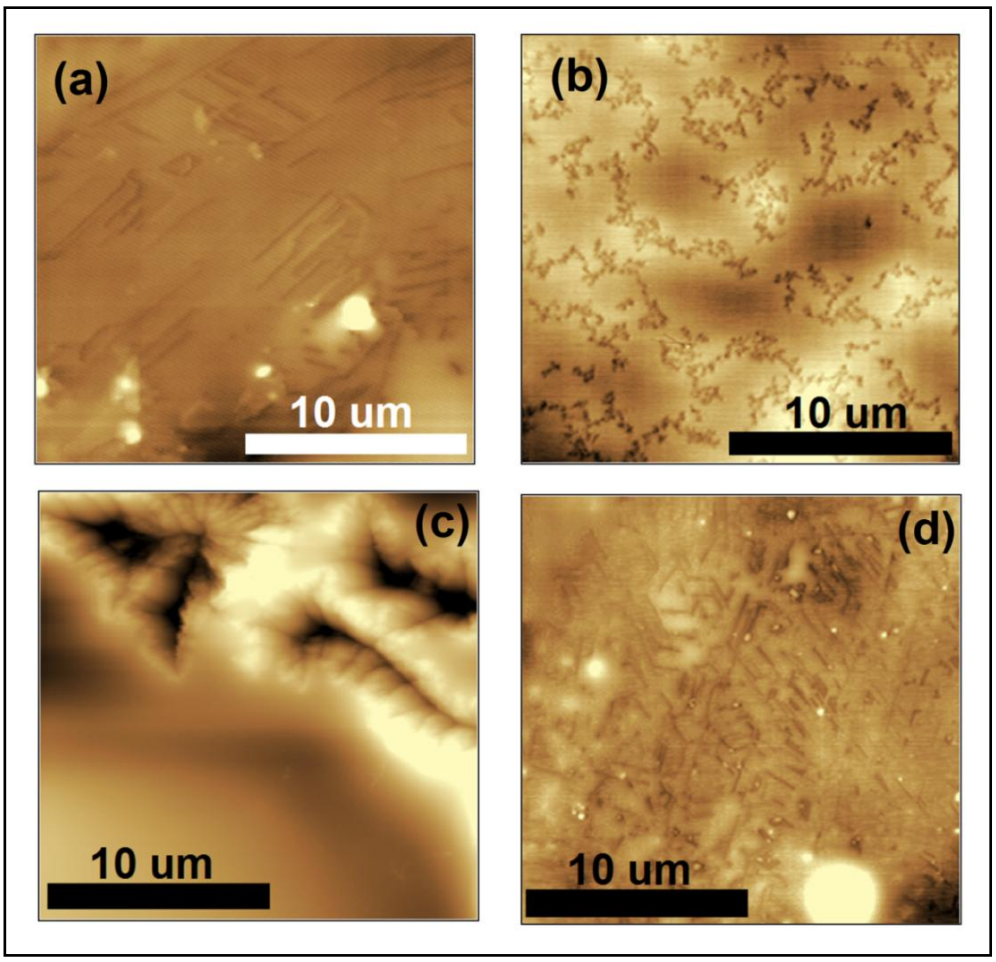

Figure 3.11 : Despite preparing with the same method, different film structures are observed on HOPG surface. (a) Sample 198, (b) Sample 201, (c) Sample 204, (d) Sample 208. Scan area of image (a), (b), (c) and (d) 20µmX20µm, scan rate is 1Hz for all.

The effect of Tris-HCl was quite interesting on the surface, as shown in optical microscope image (figure 3.12). There were very high structures on HOPG surface and they could not be observed with AFM because of the surface roughness.

Afterwards, 1µl Merck Water (Merck Water for chromatography LiChrosolv®) was taken with micropipette and it was carefully dropped on Sample 235, then the liquid on the surface was dragged with gold-coated mica and gently pulled. The method is described in figure 3.13. We call this method as "drop cast-drag-pull method". The

purpose of performing this method is reduce the roughness on the Sample 235. The reason to use gold-coated mica is its lightness in weight and the inertness of the Au surface. It is easy to use it when applying the drag and pull method. Si(001), SiO_2 or glass were not convenient for the drag and pull method. For instance, if silicon is used for dragging the liquid on the HOPG surface, the HOPG and silicon surfaces sticks to each other and silicon wafer cannot be gently pulled. So, hexagonal structures were not observed both on HOPG and silicon surfaces.

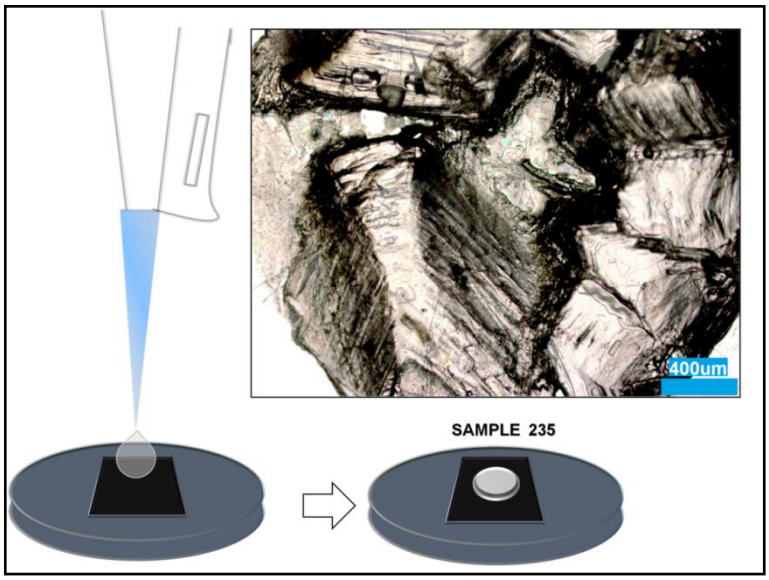

Figure 3.12: Preparation method and optical microscope image of Sample 235, Tris-HCl solution on HOPG surface.

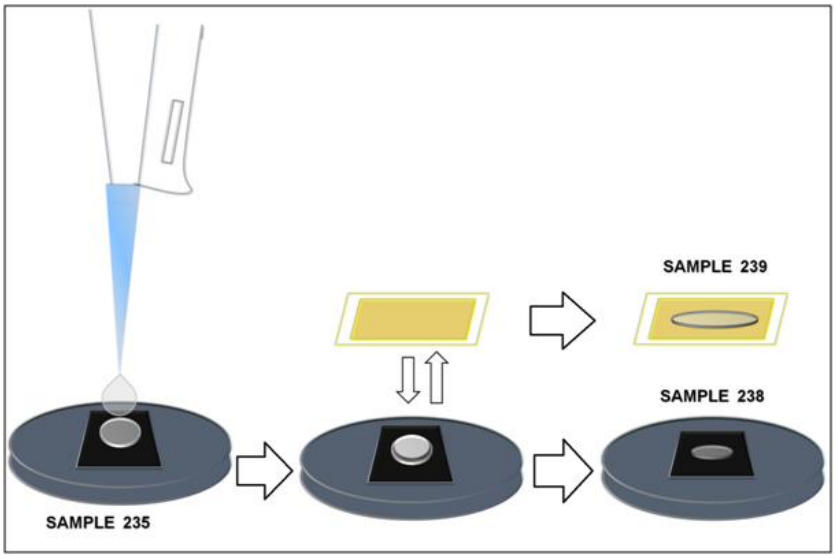

Figure 3.13: Preparation method of Sample 238 (the HOPG part after drop cast-drag-pull method) and Sample 239 (the gold-coated mica part after drop cast-drag-pull method).

After drop cast-drag-pull method, the sample was coded as Sample 238, gold-coated mica sample was coded as Sample 239. AFM images of these samples are shown in figure 3.14 and figure 3.15.

Figure 3.14(a) and (b) show that there are not hexagonal structures in HOPG part. However, the hexagonal structures occurred on gold-coated mica part as shown in figure 3.15.

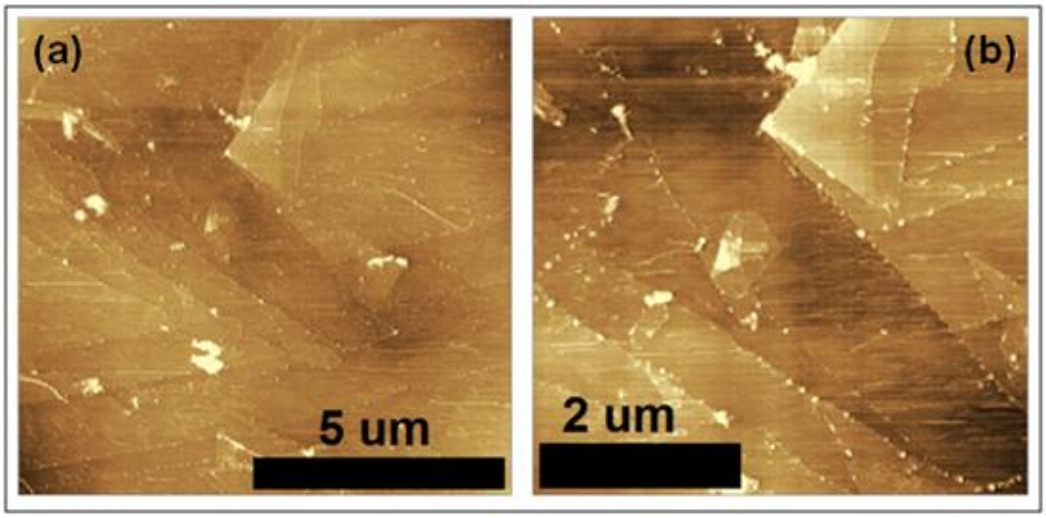

Figure 3.14: AFM images of the HOPG part (Sample 238) after drop cast-drag-pull method. Scan size of (a) is 10µmX10µm, (b) is 5µmX5µm. Scan rate is 1Hz for both.

The details of drag and pull processes are important for observing the hexagonal nanostructures on both HOPG and gold-coated mica surfaces. Because the dragging and pulling methods are applied manually by hand and adjustment of the methods can change. Moreover, surface properties such as hydrophilicity (mica) or hydrophobicity (HOPG) can be important paramaters in formation of hexagonal structures on the surfaces [12]. During the drag-pull process, hydrophilic feature of mica surface was clearly observed with naked eye, gold-coated mica surface draw toward the solution itself. In the experiments, formation of the hexagonal structures is almost not exist on the HOPG surfaces when using drop cast-drag-pull method. This may be from hydrophobic feature of HOPG surface.

Other samples were prepared with the same drop cast-drag-pull method. Figure 3.16 and figure 3.17 show optical microscope images and AFM images of the gold-coated mica part, which are coded as Sample 311 and Sample 312.

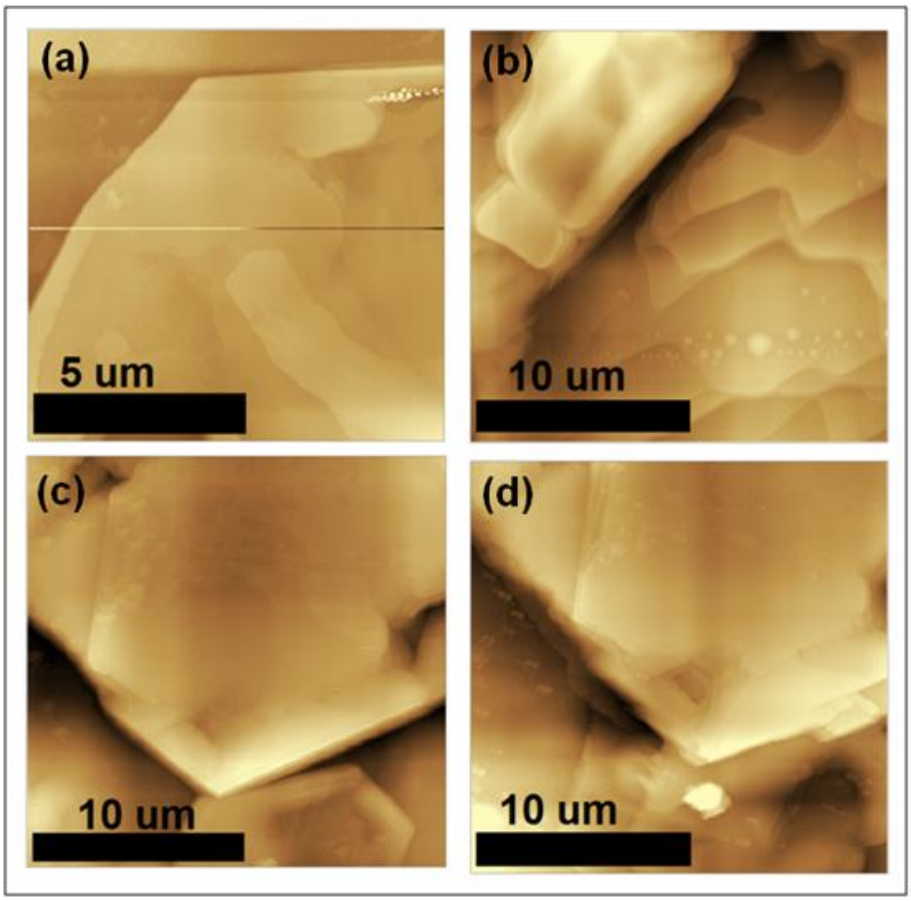

Figure 3.15: AFM images of the gold-coated mica part (Sample 239) after drop cast-drag-pull method. Scan size of (a) is 10µmX10µm, (b), (c) and (d) 20µmX20µm. Scan rate is 1Hz for all.

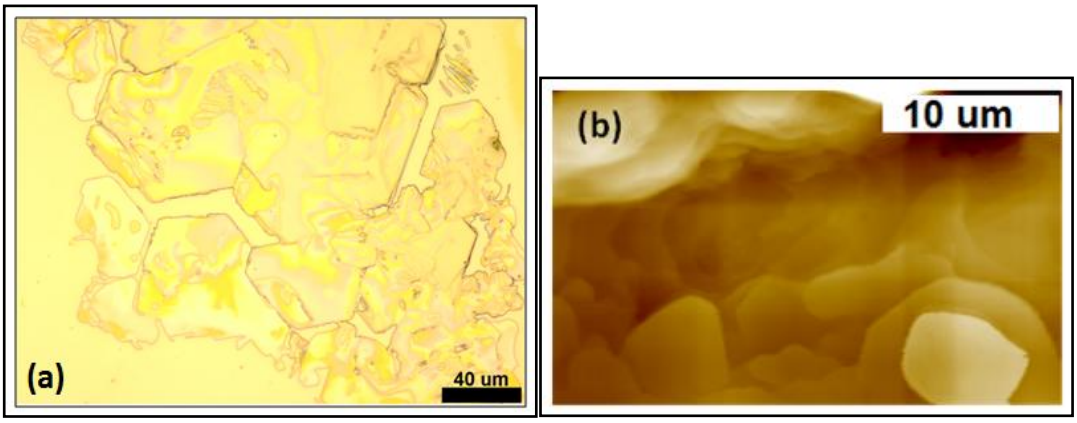

Figure 3.16: (a) Optical microscope and (b) AFM image of the gold-coated mica part, which was coded as Sample 311, after drop cast-drag-pull method. Scan size of (b) is 20µmX30µm, height of the steps changes between 10-20nm.

The hexagonal structures are even observed in the optical image. The AFM image of Sample 311, as shown in figure 3.16(b), showed that the hexagonal structures are not

observed. However, the smooth layers are observed. This is due to the structure of the hexagons and this AFM image might be from different part of a hexagonal structure. Also according to figure 3.17(d), it is clearly stated that, the hexagons are formed by smooth multi-layer structures. Step height of the layers change between 10-20 nm, as shown in figure 3.17(b) and (c).

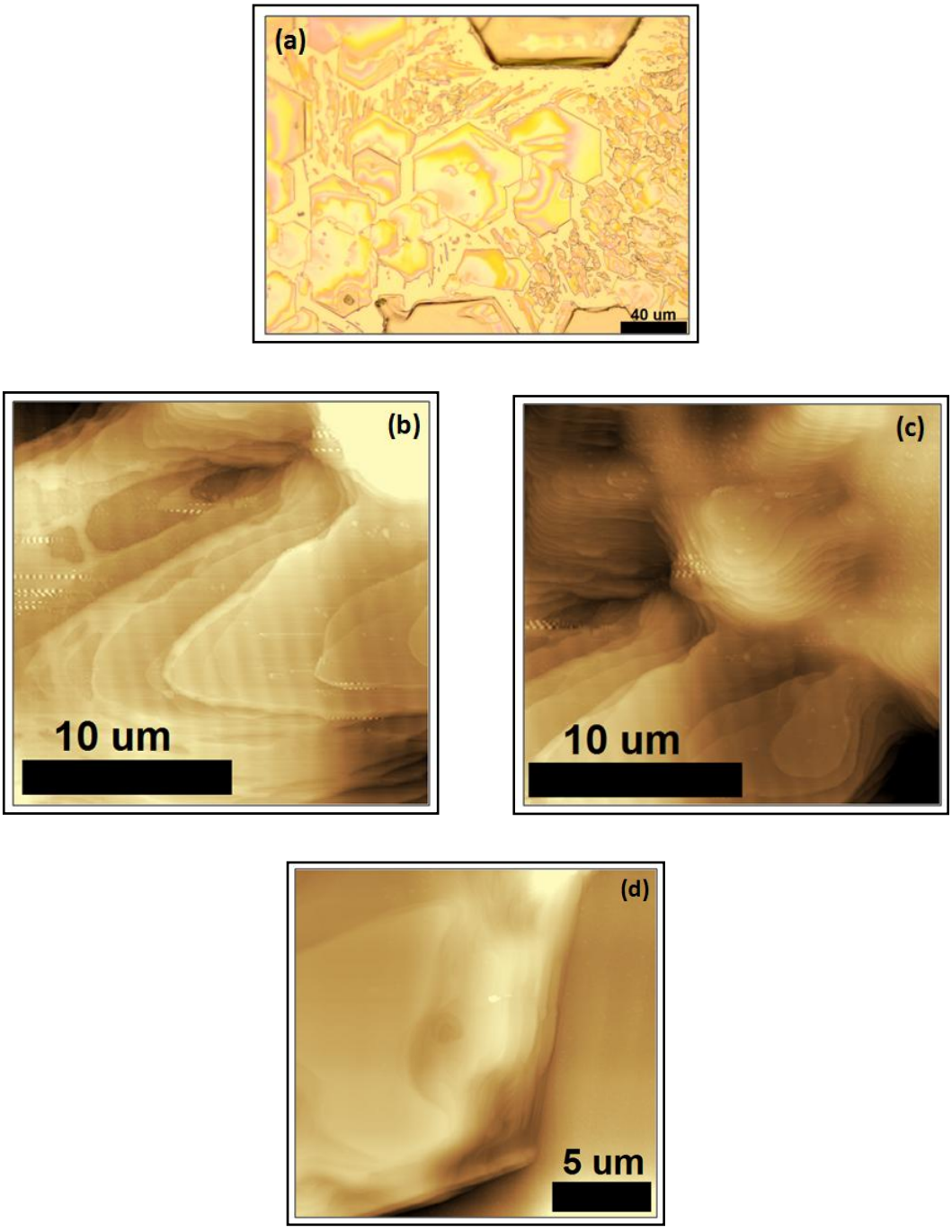

Figure 3.17: Optical microscope and AFM images of the gold-coated mica part after drop cast-drag-pull method, which was coded as Sample 312. Scan size of (b),(c) and (d) is 20µmX20µm. Scan rate is 1Hz. Step height of the layers in (b) is ~15nm.

Following the Tris-HCl investigation, EDTA solution was studied on HOPG surface using drop casting method and drop cast-drag-pull method. In contrast to Tris-HCl, the hexagonal structures could not be observed when EDTA solution was applied on the surface using the same sample preparation methods. As described in figure 3.13, drop cast-drag-pull method applied for EDTA on HOPG surface. There were not remarkable effects on both gold-coated mica and HOPG surfaces. AFM images of bare gold-coated mica, Tris-HCl on gold coated mica after drop cast-drag-pull method, EDTA on gold-coated mica after drop cast-drag-pull method, are shown in figure 3.18.

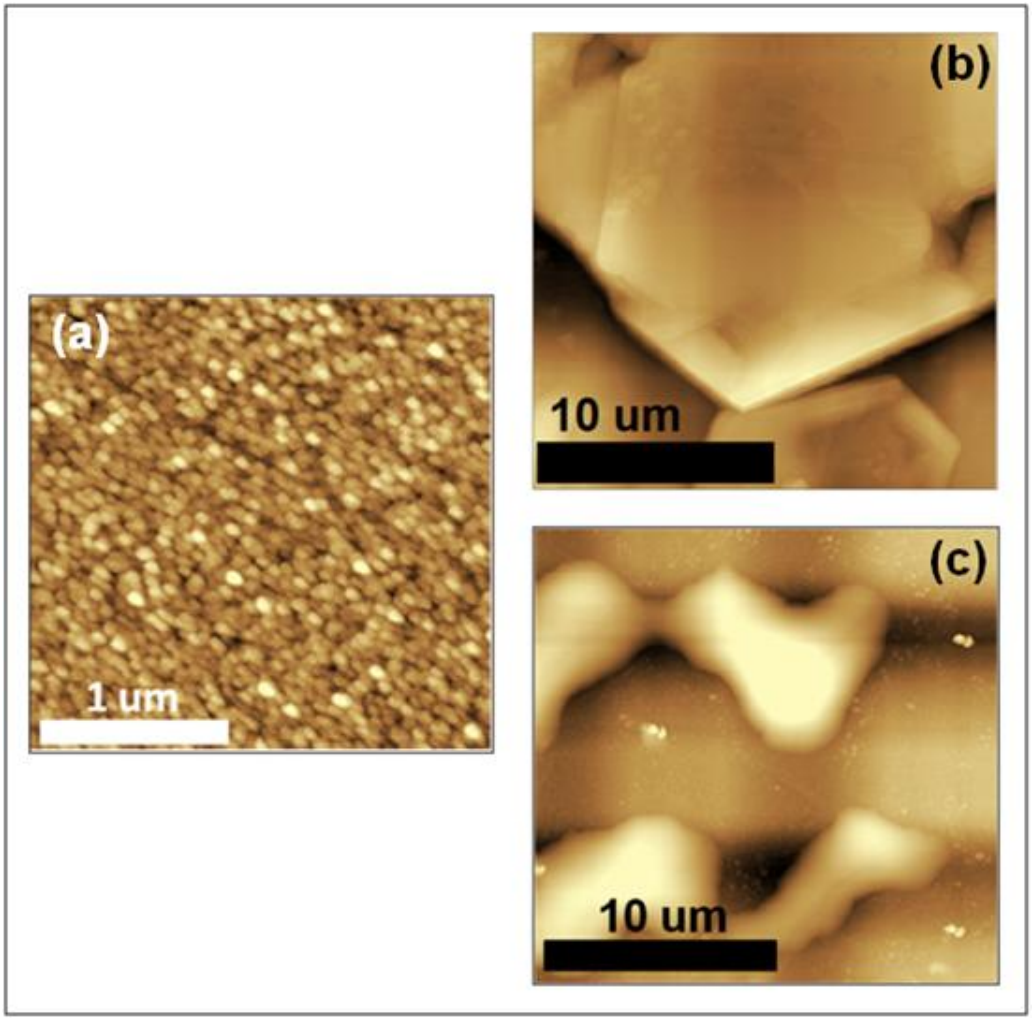

Figure 3.18: (a) AFM image of bare gold-coated mica, scan size is 2.5µmX2.5µm, (b) Tris-HCl on gold-coated mica (after drop cast-drag-pull method), scan size is 20µmX20µm, (c) EDTA on gold-coated mica (after drop cast-drag-pull method), Scan size is 20µmX20µm. Scan rate is 1Hz for all.

The hexagonal structures, which are formed by Tris-HCl solution were observed with AFM. In the experiments, not only commercial Tris-HCl solution, but also 1M

Tris-HCl which was prepared in our laboratory (see Appendix A.2) was used and same results were obtained. Furthermore, Tris-base was dissolved in only ddH_2O water (Merck Water for chromatography LiChrosolv®) without HCl. 1M Tris-water solution was prepared and drop casted on SiO_2 and silicon surfaces and dried in the desiccator. There were not hexagonal structures on both surfaces. The effect of this solution is shown in figure 3.19 with an optical microscope image.

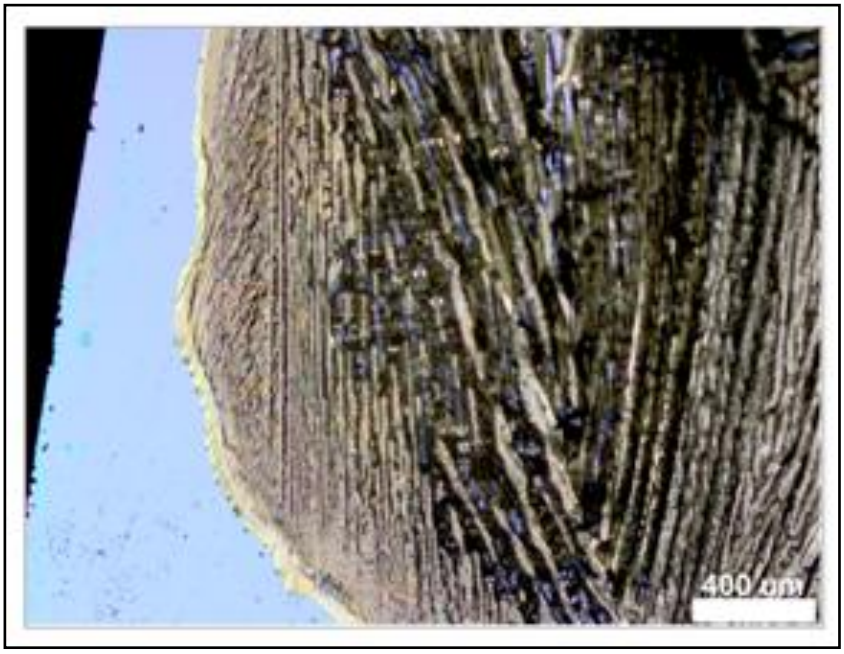

Figure 3.19: Tris-water solution without HCl on SiO_2 surface.

Besides all the experiments reported above, 1M Tris-HCl solution diluted by 1/100 using ddH_2O water (Merck Water chromatography LiChrosolv®) was also investigated. 1µl from this solution was taken with the micropipette and drop casted on Si wafer surface and dried in a desiccator. This sample was coded as Sample 339. The hexagonal structures were observed with dilution method without drop cast-drag-pull method as shown in figure 3.20. (a) is an optical microscope image of the sample without drop cast-drag-pull method. (b) and (c) are AFM images of this sample. The optical microscope images and atomic force microscope images showed that the structures are more adjacent to each other as before shown in figure 3.10 and the hexagons appeared vaguely.

Using the same sample preparation technique, 1M Tris-HCl solution diluted by 1/100 using ddH_2O water drop casted on HOPG surface. This sample was coded as

Sample 343. The hexagonal structures were observed without drag-pull method as shown in figure 3.21.

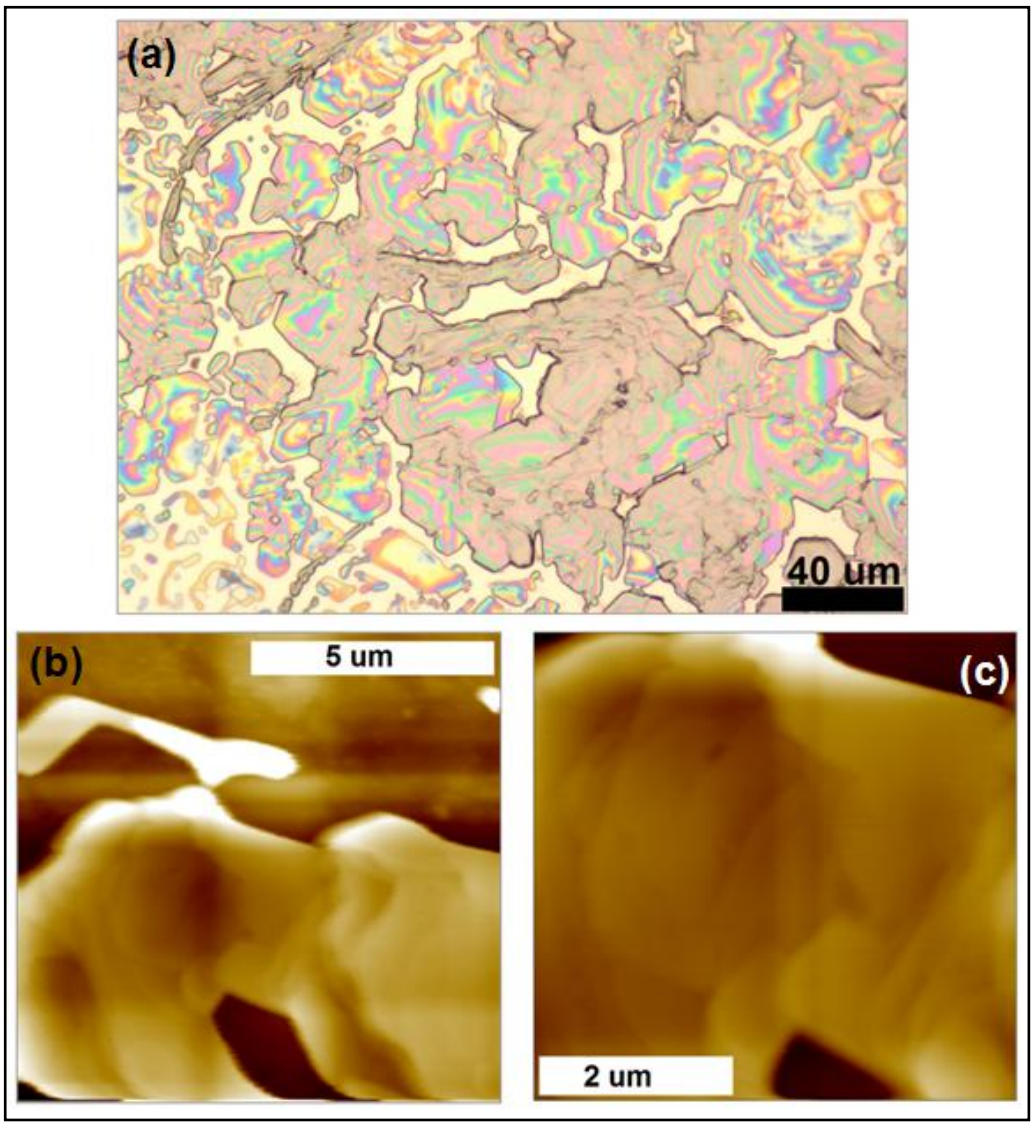

Figure 3.20: Sample 339, diluted Tris-HCl solution drop casted on Si wafer. (a) is optical microscope image, (b) and (c) are AFM images. Scan size of (b) is 10µmX10µm, (c) is 5µmX5µm.

This sample was investigated with atomic force microscopy and also scanning tunneling microscopy as shown in figure 3.22 and figure 3.23.

In figure 3.22, a hexagonal structure and its layers are shown in (a) and (b). The layers are shown in (c) and (d), the height of the layers is ~10nm. In figure 3.23, STM image of clean HOPG surface is shown in (a) and STM image of the Sample 343 is shown in (b). The STM investigation of diluted Tris-HCl solution on HOPG surface is a preliminary study.

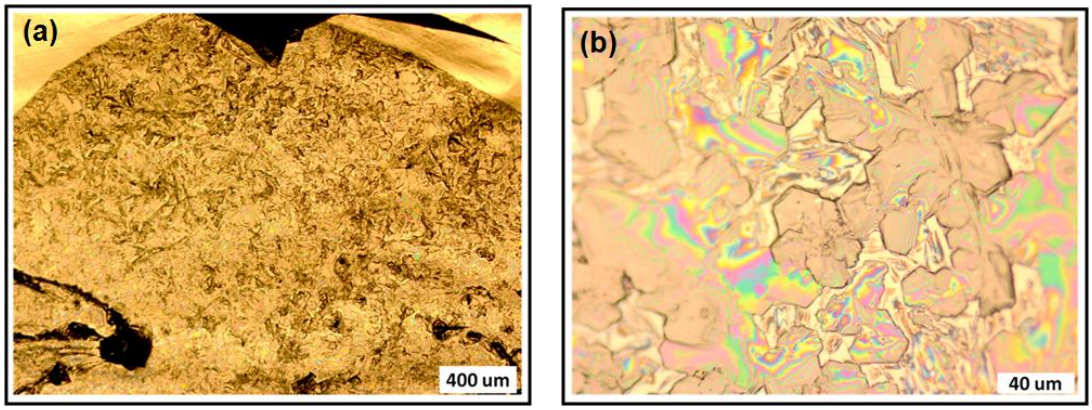

Figure 3.21: (a) and (b) Optical microscope images of Sample 343, diluted Tris-HCl solution drop casted on HOPG surface.

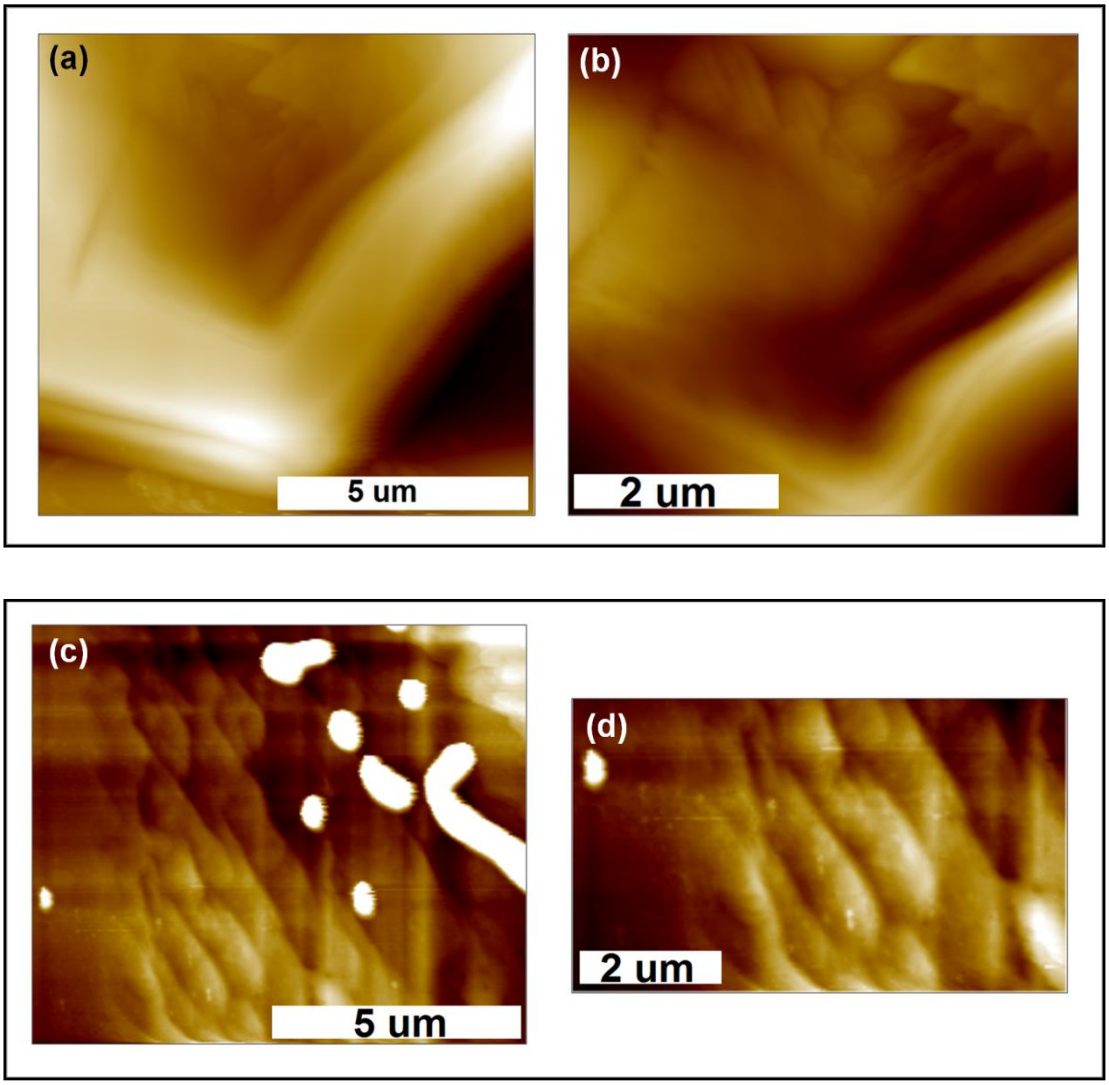

Figure 3.22: AFM images of Sample 343, diluted Tris-HCl solution drop casted on HOPG surface. Scan size of (a) is 10µmX10µm, scan rate is 3µm/s, scan size of (b) is 5µmX5µm, scan rate is 1µm/s, scan size of (c) is 10µmX8.5µm, scan rate is 1µm/s, scan size of (d) is 6.5µmX4µm, scan rate is 1µm/s.

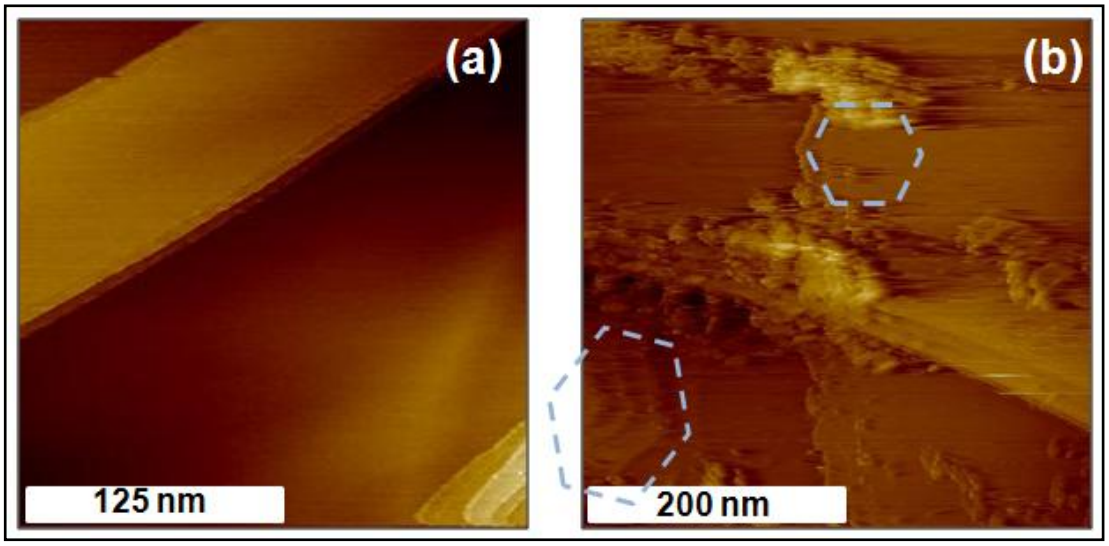

Figure 3.23: (a) STM image of HOPG, tip bias: 60mV, tunneling current: 0.5nA, scan size: 256nmX256nm (b) STM image of Sample 343, diluted Tris-HCl solution drop casted on HOPG, tip bias: 1.8V, tunneling current: 0.5nA, scan size: 400nmX400nm.

Our AFM studies clearly indicate that, T7 Primer molecules in Tris-EDTA buffer solution cannot be identified in their deposited forms on surfaces. After investigation of TE buffer solution itself, optical microscope images and AFM studies show that hexagonal structures covered the surface. The hexagonal structures can be ~50µm large and 400 nm high. These hexagonal structures are formed by smooth multi-layer structures (10-20 nm). The observed hexagonal structures are identified to be due to the Tris-HCl in the buffer. Tris-HCl solution creates hexagonal structures on solid substrates using drop cast-drag-pull method. However, EDTA and Tris-ddH_2O do not result in hexagonal structures on the surface. When using diluted Tris-HCl solution, the hexagonal structures can be observed with AFM using only drop casting method, without drag-pull method. The hexagonal layers can be observed even with scanning tunneling microscopy simply by playing with the dilution of the Tris-HCl solution.

4. INVESTIGATION OF CdSe QUANTUM DOTS

4.1 Literature Review

Quantum dots were suggested by A.Ekimov et al. at the beginning of the 1980s [16] and experimentally observed in solution using Raman spectra, by L.E.Brus et al. [17]. Quantum dots are applicable in many fields such as LEDs, diode laser, transistors, solar cells and medical imaging [19-20].

Quantum dots (QDs) are semiconductor crystals with 2-10 nm radius. Because of their small size, quantum dots have unique optical and electrical properties, which are different from those of their bulk form. Quantum dots have discrete, quantized energy levels, so quantum dots are related to atoms more closely than the bulk material. They can be called artificial atoms. Moreover, apparent of quantum dots is the emission of photons under excitation. The wavelength of these photon emissions depend size of the quantum dot. If the size of a quantum dot is smaller, its band gap is larger [18] (Figure 4.1-4.2).

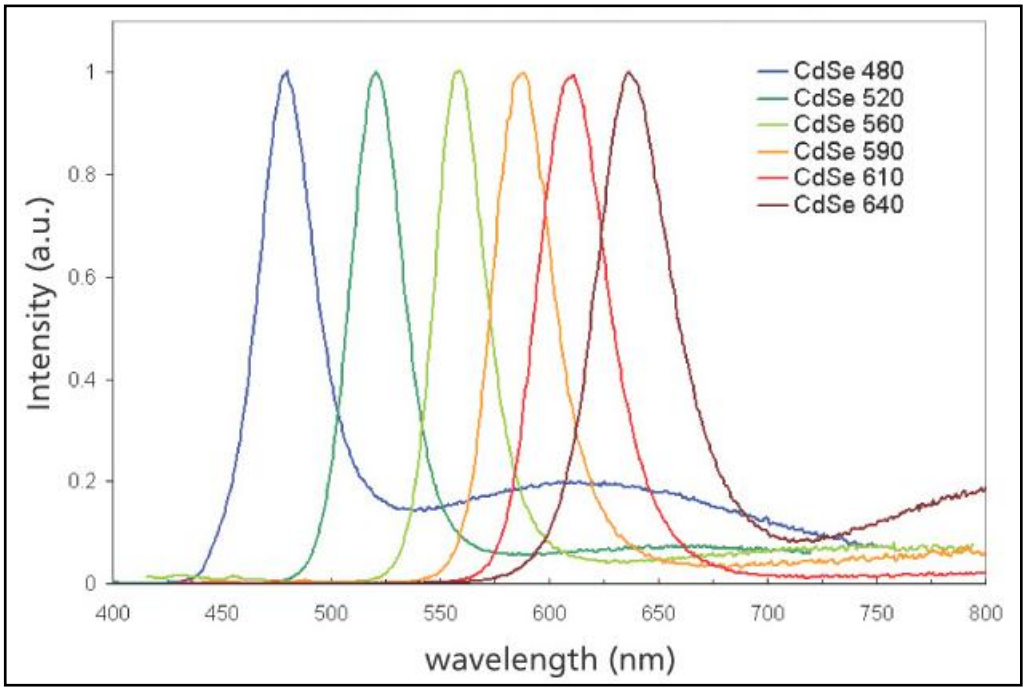

Figure 4.1: Photoluminescence spectra of different size of quantum dots (Sigma-Aldrich) [63].

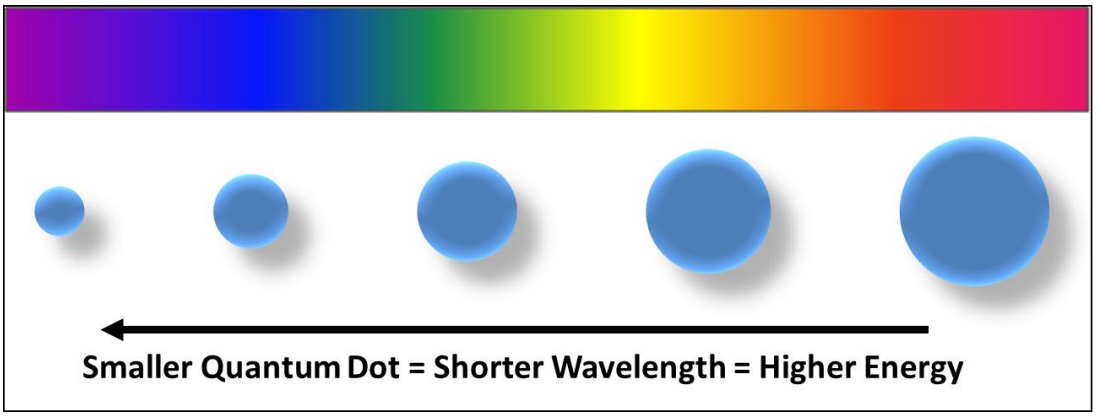

Figure 4.2 : Relationship between the size of quantum dot and its energy.

The synthesis of quantum dots are realized by quite a standard chemical process. It is based on three components; premise matters, ligand and solvents. In high temperature, the premise matter turn into monomers. When monomers reach the saturation, nanocrystals growth starts. The temperature is one of the critical factors for nanocrystal growth. Monomer concentration is very important for the growth.

Quantum dots are suspended in different solvents such as deionized water, toluene or methanole. Moreover, QDs are surrounded by different types of ligands that bind onto their surfaces. The ligands can be important, when studying with scanning probe techniques for the topographic imaging. Annealing method when the quantum dots covered the surface, can help improve the imaging quality of scanning probe microscopies [15,19,20] .

In this section, preparation of quantum dot surface systems and investigation of these system with scanning probe microscopies will be discussed.

4.2 Experiments

In this study, CdSe type quantum dots in toluene, which were purchased from Sigma-Aldrich, were studied with AFM on the HOPG surface. The properties of components of the quantum dots are very important to understand the quantum dots behavior on the surface.

Fluorescence emission wavelength of the CdSe quantum dots we used is 640 nm. The ligand of the quantum dots is Hexadecylamine / Trioctylphosphine (HDA/TOPO). The size of the quantum dots is 6.5nm and “The soft ligands increase

hydrodynamic diameter of the nanocrystals by ~4.5-5 nm" [63]. In figure 4.3, quantum dots and their ligand are shown. The quantum dots are suspended in toluene and the density of the solution is given to be 5mg/mL. 1µL of this QDs solution contains 6061x10^9 QDs (see Appendix A.3).

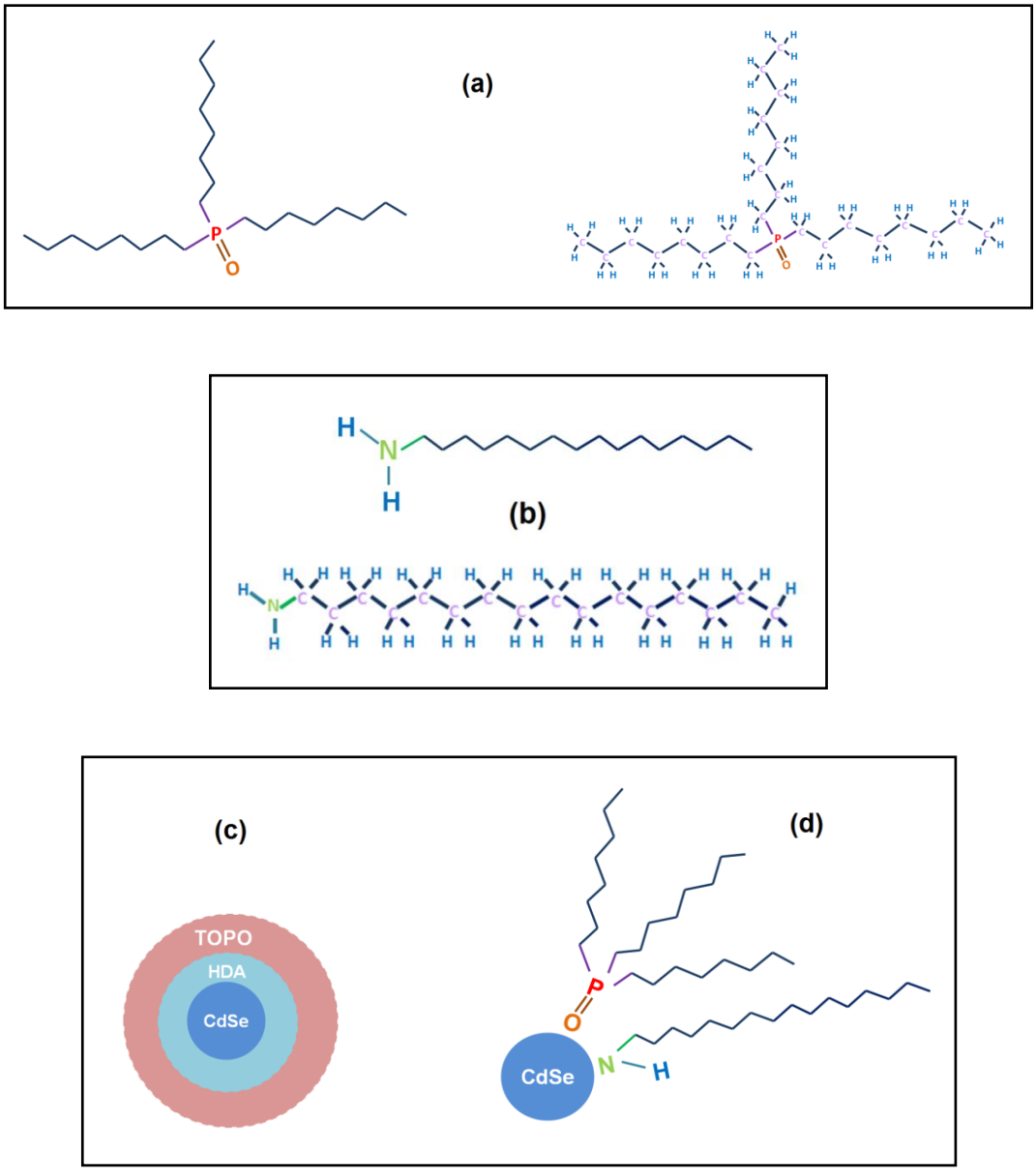

Figure 4.3 : (a) Chemical shape of Trioctylphosphine (TOPO), (b) Chemical shape of Hexadecylamine (HDA), (c) and (d) Shape of CdSe nanocrystal with its ligands.

Due to the density of the QDs solution, the solution was diluted by 1/100 (with toluene) and 1µl from this solution was taken with a micropipette and it was carefully drop casted on HOPG surface at room temperature. Then, the sample was placed in a desiccator to dry. The sample, which was coded as Sample 254, shown in figure

4.4. Image (a) and (b) are optical microscope images. (c) and (d) are AFM images. The AFM images show that there are some clusters on HOPG steps. Height of the clusters is approximately ~60 nm. As shown in figure 4.4, image (c) show that the quantum dots clusters accumulated on the HOPG steps.

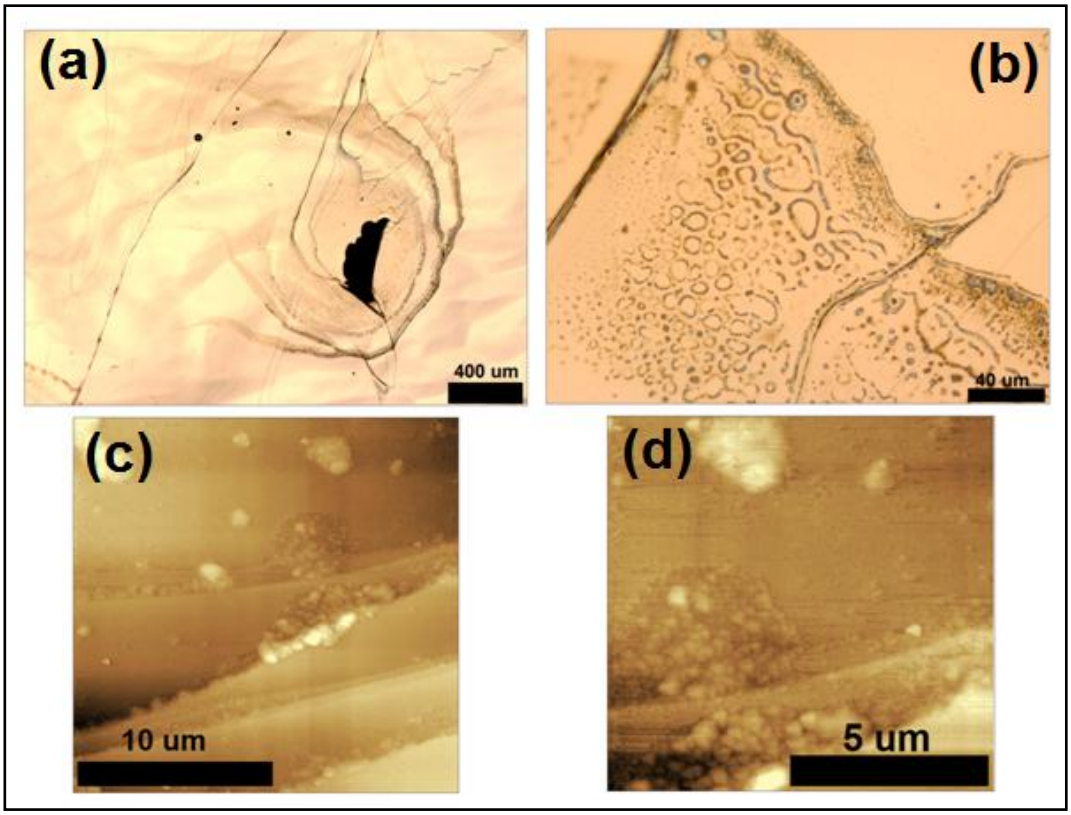

Figure 4.4: Sample 254, QDs solution (diluted by 1/100) on HOPG surface. (a) and (b) are optical microscope images. (c) and (d) are AFM images. The scan area of (c) is 20µmX20µm, and (d) is 10µmX10µm. Scan rate is 1Hz.

Another sample with the code Sample 263, was prepared. The solution was diluted by 1/200 with toluene and it was carefully drop casted on HOPG surface at room temperature. Then, the sample was placed in the desiccator to dry. Optical microscope images and AFM images are shown in figure 4.5. From the AFM images of this sample, a film formation is observed on the surface and the height of the film is ~18nm. In such images distinguishing the quantum dots are impossible.

Sample 270 was prepared and this time QDs solution was diluted by 2.5/5000 (µl) with toluene and it was carefully drop casted on HOPG surface at room temperature. Then, the sample was placed in the desiccator to dry. Optical microscope images

and AFM images are shown in figure 4.6. Although the AFM images of this sample are quite interesting. It is impossible to distinguish between the effect of the solution and the quantum dots. The sample seems to be wet in AFM images.

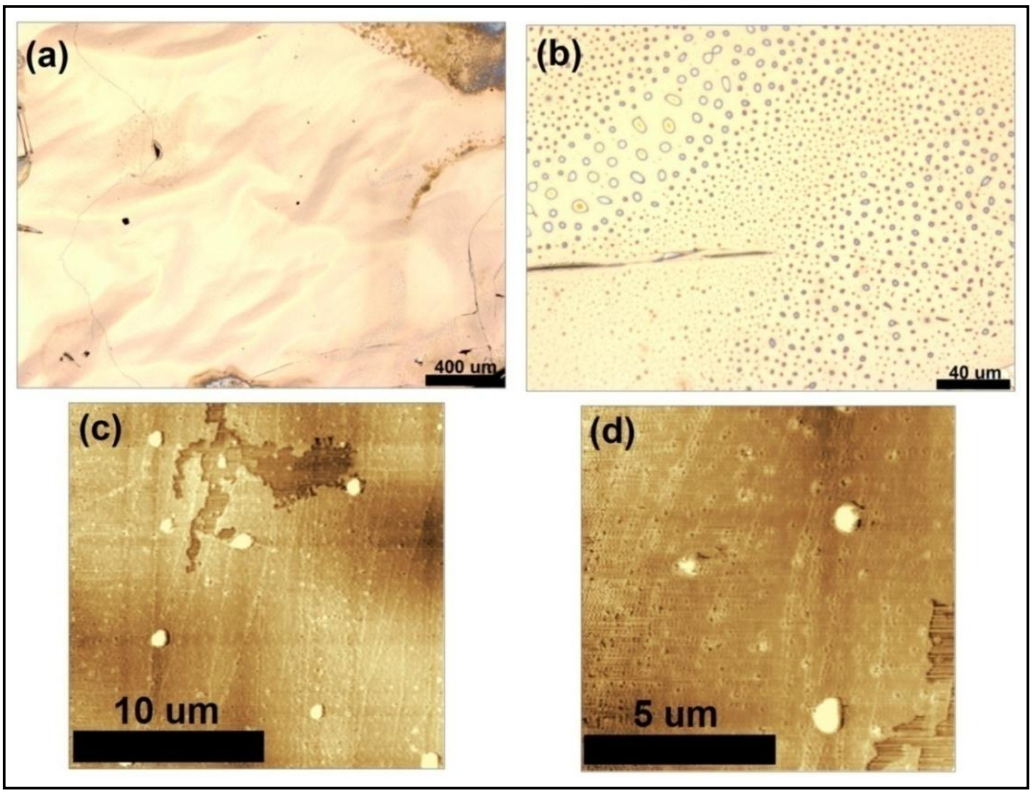

Figure 4.5 : Sample 263, QDs solution (diluted by 1/200) on HOPG surface. (a) and (b) are optical microscope images, (c) and (d) are AFM images. Scan area of Image (c) 20µmX20µm and (d) 10µmX10µm. Scan rate is 1Hz.

Then the Sample 270 was gently washed with toluene and dried in desiccator. After these processes, the sample was coded as Sample 274. Optical and AFM images are shown in figure 4.7. Washing with toluene did not result in much difference on the surface. Moreover, Sample 274 was annealed using tube oven in H_2-Ar atmosphere at 300^0C, 1 hour. The sample was coded as Sample 280 shown in figure 4.8. AFM images showed that annealing process removed the contaminants, which were on the surface from the solution.

In figure 4.9, a cluster of quantum dots are occured. On the HOPG surface, there are many quantum dot clusters. As in figure 4.9, the hight of a cluster approximately 9nm. Although AFM investigation of the quantum dot clusters could be measured, STM investigation of the clusters could not be performed yet.

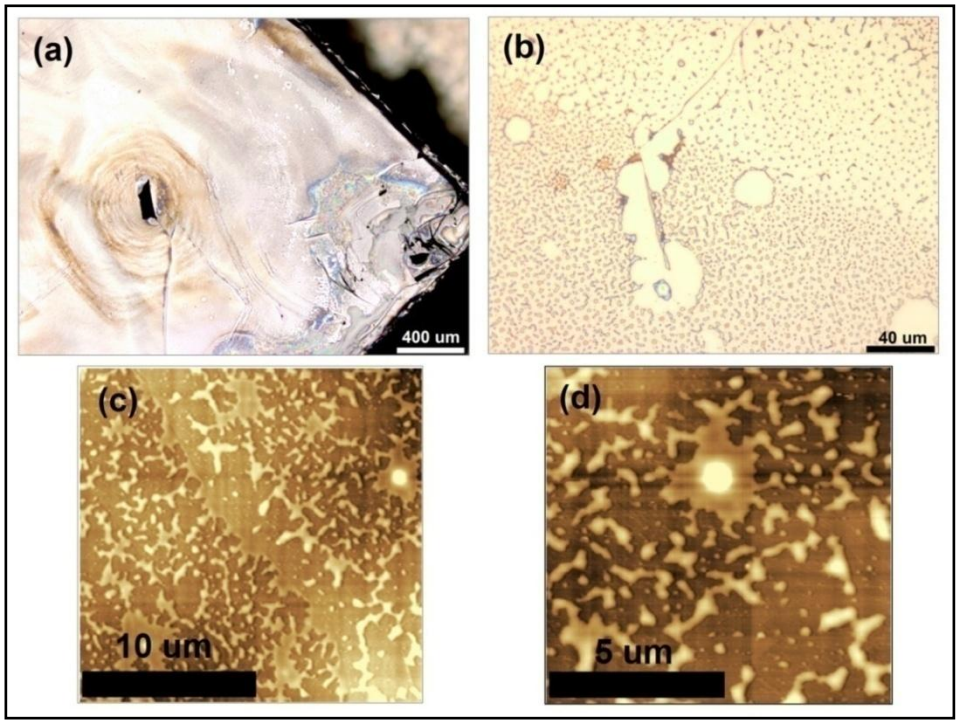

Figure 4.6 : Sample 270, QDs solution (diluted by 2.5/5000) on HOPG surface. (a) and (b) are optical microscope images, (c) and (d) are AFM images. Scan area of image (c) is 20µmX20µm, (d) is 10µmX10µm. Scan rate is 1Hz.

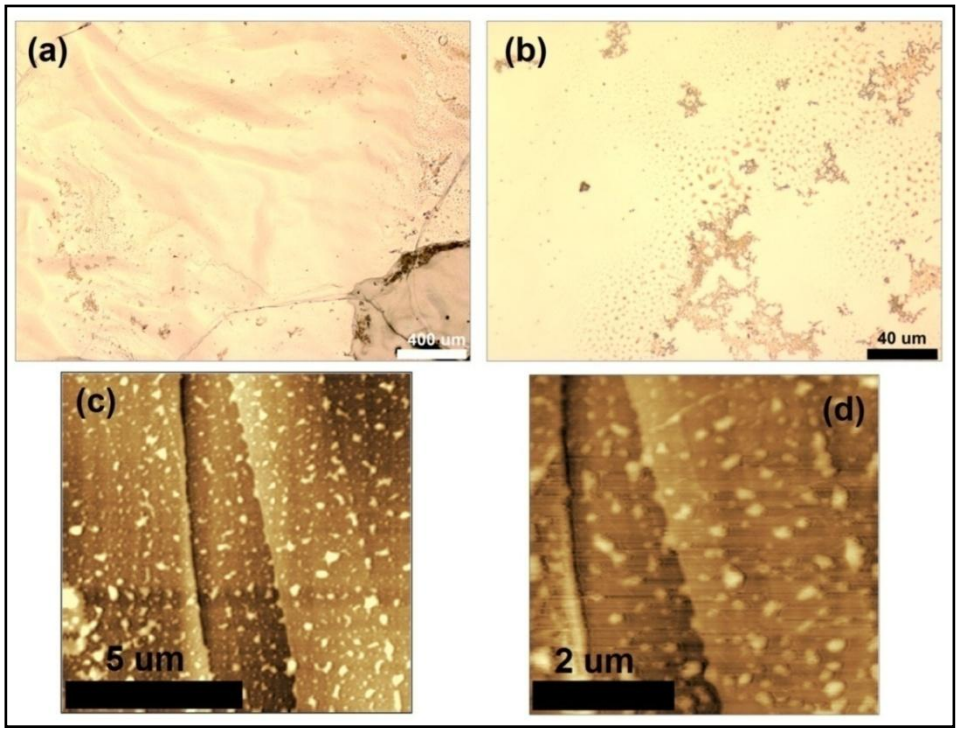

Figure 4.7 : Sample 274 was prepared by washing with toluene of Sample 270. (a) and (b) are optical microscope images, (c) and (d) are AFM images. Scan area of image (c) 20umX20um, (b) 10umX10um. Scan speed is 1Hz.

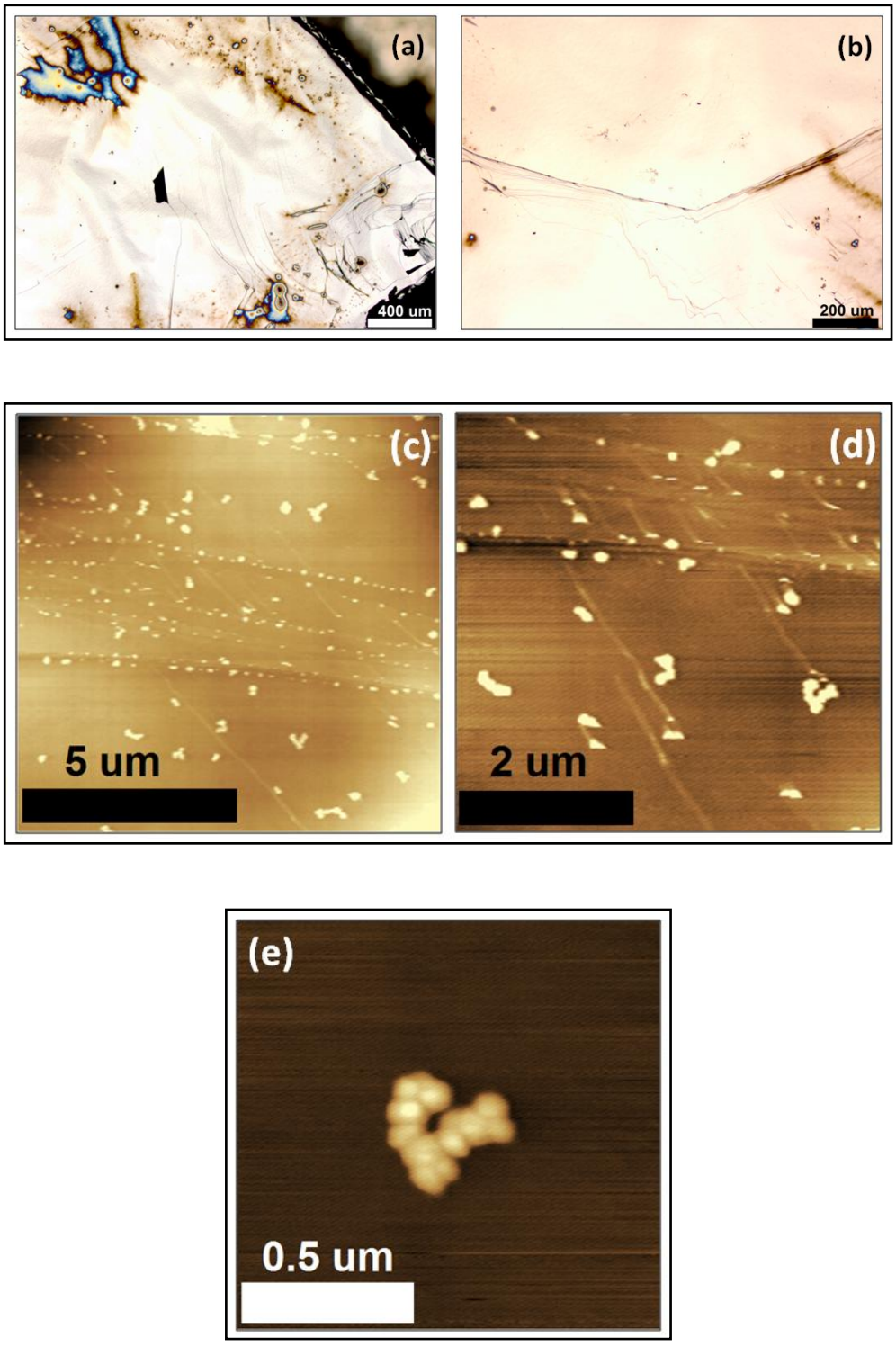

Figure 4.8 : Sample 280 was prepared by annealing of the Sample 274 under H_2-Ar atmosphere. Scan area of image (c) 10µmX10µm, (d) 5µmX5µm, (e) 1.25µmX1.25µm. Scan rate is 1Hz.

Sample 300 was prepared using a QDs solution that was diluted by 2.5/5000 (µl) with toluene and it was carefully drop casted on HOPG at room temperature. Then, the sample was placed in the desiccator to dry. Then, the sample was annealed in

tube oven in H_2-Ar atmosphere at 150^0C, 1 hour. In figure 4.10(a) and (c) are before the annealing of Sample 300, (b) and (d) are after annealing of the sample. According to the previous work [15,19,20], the temperature of the tube oven was changed. However, the results are not same with Sample 280.

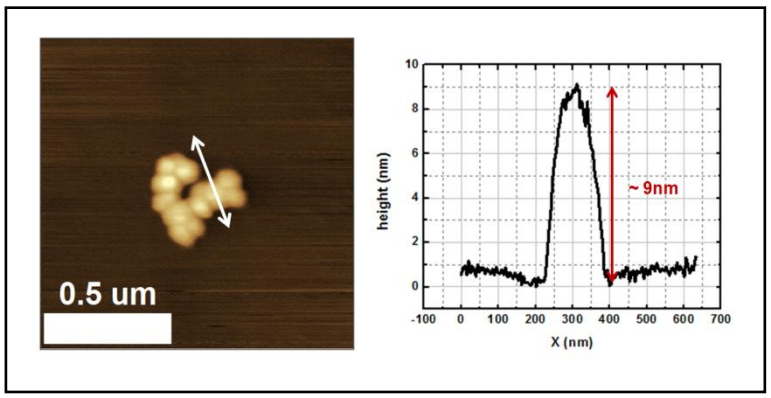

Figure 4.9 : The height of a quantum dot cluster.

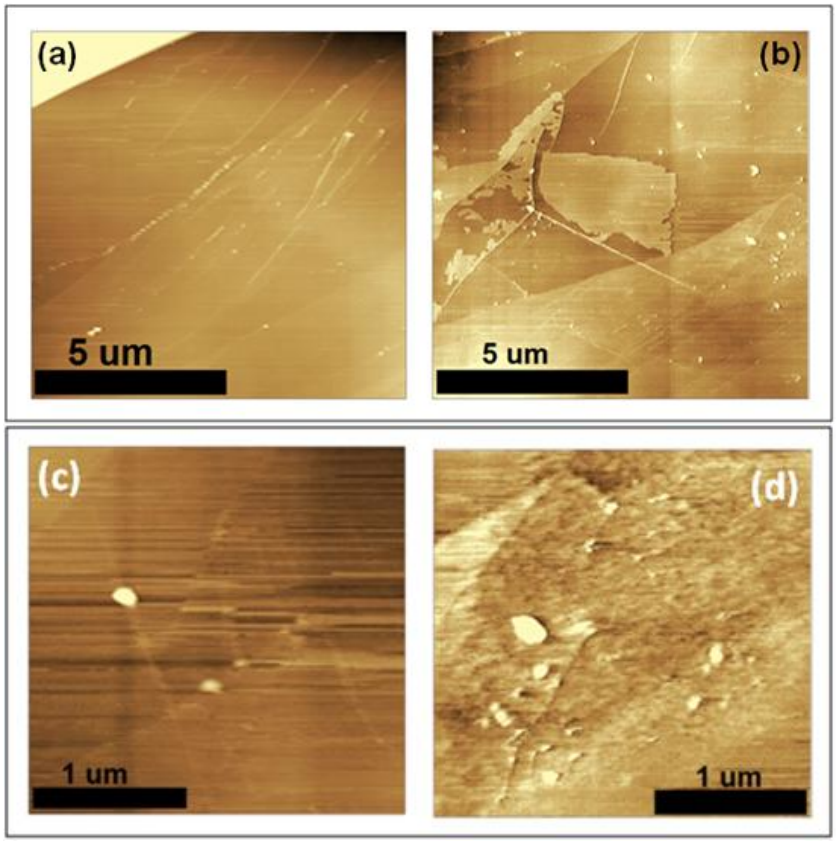

Figure 4.10 : Sample 300, AFM images of quantum dots on HOPG, (a) and (c) before annealing, (b) and (d) after annealing. Scan size of (a) and (b) is 10µmX10µm, (c) and (d) 2.5µmX2.5µm. Scan rate is1Hz for all.

Also, effects of pure toluene solution are investigated on the HOPG surface using AFM. 1µl toluene solution drop casted on HOPG surface and the sample was placed in the desiccator to dry. Then the sample was investigated by AFM, as shown in figure 4.11, the solution creates spherically symmetric structures on the HOPG edges.

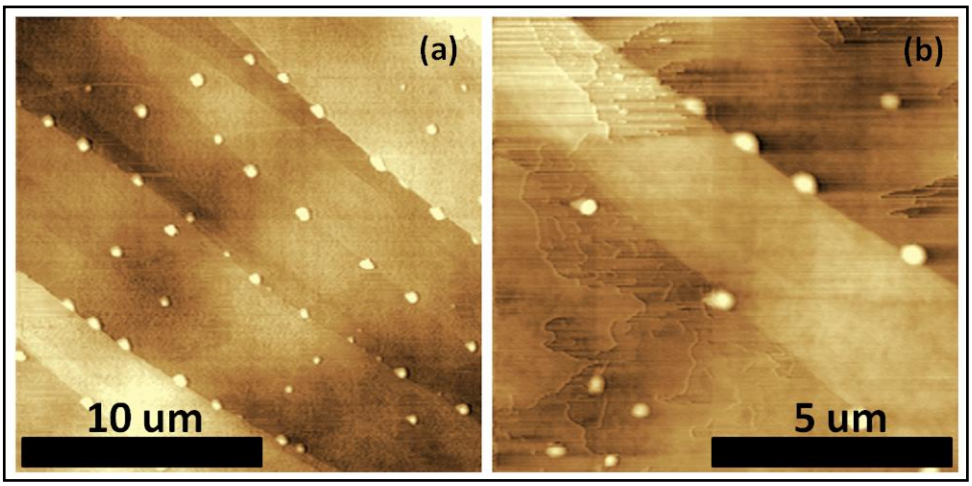

Figure 4.11: Pure toluene on HOPG surface, scan size of (a) is 20µmX20µm, (b) 10µmX10µm, scan rate is 1Hz for both.

The results show that, the annealing process, the correct temperature are very important to get rid of the solution effects and ligand, when investigating quantum dots on solid surface using SPM techniques. Preparation of quantum dots surface systems and to study of these systems with SPM prove not to be so straight forward. Informatio on the exact contents of the quantum dot solutions is definitely important. Although there are many advanced studies of quantum dots, a single quantum dot is still not reported on any surface using SPM. Clearly on of the major problems is the formation clusters not only due to the quantum dots but also because of the remnants in the solutions.

5. AN ALTERNATIVE METHOD FOR GRAPHENE PRODUCTION

5.1 Literature Review

Graphene is a single layer of graphite. The structure of graphene consists of sp2 bonded carbon atoms, which are in a two dimensional (2D) honeycomb lattice. They can be wrapped up to form 0D structures or buckyballs. If it is rolled, it is called 1D nanotube. If it is stacked, it is called 3D graphite.

Investigation of the electronic properties of graphene started in 1947. The energy-band structure of graphene was discussed theoretically by P.R.Wallace [28]. However, a graphene sheet was obtained experimentally for the first time in 2004 by A.K.Geim and K.S.Novoselov et.al.This group used mechanical exfoliation method, by cleaving graphite to its layers and rubbing the layers onto another surface. Moreover, multi layer graphene flakes on SiO_2 substrate was processed into device and its electronic properties were analyzed [25].

Most of the research on graphene have been oriented in the field of exploration of its electronic properties. In graphene, effective mass of electrons, which are in honeycomb lattice, is zero and electrons and holes behave like relativistic particle described by the Dirac equation rather than the Schrödinger equation. The massless electrons (Dirac fermions) in graphene move with Fermi velocity ($v_F \sim 10^6$ m/s). The electrons in graphene can propagate without scattering for submicrometer distances [25].

Dirac fermions in graphene behave extraordinary if it is exposed to magnetic fields. When applying a gate voltage (Vg) to the graphene under magnetic field, charge density can be controlled and carrier mobility(μ) can be calculated. Carrier mobility values of few layer graphene were reported between 3000 and 10.000 cm^2/V.s at room temperature. The values of carrier mobility of graphene were measured at 300^0K, ~15.000 cm^2/V.s and at 4^0K, 60.000 cm^2/V.s [25]. In 2008, carrier mobility of single layer graphene was measured at 5^0K, 200.000 cm^2/V.s [64]. The high carrier mobility results high electrical conductivity, so graphene enables to use more

than silicon in transistor technology because of the typical electron mobility of silicon (Si) at 300^0K is 1400 cm^2/V.s. Besides these features, graphene has strong mechanical properties (breaking strength of graphene is 200 times greater than steel) and high thermal conductivity (for graphene $5.3x10^3$ W/mK, for diamond 2200 W/mK).

Graphene is generally prepared by four different methods; the mechanical exfoliation method [25], epitaxial growth on insulating or semiconductor surfaces (high temperature treatment of SiC) [33], epitaxial growth by chemical vapor deposition (CVD) [31,32] and by the formation of colloidal suspensions (graphene oxide) [34,35].

Mechanical exfoliation method is the first and a very simple method which consists the peeling off of the graphite layers using scotch tape and rubbing the layers to another surface. Then, the graphene flakes can be characterized by optical microscope on 290-300 nm oxidized silicon wafer.

In this section, an alternative method for graphene production, using both mechanical exfoliation method and chemical materials, will be discussed.

5.2 Experiments

In this study, an alternative method, which involves the preparation of a solution with graphite and graphene flakes, for graphene production was studied. The graphite and graphene flakes were obtained using mechanical exfoliation method, which is separation of graphite layers from the HOPG surface. Scotch tape was adhered to the HOPG surface and it was gently pulled. Thus, a few layer of graphite adhered on the tape. The tape, which has graphite on it, was adhered on itself and was pulled. This process continued several times until graphite pieces got thinner and homogenous. After this process, the tape was dissolved in pure acetone. The tape turned to mucus structure in acetone. The mucus structure was put on a very clean glass lamel and it was rubbed to the lamel surface. The graphite and graphene flakes remained on the glass, the tape was separated. Then, the glass was washed in 2-propanol in ~15 minutes using ultrasonic bath. After that, the propanol solution contains the graphite and graphitic flakes in it. In the experiments, the drop casting method was used as a sample preparation method. SiO_2 and gold-coated mica were used as substrates. The solution was drop casted on SiO_2 or gold-coated mica substrates.

1µl from the solution was taken with a micropipette and it was carefully drop casted on a piece of gold-coated mica at room temperature and dried. This sample was coded as Sample 16 and its optical microscope images are shown in figure 5.1. The figure shows that there are many types of flakes and the flakes are in different colors. In image (b) gray-white-color layer folded on itself, the folded part is seen in blue. This image is quite interesting. Moreover, the Sample 16, by making conductive using silver paste, was investigated by scanning tunneling microscopy.

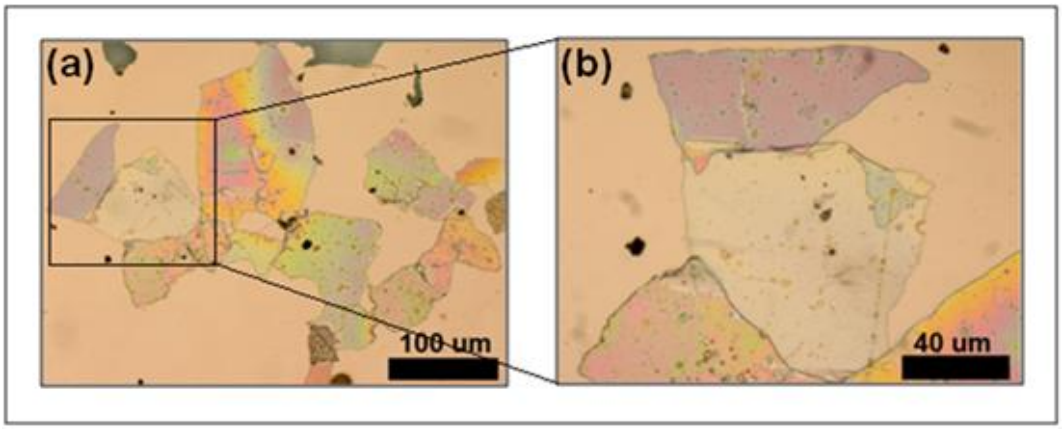

Figure 5.1: (a) and (b) are optical microscope images of Sample 16, which was prepared by drop casted method of graphitic solution on gold-coated mica.

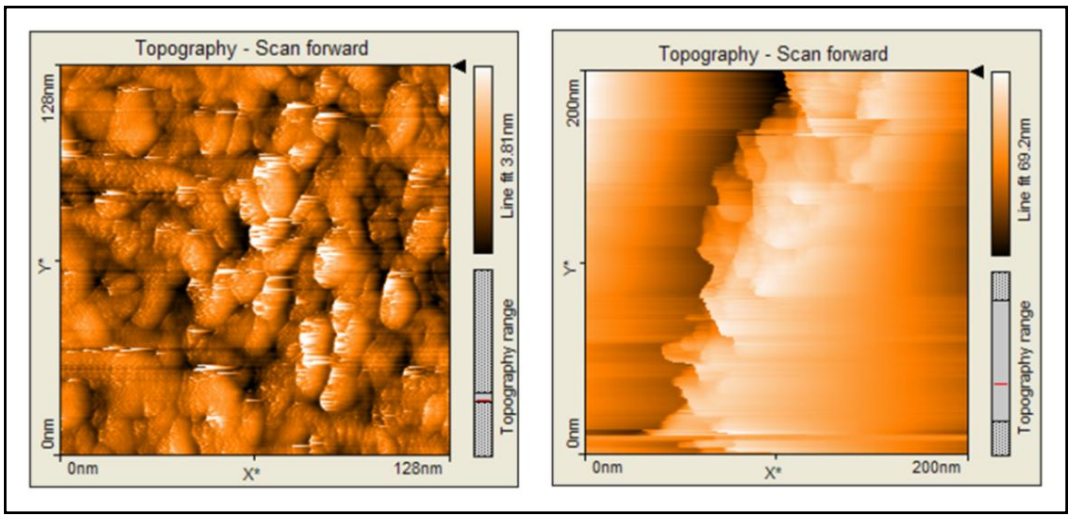

Figure 5.2: Left: STM image of gold part of Sample 16, scan size : 128nmX128nm, tunneling current : 1nA, tip bias :0.61V. Right: STM image of gray-white-color flake on Sample 16, scan size:200nmX200nm, tunneling current :1nA, tip bias:0.61V.

In figure 5.2, the STM images of the sample are shown, figure 5.2(left) is STM image of gold part of the sample, figure 5.2(right) is STM image of gray-white color layer, which is shown in figure 5.1(b). The STM image of white-color flake is not meaningful. However, this meaningless can be due to the remnants from the solution.

In this study, we used reference graphene sample on SiO_2, prepared by mechanical exfoliation technique with lithographic gold contacts on it. This sample was supplied from National University of Singapore (NUS). We called it "NUS sample". Optical microscope image of NUS sample is shown in figure 5.3. Optical contrast of monolayer, bilayer and multilayer graphene can be distinguished on 290-300 nm oxidized silicon wafer [25]. As shown in figure, the graphene sheets can be identified and the bottom edge of the left side graphene sheet is darker than the other parts. It is stated that, this edge is not monolayer graphene.

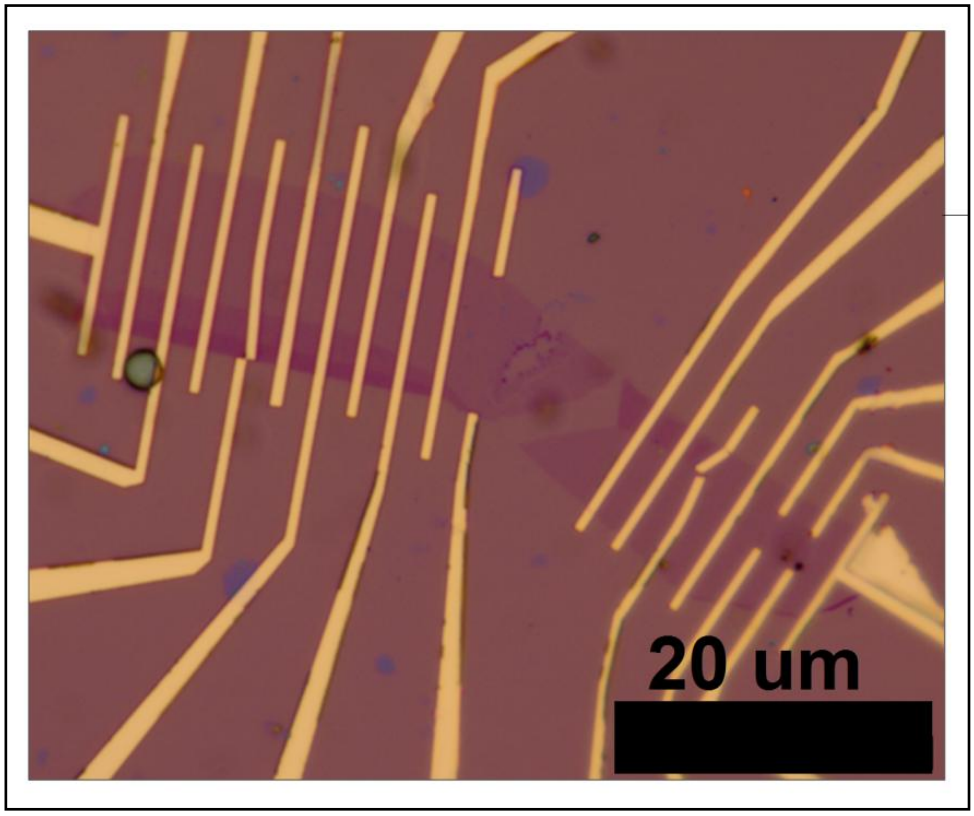

Figure 5.3: Reference graphene sample, which was coded as NUS sample. Two pieces of graphene layers are on SiO_2 surface and gold contacts are on the graphene layers.

NUS sample was clearly identified using atomic force microscopy. The typical apperent step height of graphene and gold contacts on SiO_2 were observed by atomic force microscopy. In figure 5.4, AFM images of different parts of the NUS sample are shown. The step height of the gold contacts were also measured using AFM data. In figure 5.5, the height of the graphene flake and the height of the gold contacts are shown. The apparent height of graphene flake with respect to the SiO_2 surface is 3.06 nm. It corresponds to 9 graphene layers. Because the distance among graphene layers in graphite is 0.335 nm.

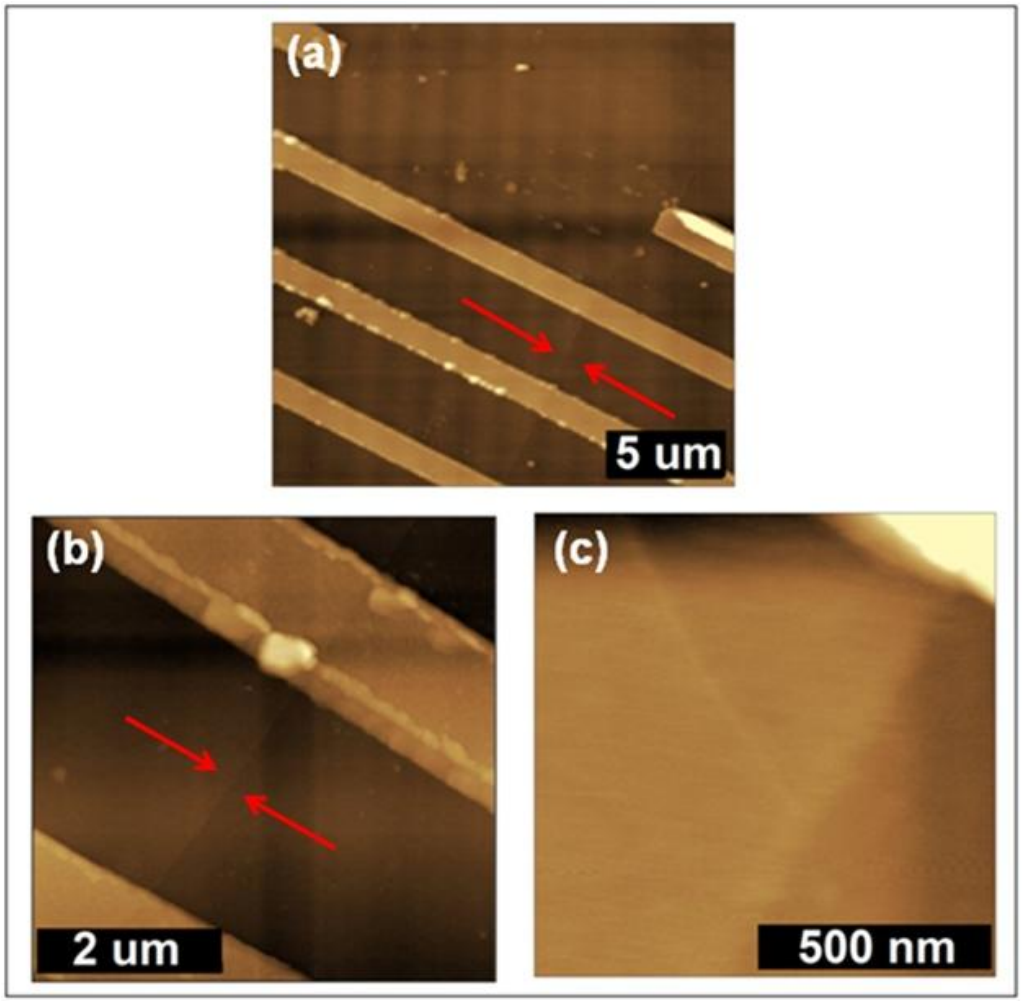

Figure 5.4: AFM images of NUS sample. In image (a) the gold contacts are observed and the graphene edge can be seen, scan size of image is 20µmX20µm. In image (b) the graphene edge is seen between the two gold contacts, scan size of image is 5µmX5µm. Image (c) is zoom of (b), scan size of image is 1µmX1µm. Scan rate is 1Hz for all.

The reference graphene device was used not only for AFM measurements, but also it was used for STM measurements. This sample, by making conductive using silver paste, was investigated by scanning tunneling microscopy. In figure 5.6, STM images of graphene flake on the NUS sample are shown. The STM images show that the investigation of graphene is not an easy task. This device was generated using lithography method. This method can cause photoresist residue on the surface. As shown in top image, the residue effect might be observed in figure 5.6. According to the right-down image, atomic resolution might be observed. However it was not clear like atomic resolution of HOPG. In figure 5.7, atomic resolution of HOPG surface was also given.

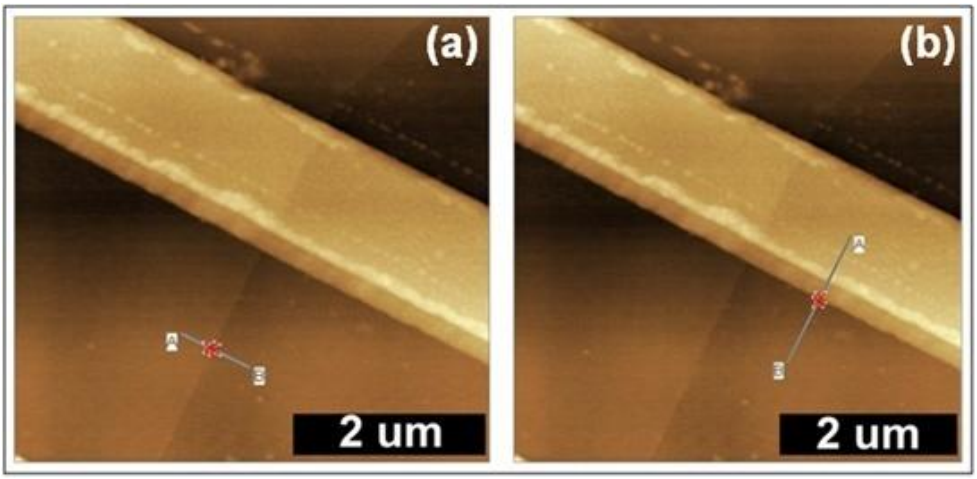

Figure 5.5: AFM images of NUS Sample, (a) The step height of the graphene flake is 3.06 nm. This corresponds to 9 graphene layers (the distance among graphene layers in graphite is 0.335 nm). (b) The step height of the gold contact is ~15nm. Scan size of (a) and (b) is 5µmX5µm. Scan rate is 1 Hz.

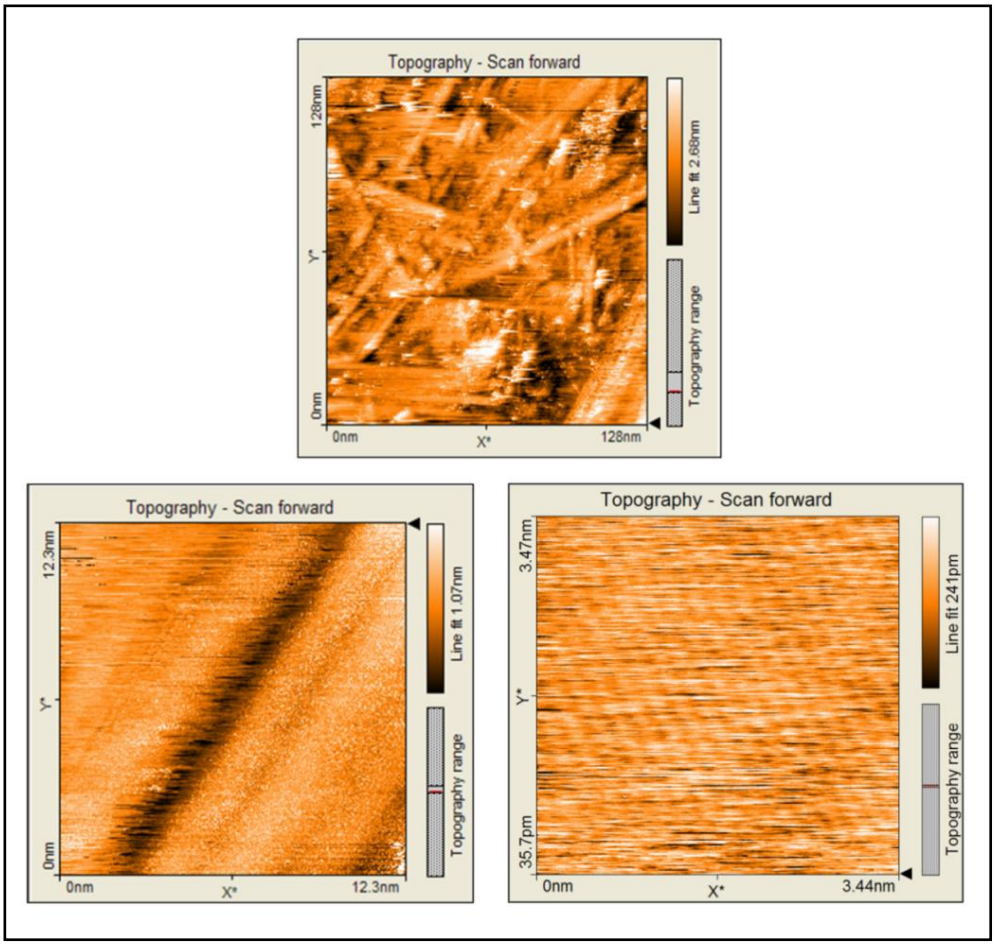

Figure 5.6 : STM measurement of the graphene on the NUS sample. Top: scan size:128nmX128nm, tunneling current(I_t):1nA, tip bias(V_b):50mV. Left-down: scan size:12.3nmX12.3nm, I_t:1nA, V_b:0.2V. Right-down: scan size: 3.44nmX3.44nm, I_t:1nA, V_b:50mV.

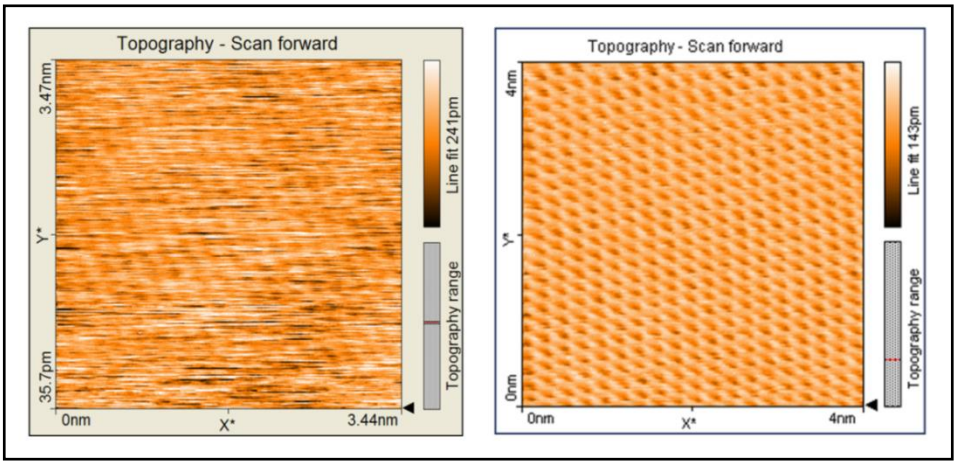

Figure 5.7: Left: STM image of graphene flake on NUS sample, scan size: 3.44nmX3.44nm, I_t:1nA, V_b:50mV. Right: STM image of atomic resolution of HOPG, scan size:4nmX4nm, I_t:0.45nA, V_b:50mV.

For graphene study, one of the most important characterization technique is the micro Raman Spectroscopy. Raman spectra of graphene and graphitic flakes are generally measured at 514 nm and 633nm wavelengths and on 290-300 nm SiO_2. Graphene layer has three eminent peaks in the Raman spectrum. The G peak is always observed in graphite samples at ~1580cm^{-1}. The D peak is at ~1350cm^{-1}, D'or 2D peak is at ~2700cm^{-1}. The 2D peak is fingerprint of graphene. For monolayer graphene, the 2D peak is at ~2640cm^{-1}. This peak shifts to 2700cm^{-1} for multi layer graphene [53].

Raman spectra of graphite and graphene, the G and 2D peaks, and Raman spectrum shifts of 2D peak for graphene layers and graphite are shown in figure 5.8 [53].

Raman spectroscopy is used to characterize the graphene flakes, which was described in this study. During the characterization with Raman spectroscopy, the NUS sample and HOPG were used as reference sample. The Raman spectra of HOPG and NUS sample are shown in figure 5.9. During the whole Raman spectroscopy measurements, green laser at 514 nm was used to excite the sample surface.

In this study, graphene or graphitic flakes solution described above was also investigated on SiO_2 surface. The sample 58 was prepared with drop casting method on SiO_2 wafer (290nm oxide) and dried in the laboratory conditions. The sample was annealed under H_2-Ar atmosphere at 400^0C to get rid of the residues from the solution. The optical microscopy images are shown in figure 5.10. After annealing proccess, the color of the graphitic flake changed.

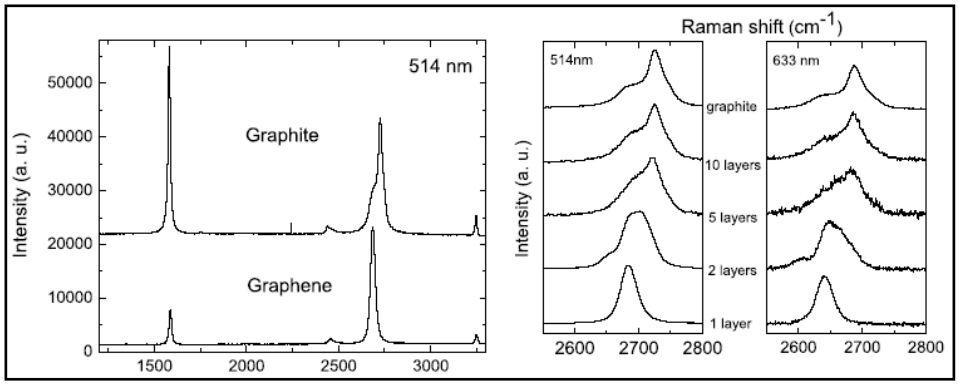

Figure 5.8 : (a) Raman Spectra of Graphene and Graphite, (b) Raman spectrum shifts of 2D peak for graphene layers [53].

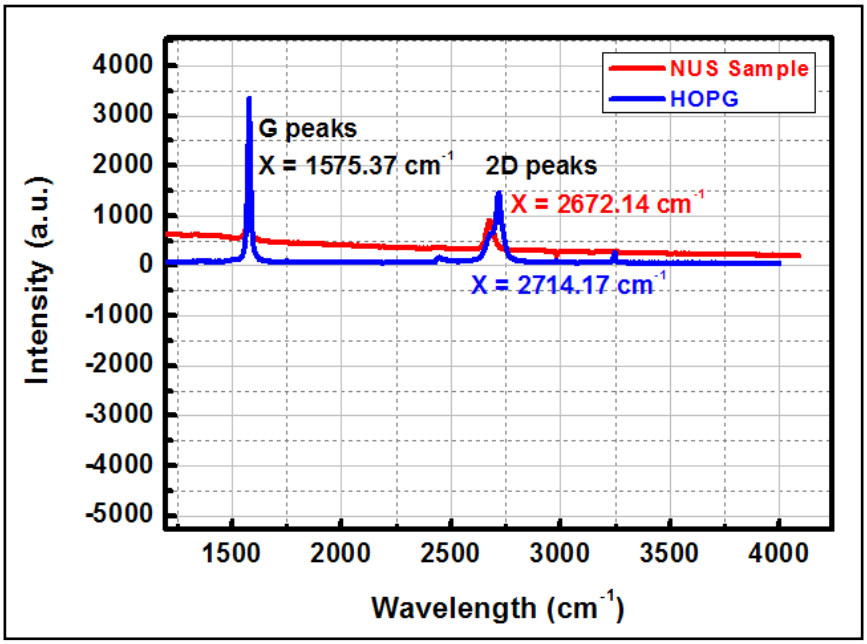

Figure 5.9: The Micro Raman spectrum peaks of HOPG and Graphene sample (NUS).

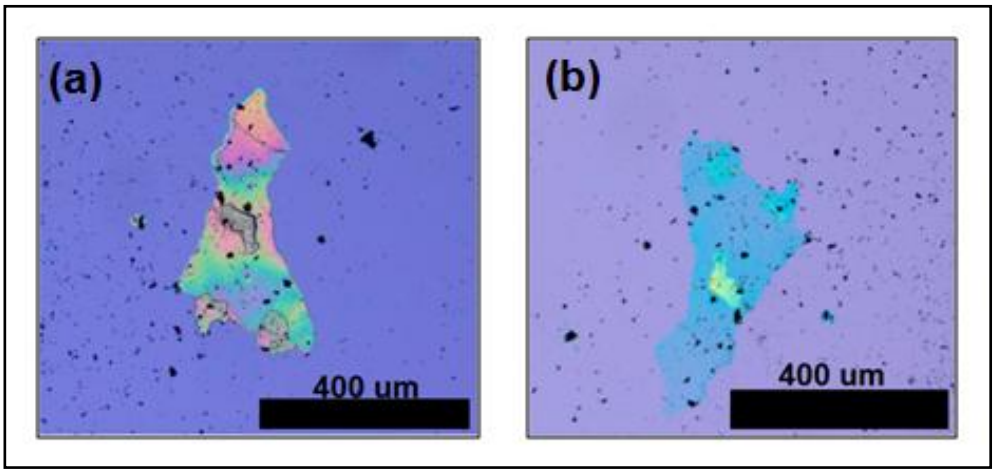

Figure 5.10 : Sample 58, prepared by graphitic solution , Image (a) is after drop casted and drying, image (b) is after annealing at 400^0C under H_2-Ar atmosphere.

Moreover, the Sample 58 was observed before annealing and after annealing process by Micro Raman Spectroscopy. The Raman spectrum of Sample 58 is shown in figure 5.11. Before annealing, we could not see G peak and 2D peak on the sample with Raman spectrum. After annealing, we can see G peak on the sample with Raman spectrum, however the 2D peak is still invisible.

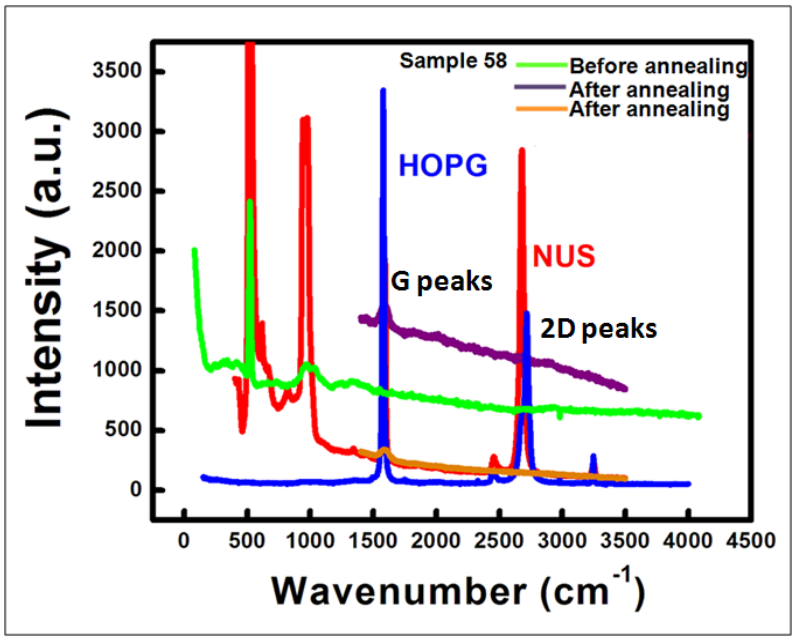

Figure 5.11: Raman spectrum of before and after annealing process of Sample 58, HOPG and reference graphene (NUS) sample.

Another sample, we called this sample "SiO device", was prepared with the same method as Sample 58. Optical image and Raman spectrum of this sample are shown in figure 5.12. In figure 5.13 and figure 5.14, comparison of the NUS sample and SiO device sample is shown.

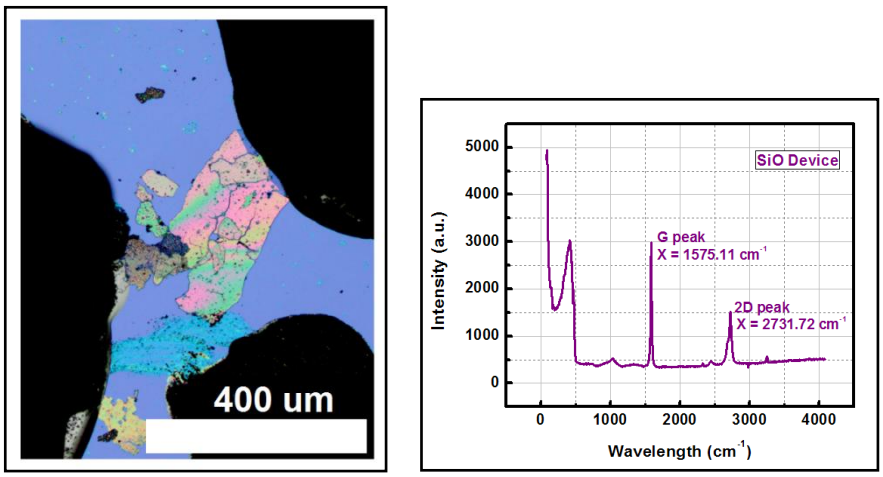

Figure 5.12: Another sample (SiO device) prepared by graphene solution. Left: Optical microscope image, Right: Raman spectrum of the sample.

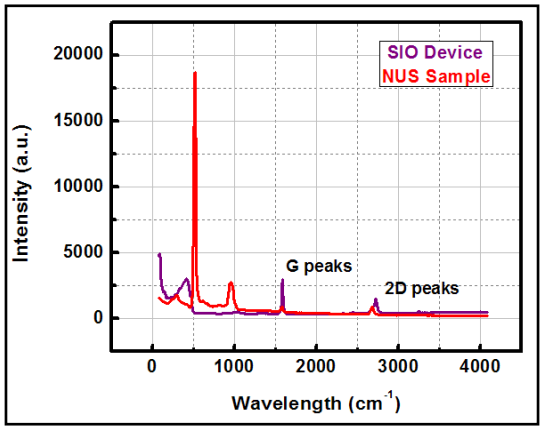

Figure 5.13: Raman spectrum of graphene sample (NUS) and the flake on SiO_2, which was called as SiO device.

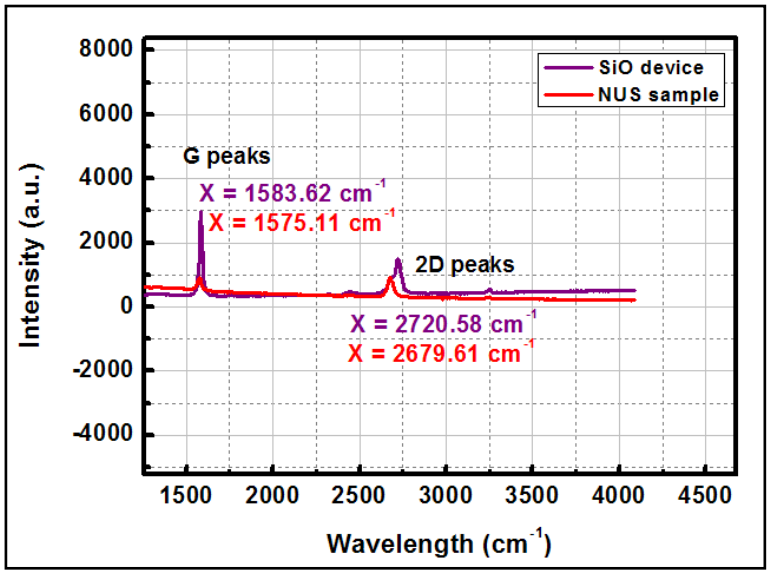

Figure 5.14: Raman spectrum of graphene sample (NUS) and graphene flake on SiO_2, which was called as SiO device. According to peaks, the flake, which is on the SiO device, is multi layer graphene flakes.

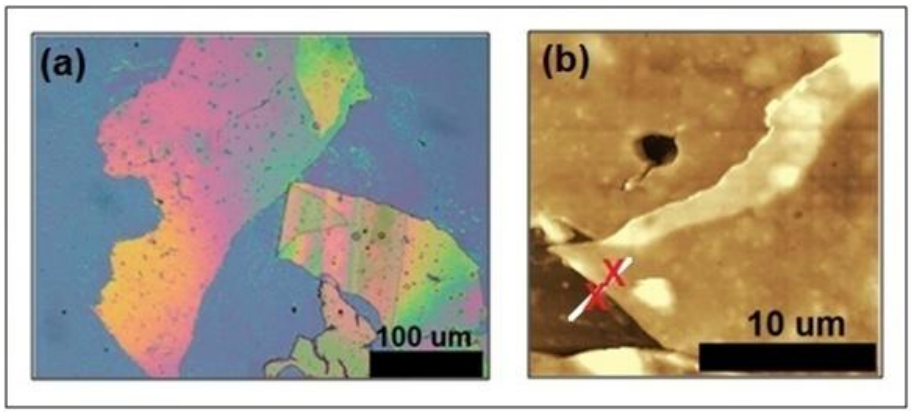

Figure 5.15: Sample 188, solution of graphitic flake drop casted on SiO_2. (a) is optical microscope image, (b) is AFM image of the Sample 188, height of the flake is ~150 nm. Scan size of (b) is 20µmX20µm, scan rate is 1Hz.

The figure 5.12, figure 5.13 and figure 5.14 showed that, the flake on SiO device is not a monolayer graphene sheet. It is multi layer graphene flakes.

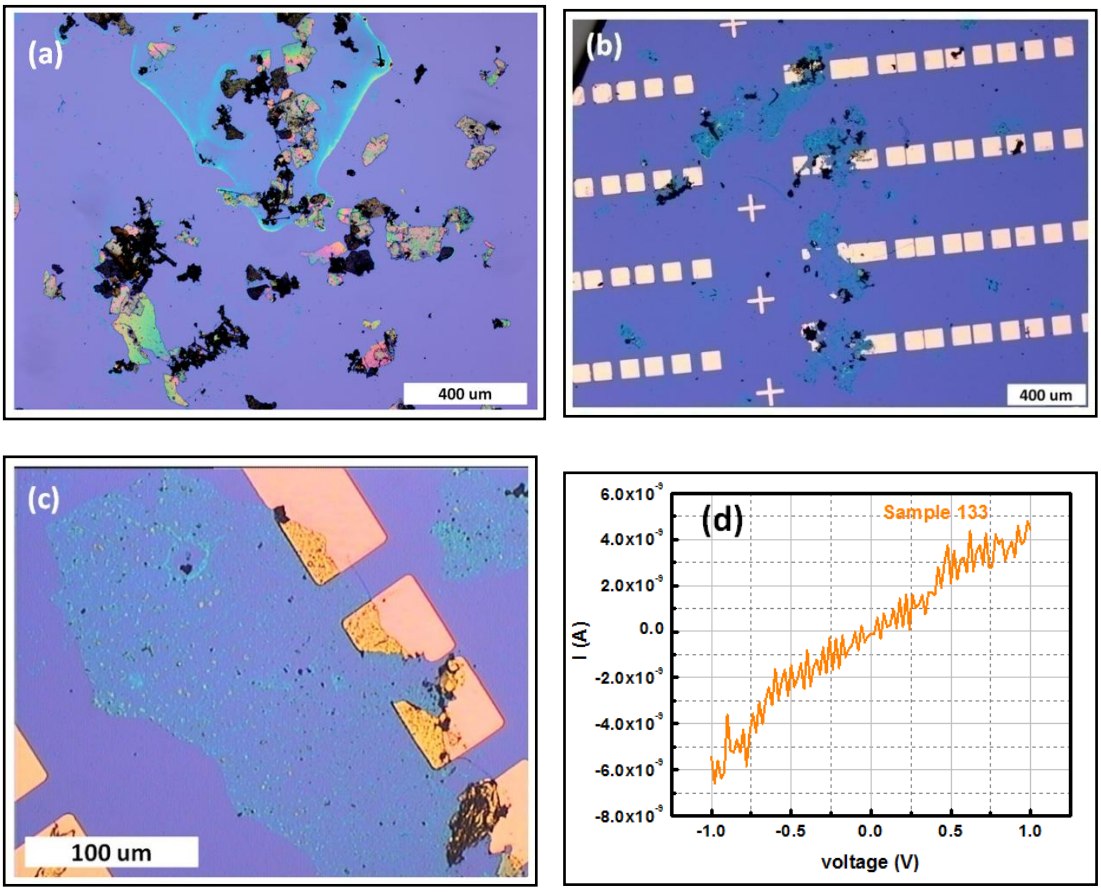

Figure 5.16: Sample 133, solution of graphitic flake drop casted on SiO_2. (a) is optical microscopy image before annealing, (b) is optical microscope image after annealing and lithograpy, (c) is optical microscope image of one of the flakes, (d) is I-V measurement of the flakes, which is shown in (c).

Sample 188 was prepared with the same method on SiO_2. The sample and the flakes are shown in figure 5.15, image (a) is optical microscopy image. This sample was also investigated with atomic force microscopy. (b) is AFM image of the sample. The height of the flake as shown in (b) is 150nm. The AFM investigation shows that the flake is higher than a monolayer graphene sheet.

Another sample was prepared with the same method on SiO_2. This sample was coded as Sample 133 and optical microscope images are shown in figure 5.16. In image 5.16(a), the sample is observed dirtier than others, the black-color materials are graphite. This sample was annealed under H_2-Ar atmosphere ~300^0C. Then the sample was made conductive using lithograpy technique. Gold (Au) on Titanyum (Ti) pads are ~50µm wide and ~30nm high (figure 5.16(b)). Another characterization technique was applied and current versus voltage characteristic of the sample was

investigated. I-V curve of one of the flakes, as shown in figure 5.16(c), was measured and the measurement is shown in figure 5.16(d).

Moreover, I-V curves of the NUS sample and HOPG were measured, as shown in figure 5.17. I-V curve of HOPG is shown in figure 5.17(a), I-V curve of the NUS sample is shown in figure 5.17(b).

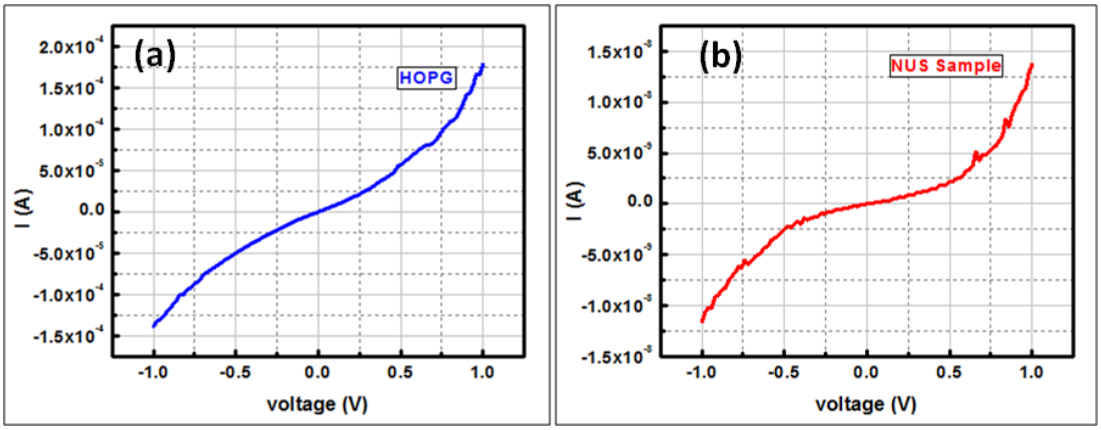

Figure 5.17: (a) I-V curve measurement of HOPG, (b) I-V curve measurement of the NUS sample.

In this section, an alternative method for graphene production, preparing a solution using adherent-graphite-layers on tape, was explained. Our initial results on the samples we prepared using our graphene production recipe hints at the possible successful multi-layer graphene flakes with considerably large sizes even visible to the naked eye. According to the Raman spectrum data, it is clearly mentioned that, the annealing method, based on information in the literature, gave quite well results. The flakes are made of graphite and Raman spectrum of the flakes show G peaks, but not 2D peaks. One of the samples' Raman spectrum data showed that even before annealing, the flake gave us the peaks of multi layer graphene. AFM images of another sample showed that, apparent relative heights of the flakes are approximately ~150 nm and it can be stated that the flake is graphitic. Finally, one of the samples was made conductive using lithography method and I-V characteristic of a flake on the sample was investigated but results show us the sample is more likely graphitic.

6. CONCLUSION

In this study, morphological, electronic and optical properties of novel nano-scale structures were investigated.

In the first chapter, we investigated T7 Primer molecules on HOPG surface by using scanning probe microscopy techniques. However, the solution of T7 Primer molecules formed different thin film structures on HOPG surfaces. According to AFM images we can clearly state that, this film structures prevented the observation of T7 Primer molecules on the surface. Then, we started to investigate the solution of T7 Primer molecules itself, which is Tris-EDTA buffer solution. TE buffer solution created hexagonal nanostructures on solid substrates. The hexagonal structures were observed by using AFM. The results of many experiments were not similar. To understand the hexagonal effects, the components of TE buffer, which are Tris-HCl and EDTA, were investigated on solid substrates by using AFM. The AFM images and even optical microscope images clearly showed that Tris-HCl buffer solution generates quite large hexagonal structures on solid substrates. These effects can be observed using drop cast-drag-pull method. Moreover, the hexagonal structures can be formed without drag-pull method by using diluted Tris-HCl buffer solution. EDTA and Tris-water (without HCl) solutions are shown not to form any hexagonal structures.

In the second chapter, we investigated CdSe quantum dot systems on HOPG surface using different dilution ratio of quantum dot solution. Quantum dots were observed with atomic force microscopy, but in cluster form. Rinsing and annealing the sample made AFM investigations much better. Here it was shown that the important parameter is annealing temperature.

In the third chapter, an alternative method for graphene production was studied. The method consists preparing a solution using “graphite on tape” and it results in multi layer graphene and graphitic flakes. On gold-coated mica and oxidized silicon wafer, flakes were observed by optical microscopy, atomic force microscopy and micro

Raman spectroscopy. The solution effect made the graphitic flakes higher, so we used annealing method to get rid of the solution remnants. Micro Raman spectroscopy showed that the flakes are graphitic. Moreover, another characterization technique, current versus voltage characteristic, was investigated. One of the graphene sample was made conductive using lithography method and its I/V measurement showed the flake is more likely graphitic.

REFERENCES

[1] **Binning, G., Quate, C. F. and Gerber, C.** (1986). Atomic Force Microscope. *Physical Review Letters, 56, 930-933.*

[2] **Binning, G., Rohrer, H., Gerber, C. and Weibel, E.** (1982). Tunneling through a controllable vacuum gap. *Applied Physics Letters, 40, 178-180.*

[3] **Lyubchenko, Y., Shlyakhtenko, L., Harrington, R., Oden, P. and Lindsay, S.** (1993). Atomic Force Microscopy of long DNA: Imaging in air and under water. *Proc. Natl. Acad. Sci. U.S.A., 90, 2137-2140.*

[4] **Hansma, H. G., Sinsheimer, R. L., Li, M. Q. and Hansma, P. K.** (1992). Atomic Force Microscopy of single- and double-stranded DNA. *Nucleic Acids Research, Vol.20, No.14, 3585-3590.*

[5] **Salmeron, M., Beebe, T., Odriozola, J., Wilson, T., Ogletree, D. F. and Siekhaus, W.** (1990). Imaging of biomolecules with the scanning tunneling microscope: problems and prospects. *J. Vac. Sci. Technol. A, Vol.8, No.1, 635-641.*

[6] **Hansma, H. G., Revenko, I., Kim, K. and Laney, D. E.** (1996). Atomic Force Microscopy of long and short double-stranded, single-stranded and triple-stranded nucleic acids. *Nucleic Acids Research, Vol.24, No.4, 713-720.*

[7] **Arscott, P. G., Lee, G., Bloomfield, V. A. and Evans, D. F.** (1989). Scanning Tunneling Microscopy of Z-DNA. *Nature, 339, 484-486.*

[8] **Keller, D., Bustamante, C. and Keller, R. W.** (1989). Imaging of single uncoated DNA molecules by Scanning Tunneling Microscopy. *Proc. Natl. Acad. Sci. U.S.A,. Vol.86, 5356-5360.*

[9] **Lee, G., Arscott, P. G., Bloomfield, V. A. and Evans, D. F.** (1989). Scanning Tunneling Microscopy of Nucleic Acids. *Science, Vol.224, 475-477.*

[10] **Dunlap, D. D. and Bustamante, C.** (1989). Images of single-stranded nucleic acids by Scanning Tunneling Microscopy, *Nature, 342, 204-206.*

[11] **Klinov, D. V., Yaminsky, I. V. and Dubrovin, E. V.** (2003). Scanning Probe Microscopy of DNA on mica and graphite. *AIP Conf. Proc., 696, 452-456.*

[12] **Wang, H., Zhang, L., Zhang, F., An, H., Chen, S., Li, H., Wang, P., Wang, X., Wang, Y. and Yang, H.** (2007). Investigation on the morphology of precipitated chemicals from TE buffer on solid substrates. *Surface Review and Letters, Vol.14, No.6, 1121-1128.*

[13] **Jiang, X. and Lin, X.** (2004). Atomic Force Microscopy of DNA self-assembled on a highly oriented pyrolytic graphite electrode surface. *Electrochem. Commun., 6, 873.*

[14] **Nogues, C., Cohen, S. R., Daube, S. S. and Naaman, R.** (2004). Electrical properties of short DNA oligomers characterized by conducting AFM. *Phys. Chem. Chem. Phys., 6, 4459-4466.*

[15] **Jdira, L., Overgaag, K., Gerritsen, J., Vanmaekelberg, D., Liljeroth, P. and Speller, S.** (2008). Scanning Tunneling Spectroscopy on Arrays of CdSe Quantum Dots: Response to wave functions to Local Electric Fields. *NanoLetters, Vol.8, No.11, 4014-4019.*

[16] **Ekimov, A. I. and Onushchenko, A. A.** (1984). Size quantization of the electron energy spectrum in a microscopic semiconductor crystal. *JETP Lett., Vol.40, No.8, 1136-1139.*

[17] **Rossetti, R., Nakahara, S. and Brus, L. E.** (1983). Quantum size effects in the redox potentials, resonance Raman spectra, and electronic spectra of CdS crystallizes in aqueous solution. *J. Chem. Phys., 79(2),1086-1088.*

[18] **Alivisatos, A. P.** (1996). Semiconductor clusters, nanocrystals and quantum dots. *Science, 271, 933.*

[19] **Hummon, M. R., Stollenwerk, A. J., Narayanamurti, V., Anikeeva, P. O., Panzer, M. J., Wood, V. and Bulovic, V.** (2010). Measuring change trap occupation and energy level in CdSe/ZnS quantum dots using a scanning tunneling microscopy. *Physical Review B, 81, 115439.*

[20] **Ou, Y. C., Cheng, S. F. and Jian, W. B.** (2009). Size dependence in tunneling spectra of PbSe quantum dot arrays. *Nanotechnology, 20, 285401 (5pp).*

[21] **Kim, S., Fisher, B., Eisler, H. J. and Bawendi, M.** (2003). Type II Quantum Dots: CdTe/CdSe (Core/Shell) and CdSe/ZnTe (Core/Shell) heterostructures. *J. Am. Chem. Soc., 125, 11466-11467.*

[22] **Bernard, R., Comtet, G., Dujardin, G., Huc. V. and Mayne, A. J.** (2005). Imaging and spectroscopy of individual CdSe nanocrystals on atomically resolved surfaces. *Applied Physics Letters, 87, 053114.*

[23] **Coe, S., Woo, W. K., Bawendi, M. and Bulovic, V.** (2002). Electroluminescence from single monolayers of nanocrystals in molecular organic devices. *Nature(London), Vol.420.*

[24] **O'Regan, B. and Gratzel, M.** (1991). A low-cost, high-efficiency solar cell based on dye-sensitized colloidal titanium dioxide films. *Nature(London), 353, 737.*

[25] **Novoselov, K. S., Geim, A. K., Morozov, S. V., Jiang, D., Zhang, Y., Dubonos, S. V., Grigorieva, I. V. and Firsov, A. A.** (2004). Electric Field effect in atomically thin carbon films. *Science, 306, 666-669.*

[26] **Novoselov, K. S., Geim, A. K., Morozov, S. V., Jiang, D., Katsnelson, M. I., Grigorieva, I. V., Dubonos, S. V. and Firsov, A. A.** (2005). Two-dimensional Gas of Massless Dirac Fermions in Graphene. *Nature, 438, 197.*

[27] **Chen, J. H., Jang, C., Xiao, S., Ishigami, M. and Fuhrer, M. S.** (2008). Intrinsic and extrinsic performance limits of graphene devices on SiO_2. *Nature Nanotechnology,3, 206-209.*

[28] **Wallace, P. R.** (1947). The band theory of graphite. *Physical Review, 71(9), 622.*

[29] **Geim, A. K. and Novoselov, K. S.** (2007). The rise of graphene. *Nature Materials, 6, 183-191.*

[30] **Schwierz, F.** (2010). Graphene Transistors. *Nature Nanotechnology, 5, 487-496.*

[31] **Eizenberg, M. and Blakely, J. M.** (1970). Carbon monolayer phase condensation on Ni(111). *Surface Science, 82, 228-236.*

[32] **Aizawa, T., Souda, R., Otani, S., Ishizawa, Y. and Oshima, C.** (1990). Anomalous bond of monolayer graphite on transition-metal carbide surfaces. *Phys. Rev. Lett., 64, 768-771.*

[33] **Berger, C. et.al.** (2006). Electronic confinement and coherence in patterned epitaxial graphene. *Science, 312, 1191-1196.*

[34] **Dikin, D. A., Stankovich, S., Zimney, E. J., Piner, R. D., Dommett, G. H. B., Evmenenko, G., Nguyen, S. B. T. and Ruoff, R. S.** (2007). Preparation and characterization of graphene oxide paper. *Nature, 448.*

[35] **Park, S., An, J., Jung, I., Piner, R. D., An, S. J., Li, X., Velamakanni, A. and Ruoff R. S.** (2009). Colloidal suspensions of highly reduced graphene oxide in a wide variety of organic solvents. *NanoLetters, Vol.9, No.4, 1593-1597.*

[36] **Seeman, N. C.** (2010). Nanomaterials based on DNA. *Annual review of biochemistry, 79, 65-87.*

[37] **Ding, B., Sha, R. and Seeman, N. C.** (2004). Pseudohexagonal 2D DNA crystals from double crossover cohesion. *J. Am. Chem. Soc.,126, 10230-10231.*

[38] **Liu, F., Sha, R. and Seeman, N. C.** (1999). Modifying the surface features of 2D DNA crystals. *J. Am. Chem. Soc., 121, 917-922.*

[39] **Mao, C., Sun, W. and Seeman, N. C.** (1999). Designed two dimensional DNA holliday junction arrays visualized by AFM. *J. Am. Chem. Soc., 121, 5437-5443.*

[40] **Chhabra, R., Sharma, J., Liu, Y., Rinker, S. and Yan, H.** (2010). DNA self-assembly for nanomedicine. *Advanced Drug Delivery Review, 62, 617-625.*

[41] **Jamieson, T., Bakhshi, R., Petrova, D., Pocock, R., Imani, M. and Seifalian, A. M.** (2007). Biological applications of quantum dots. *Biomaterials, 28, 4717-4732.*

[42] **Wilson, N. R. and Macpherson, J. V.** (2009). Carbon nanotube tips for atomic force microscopy. *Nature Nanotechnology, 4, 483-491.*

[43] **Bao, W., Liu, G., Zhao, Z., Zhang, H., Yan, D., Deshpande, A., LeRoy, B. and Lau, C. N.** (2010). Lithography-Free Fabrication of high quality substrate-supported and free standing graphene devices. *Nano Res., 3, 98-102.*

[44] **Chen, J. H., Jang, C., Adam, S., Fuhrer, M. S., Williams, E. D. and Ishigami, M.** (2008). Charged-impurity scattering in graphene. *Nature Physics, 4, 377-381.*

[45] **Ishigami, M., Chen, J. H., Cullen, W. G., Fuhrer, M. S. and Williams E. D.** (2007). Atomic Structures of Graphene on SiO_2. *NanoLetters, Vol.7, No.6, 1643-1648.*

[46] **Wiesendanger, R.** (1994). Scanning Probe Microscopy and Spectroscopy: Methods and Application. *Cambridge University Press.*

[47] **Chen, C. J.** (1993). Introduction to Scanning Tunneling Microscopy. *Oxford University Press.*

[48] **Binns C.** (2010). Introduction to Nanoscience and Nanotechnology. *Wiley Survival Guides in Engineering and Science.*

[49] **Giessibl, F. J.** (2003). Advances in Atomic Force Microscopy. *Reviews of modern physics, Vol.75.*

[50] **Wolf, I. D.** (1996). Micro-Raman Spectroscopy to study local mechanical stress in silicon integrated circuits. *Semicond. Sci. Technol., 11, 139-154.*

[51] **Lyon, L. A., Keating, C. D., Fox, A. P., Baker, B. E., He, L., Nicewarner, S. R., Muluaney, S. P. and Natan, M. J.** (1998). *Anal. Chem., 70, 341R-361R.*

[52] **Schrader, B.** (1995). Infrared and Raman Spectroscopy: Methods and Application. *VCH.*

[53] **Ferrari, A. C., Meyer, J. C., Scardaci, V., Casiraghi, C., Lazzeri, M., Mauri, F., Piscanec, S., Jiang, D., Novoselov, K. S., Roth, S. and Geim, A. K.** (2006). Raman Spectrum of Garphene and Graphene Layers. *Physical Review Letters, 97, 187401.*

[54] **Hansma, H. G., Laney, D. E., Bezanilla, M., Sinsheimer, R. L. and Hansma, P. K.** (1995). Applications for Atomic Force Microscopy of DNA. *Biophysics Journal, Vol.68, 1672-1677.*

[55] **Rose, F., Martin, P., Fujita, H. and Kawakatsu, H.** (2006). Adsorption and combing of DNA on HOPG surfaces of bulk crystals and nanosheets: application to the bridging of DNA between HOPG/Si heterostructures. *Nanotechnology, 17, 3325-3332.*

[56] **Gomori, G.** (1946). *Proc. Soc. Exptl. Biol. Med., 62, 33-34.*

[57] **Rudman, R., Eilerman, D. and LaPlaca, S. J.** (1978). The structure of crystalline Tris: A plastic crystal precursor, buffer and acetylcholine attenuator. *Science, Vol.200, No.4341, 531-533.*

[58] **Eilerman, D. and Rudman, R.** (1980). Polymorphism of crystalline poly(hydroxymethyl) compounds. III. The structures of crystalline and plastic tris(hydroxymethyl)aminomethane. *J. Chem. Phys., Vol.72, 5656-5666.*

[59] **Divi, S., Chellappa, R. and Chandra, D.** (2006). Heat capacity measurement of organic thermal enery storage materials. *J. Chem. Thermodynamics, 38, 1312-1326.*

[60] **Harsha, S. S. and Grischkowsky, D.** (2010). Terahertz characterization of Tris(hydroxymethyl)aminomethane using high reolution waveguide THz-TDS. *J. Phys. Chem. A, 114, 3489-3494.*

[61] **Kanesaka, I. and Mizuguchi, K.** (1998). Vibrational study of hydrogen bonds and structure of Tris(hydroxymethyl)aminomethane. *Journal of Raman Spectrosc., 29, 813-817.*

[62] **Emmons, E. D., Fallas, J. C., Kamisetty, V. K., Chien, W. M., Covington, A. M., Chellappa, R. S., Gramsch, S. A., Hemley, R. J. and Chandra, D.** (2010). High pressure raman spectroscopy of Tris(hydroxymethyl)aminomethane, *J. Phys. Chem., 114, 5649-5656.*

[63] Url-1<http://www.sigmaaldrich.com/catalog/ProductDetail> data received 02.03.2011

[64] **Bolotin, K. I., Sikes, K. J., Hone, J., Stormer, H. L. and Kim, P.** (2008). Temperature dependent transport in suspended graphene. *Physical Review Letters, 101, 096802.*

APPENDICES

APPENDIX A.1 : Weight of a T7 Primer molecule

APPENDIX A.2 : Preparation of Tris-HCl buffer

APPENDIX A.3 : Weight of a CdSe quantum dot

APPENDIX A.1

For 20 b oligonucleotide (ssDNA) ;

1 picomole = 6.6 ng.

1 picomole/µl = 6.6 ng/µl

1µl solution consists 6.6 ng T7 Primer.

OR

For ssDNA, to convert picomole to µg :

picomole x N x 330 picogram/picomole x 1µg/10^6 picogram = µg

where N is the number of nucleotides and 330 picogram/picomole is the average molecular weight of a nucleotide

So,

T7 Primer : 5'd(TAATACGACTCACTATAGGG)3'

T : 2.094260436 x 10^{-22} g.

A : 2.243874189 x 10^{-22} g.

G : 2.509558986 x 10^{-22} g.

C : 1.84484883 x 10^{-22} g.

Total weight of a "T7 Primer"; 5T + 7A + 4G + 4C = 43.59605277 x 10^{-22}g.
= 43.59605277 x 10^{-13} ng.

A "T7 Primer" is (43.59605277 x 10^{-22} g.),
1µl solution consists 6.6 ng T7 Primer molecules,
so **1µl solution consists (1.514 x 10^{12}) T7 Primer molecules.**

APPENDIX A.2

For 1M, 0.25L, pH:7.2 Tris-HCl ;

Tris base : 30.285 g.

HCl : 18.44 mL.

ddH_2O is added until 0.25L.

for different ratios, more details in “Henderson-Hasselbalch Calculator”.

APPENDIX A.3

Concentration is 5mg/mL in toluene. 1µL solution consist 5µg quantum dots.

Crystal Structure	Lattice Parameter, a (Å)
CdS	5.80
CdSe	6.05
ZnS	5.41

For CdSe ; $V_{unit\ cell} = a^3 = (0.605\ nm)^3 = 0.22144\ nm^3$

640nm CdSe ; size:6.5 nm, r = 3.25 nm

$V_{CdSe} = 4/3\ \pi\ r^3 = 143.72\ nm^3$

$N_{unit\ cell} = V_{CdSe} / V_{unit\ cell} = 143.72 / 0.22144 = 649.0245665 = \sim 649$ unit cell

In 1 quantum dot;

number of Cd atoms : 649 x 4 = 2596

number of Se atoms : 649 x 4 = 2596

Total atom in a 6.5nm-quantum dot ; 2596 Cd + 2596 Se

Element	Atomic mass (akb)
Cd	112.411
Se	78.96
Zn	65.39
S	32.06

Weight of a quantum dot;

$W_{CdSe} = 2596 \times 112.411 + 2596 \times 78.96 = 496799.116$ akb

1 akb = 1 u = $1.660538782(83) \times 10^{-24}$ g.

$W_{cdSe} = 8.2495424 \times 10^{-19}$ g. So, **1µl solution consists (6061×10^9) QDs.**

CURRICULUM VITAE

Name Surname: Merve ALTAY

Place and Date of Birth: Bandırma/Balıkesir, 24.12.1986

Address: Merkez mah.Perihan sok. No : 85/3, Şişli/İstanbul

E-Mail: altaymerve@itu.edu.tr, altaymerve86@gmail.com

B.Sc.: Balıkesir University, Physics

PUBLICATIONS/PRESENTATIONS ON THE THESIS

- **Altay M.,** Avşar A., Özyılmaz B., Gürlü O., 2006 : Poster Presentation. "An Alternative Approach to Graphene and Graphitic Flake Preparation and Their Morphology on Au and SiO Substrates", NanoTR VI, Haziran 2010, Çeşme/İzmir
- **Altay M.,** Karacor B., Kumru M., Akarsubaşı A.T., Gürlü O., 2007 : Poster Presentation. "Morphology of tris-edta buffer remnants on solid substrates", NanoTR VII, Haziran 2011, Sabancı University/İstanbul
- **Altay M.,** Yılmaz R., Gürlü O., 2007 : Poster Presentation. "Effects of various solvents for quantum dots on hopg and gold surfaces" , NanoTR VII, Haziran 2011, Sabancı University/İstanbul
- Tamer M.S., **Altay M.,** Yılmaz R., Gürlü O., 2007 : Poster Presentation. "Photon scanning tunneling microscopy system for observing optical excitations at nanoscale tunnel junctions", NanoTR VII, Haziran 2011, Sabancı University/İstanbul
- Uygur G., Yıldız D., **Altay M.,** Yılmaz R., Gürlü O., 2007 : Poster Presentation. "Alternative and affordable graphitic substrates for surface studies", NanoTR VII, Haziran 2011, Sabancı University/İstanbul